Lightweight Intermodal Flatcar Evaluation Program

Test Results Report (Including Appendix A-Transducer Locations)

1. Report No. FRA/ORD-80/07.II	2. Government Accession No.	3. Recipient's Catalog No.

4. Title and Subtitle	5. Report Date
Lightweight Intermodal Flatcar Evaluation Program Volume II Test Results Report (Including Appendix A - Transducer Locations)	December 1979
	6. Performing Organization Code

7. Author's) M. A. Kenworthy, Ph.D. and J. Edelman	8. Performing Organization Report No. DOT-FR-79-24

9. Performing Organization Name and Address	10. Work Unit No. (TRAIS)
Rail Transportation Engineering Division ENSCO, INC. 2560 Huntington Avenue Alexandria, VA 22303	11. Contract or Grant No. DOT-FR-64113
	13. Type of Report and Period Covered

12. Sponsoring Agency Name and Address	
U.S. DEPARTMENT OF TRANSPORTATION Federal Railroad Administration (RRD-12) 400 Seventh Street, S.W. Washington, DC 20590	Technical Report
	14. Sponsoring Agency Code FRA/ORD-12

15. Supplementary Notes

Volume I, Modal Analysis of Railcars - An Explanation and Applications Guide
Volume III, Data Appendices B through F

16. Abstract

The Lightweight Flatcar (LWFC) Evaluation Program was conducted to provide a comparative evaluation of the dynamic performance of two prototype skelton or lightweight flatcars with a conventional TTAX flatcar. For this purpose, measurements of the acceleration response of the entire vehicle system (axle, carbody, trailer, and container) were made under both controlled and revenue-service conditions. The controlled tests were conducted at zero (nominal), 50,000 and 125,000 accumulated miles of service. The results indicate that in terms of dynamic performance the lightweight flatcars were comparable overall to the conventional TTAX flatcar. This conclusion, however, must be evaluated for each special application, since situations were observed in which one flatcar was markedly superior to the other in performance.

Volume I: Modal Analysis of Railcars - An Explanation and Applications Guide
            FRA/ORD-80/07.I
Volume II: Test Results Report (Including Appendix A - Transducer Locations)
            FRA/ORD-80/07.II
Volume III: Data Appendices - Appendix B - Wear Measurements
            FRA/ORD-80/07.III- Appendix C - Axle Power Spectral Densities
                              - Appendix D - Load Power Spectral Densities
                              - Appendix E - Carbody Power Spectral Densities
                              - Appendix F - Octave RMS Histories

17. Key Words Railcar Dynamics Railcar Testing Railcar Instrumentation Intermodal Railcars TOFC/COFC Modal Analysis Railcar Lading/Dynamic Environment	18. Distribution Statement Volumes I and II of this report are available to the public through the National Technical Information Service, Springfield, VA 22161. Volume III is available from the Sponsoring Agency on a loan basis.

19. Security Classif. (of this report) Unclassified	20. Security Classif. (of this page) Unclassified	21. No. of Pages 142	22. Price

Form DOT F 1700.7 (8-72)   Reproduction of completed page authorized

TABLE OF CONTENTS

TABLE OF CONTENTS (Cont)

LIST OF ILLUSTRATIONS

LIST OF ILLUSTRATIONS (Cont)

LIST OF ILLUSTRATIONS (CONT)

LIST OF TABLES

LIST OF TABLES (CONT)

LIST OF SYMBOLS

A   modal coefficients (Section 3.2, Equation (4) elements of A-vector)

a   acceleration

B   mode shape function of bending modes

b   mode shape coefficient usually in first torsion mode

c   mode shape coefficient usually in second bending mode

d( )   elemental quantity of ( )

f   frequency

G   cross and power spectral density function

g   unit of acceleration referred to as gravity (32.2 feet/second^2)

H   matrix of transducer location

H_s integral of polar movement of inertia

i   general index

J   polar moment of inertia

j   general index

k   spring constant

L   car length

M   moment or integral of mass

m   mass

n   general index

Q   a square matrix resulting from $X^T X$

S   vertical displacement

s   general index

T   mode shape function of torsion mode

t   time

V   velocity

X   transducer location matrix (Section 2.2, Equation (13)), also data sample set when subscripted

x   principle axis in the direction of motion, or distance

y   principle horizontal axis perpendicular to the x-axis

z   principle vertical axis

$\ddot{x}$ longitudinal linear acceleration

$\ddot{y}$ lateral linear acceleration

$\ddot{z}$ vertical linear acceleration

$\ddot{x}_0$ longitudinal mode acceleration

$\ddot{y}_0$ lateral mode acceleration

$\ddot{z}_0$ vertical mode acceleration

Z   general measured acceleration vector

β bending mode

θ angular displacement about x-axis

$\ddot{\theta}_0$ roll mode acceleration

μ mean

ρ mass density

σ standard deviation

τ torsion mode

ϕ angular displacement about the y-axis

$\ddot{\phi}_0$ pitch mode acceleration

ψ angular displacement about the z-axis

$\ddot{\psi}_0$ yaw mode acceleration

Special notes of explanation:

Bending mode β_{abi}

      a indicates the axis about which bending occurs
      b indicates the direction of bending
      i indicates the number of the mode within its family

Torsion mode τ_{ai}

    a indicates the axis about which torsion occurs
    i indicates the number of the mode within its family

ASF axle identification is by number rather than the letter
code used in this text. The correlation between the two
labelling systems is:

Text Notation	AA	A	B	BB
ASF Notation	4	3	2	1

RVT - ride vibration test

OTR - over-the-road test

TTC - Transportation Test Center

ALD - automatic location detector

1.0   INTRODUCTION

1.1   BACKGROUND

As an integral part of the intermodal freight process, dedicated trains made up of flatcars carrying standardized trailers and containers operate over long distances between regions of concentrated industrial and maritime activity. This service, known as piggyback, has experienced steady growth because it is efficient and profitable. For example, one major railroad reported recently that 25 percent of net profits came from piggyback operations which comprised only 15 percent of that railroad's freight traffic.

The growing volume of intermodal traffic has resulted in an almost uninterrupted expansion of the intermodal railcar fleet. A frequent speculation during this process was whether substantial benefits could be realized if the new railcars were of a revised design. The principal issues being considered were the opportunity for increased efficiency attainable by the application of advanced technology traded-off against the requirement to be compatibile with existing intermodal equipment and terminal facilities. The need for energy efficiency prompted a special interest in new flatcar designs which featured low tare weight and were, therefore, referred to a "lightweight flatcars."

Due to the novel and in some cases radical nature of some proposed lightweight flatcar designs, it was deemed desirable to assess the ability of such flatcars to transport freight in a safe

and economical manner. To this end, the Federal Railroad
Administration, Office of Freight Systems in cooperation with:

American Steel Foundries

National Castings Division, Midland-Ross Corporation

Pullman Standard

Pullman Transport Leasing

Santa Fe Railway Company

Trailer Train Company

Transportation Systems Center

Transportation Test Center

under took a program to address this question. The effort was
referred to as the Lightweight Flatcar Evaluation (LWFC) Program.

1.2 PURPOSE

The LWFC Program evaluated the dynamic performance of two
prototype lightweight flatcars and compared their performance
to a conventional TTAX flatcar which is presently in wide-
spread use. Specifically, the objectives were to:

1. Obtain a quantitative comparison of the ride
   vibration in TOFC and COFC operations between
   a conventional TTAX flatcar and the prototype
   lightweight flatcars TLDX61 and TLDX62.

2. Obtain quantitative measurements of the ride
   vibration of containers and trailers in
   typical TOFC and COFC service conditions.

3. Experimentally determine the relationship between ride vibration and component wear incurred during actual TOFC and COFC service conditions.

4. Experimentally determine the relation between component wear and distance travelled under service conditions.

5. Determine the influence of load configuration on the ride vibration performance.

1.3 GENERAL PROGRAM DESCRIPTION

To accomplish the program objectives, a series of tests was conducted to measure the dynamic performance of a conventional TTAX flatcar and two prototype lightweight flatcars. For this purpose, each car system was instrumented with a number of acceleration transducers referred to as accelerometers. The car system included the axles, the carbody and the loads, both trailers and containers. The measured linear accelerations were transformed using modal analysis* to a generalized set of accelerations describing the acceleration response of each car subsystem in global terms. This technique provided a clear and concise basis for the comparison of the dynamic performance of the two very dissimilar flatcar designs.

---

*For a detailed explanation of modal analysis, see Volume I of this report.

The series of tests, designed to meet the program objectives, was made up of two types of tests. The first of these was a controlled test called the Ride Vibration Test (RVT). Three RVT's were conducted at specified levels of accumulated mileage (0, 50,000 and 125,000 miles). Each RVT was conducted on two test zones representing one and three miles of Class 3 and Class 5 tangent track, respectively. The test train was made up of three test cars and FRA's Data Acquisition Vehicle, T-5. The tests were conducted at a set of specified speeds held constant through the test zone while acceleration data were recorded. Upon completion of an RVT, detailed wear measurements were made on each truck. Thus, the series of RVT's was designed to address all but the second objective given in Section1.2.

To accomplish the second objective, a series of tests was conducted under actual revenue service conditions called the Over-the-Road (OTR) tests. The instrumentation and recording equipment used in the OTR test series were identical to that used in the RVT series. The OTR tests were made with the test cars and data acquisition vehicle in a regularly scheduled freight train between Los Angeles, CA, and Kansas City, MO. Acceleration measurements were made during these tests over twelve-ten mile test zones, selected to represent a cross section of track structures and operating conditions. The results of the OTR test series document the ride vibration performance of both the conventional and lightweight flatcars under actual operating conditions.

This report describes the instrumentation and test procedures
employed to make the required measurements of acceleration.
In addition, the method of transforming the data to a set of
generalized accelerations, referred to as modal analysis,
and the format of data display are described. The results
are then presented and discussed with respect to program
objectives.

2.0 TEST EQUIPMENT AND PROCEDURES

To meet the program objectives, a series of three controlled tests and six revenue service tests were conducted. The acceleration data necessary to evaluate the prototype light-weight flatcars were obtained by using linear servo-accelerometers. These tests covered two years, 125,000 miles of accumulated service, and a wide range of operating conditions.

2.1 INSTRUMENTATION

Accelerations were measured with a maximum of 48 linear servo-accelerometers per flatcar. The accelerometers were mounted in specially designed mechanical isolators to protect them from high frequency impact accelerations. The signals were electrically filtered to make maximum use of the range and resolution of the accelerometers.

Acceleration signals were transmitted by cable to the data acquisition vehicle where they were anti-alias filtered, digitized and recorded on magnetic tape. The data were reproduced on strip charts to provide a visual record and a method of monitoring the signals.

2.1.1 ACCELEROMETERS

Accelerations on the flatcars were measured with Schaevitz single-axis linear servo-accelerometers, shown in Figure 2-1. These accelerometers are closed loop, solid-state, force balance instruments which provide state-of-the-art levels of accuracy. Accelerometers with a range of ±5 g were used to measure the dynamic response of the carbody, trailers and containers (see Section 2.2 and 2.3). These accelerometers were damped with an electronic network which limited the response of the 5 g accelerometer to 130 Hz with an overall resolution of approximately 0.005 g. In contrast, the
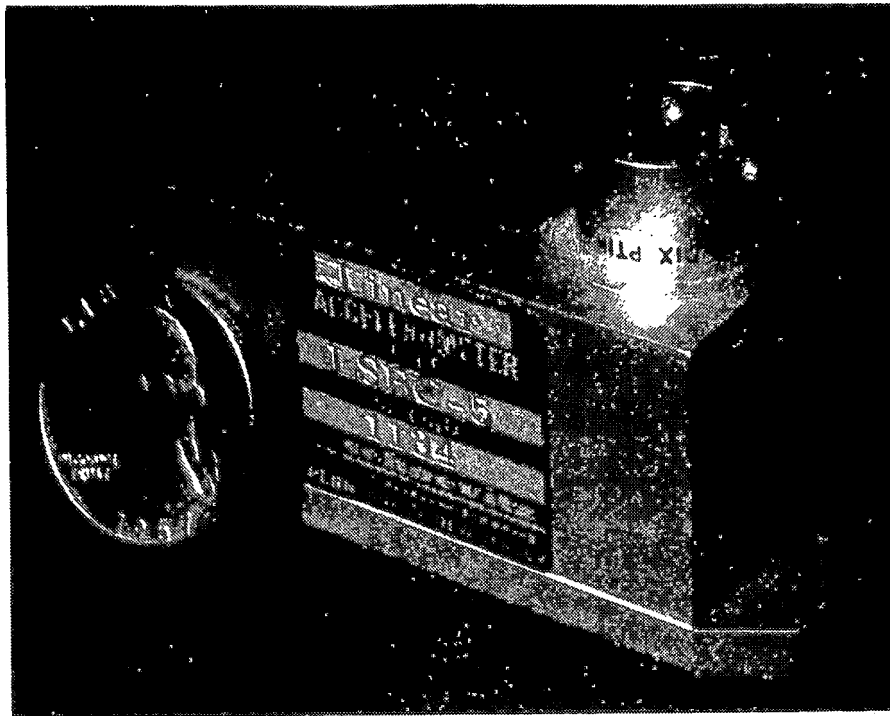
Figure 2-1. Accelerometer

accelerometers used to measure the dynamic environment
experienced by the axle of each flatcar had a range of
±30 g. Viscous damping used with the 30 g accelerometer
limited the frequency response to 30 Hz while providing some
protection against high frequency-high amplitude impulses.
The manufacturers specifications for the 5 g and 30 g accel-
erometers are summarized in Table 2-1.

2.1.2 MECHANICAL ISOLATOR

An accelerometer capable of withstanding the most severe
vibrations which occur at the bearing pad or which are
caused by mismatched track joints would lack the resolution
necessary to measure the smaller accelerations in the low
frequency range. Therefore, it was necessary to physically
isolate the accelerometers from the high frequency inputs.
inputs.

TABLE 2-1

ACCELEROMETER SPECIFICATIONS

	5 g	30 g
Scale Factor	1 volt/g	0.167 volt/g
Static Linearity	0.007%	0.02%
Cross Axis Sensitivity	0.001 volts/g	0.001 volts/g
Noise	0.001 volts rms	0.001 volts rms
Mechanical Alignment Accuracy	0.002 volts	0.005 volts
Natural Frequency (Nominal)	130 Hz	30 Hz

To isolate and protect the accelerometers, a mechanical
isolator, or filter, was designed (Figure 2-2). The inner
and outer cups were formed from one-eighth-inch aluminum
with the space between filled with a firm open cell foam
rubber. The mechanical isolator attenuated acceleration
inputs above 150 Hz; an idealized plot of truck acceleration
input and the mechanical isolator response are shown in
Figures 2-3 and 2-4, respectively. The isolator response
curve (Figure 2-4) is typical of a lightly damped second
order system. The benefit of light damping is that it pro-
duces only a very small phase shift for frequenices between
0 and 30 Hz. The phase shift error was of the order of 1°
at 30 Hz and was thus considered negligible. Flat lead
strips were placed beneath the accelerometers to add mass,
as needed, to the inner structure in order to achieve a
consistent 150 Hz corner frequency.
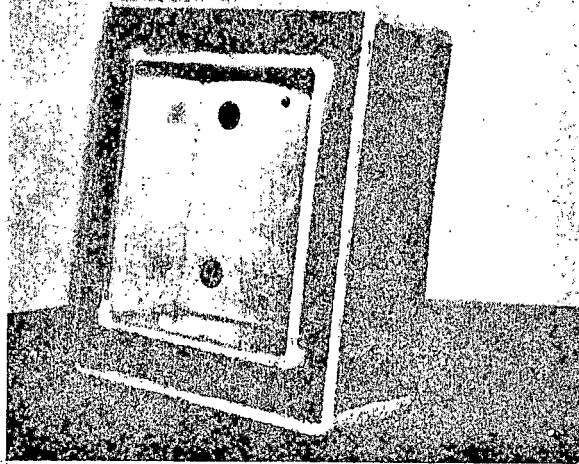
Figure 2-2.   Mechanical Isolator
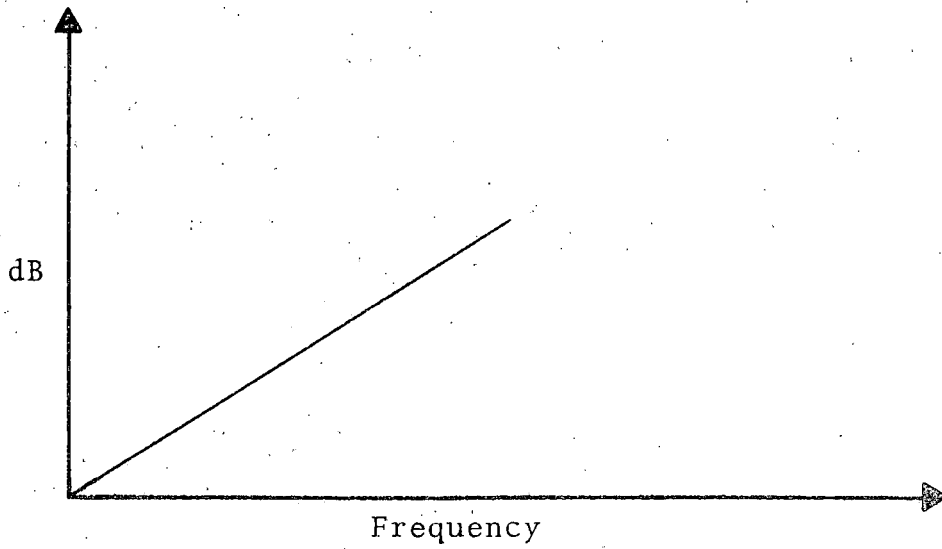
Figure 2-3.   Truck Acceleration Amplitude (Idealized)

6 dB/octave

150 Hz
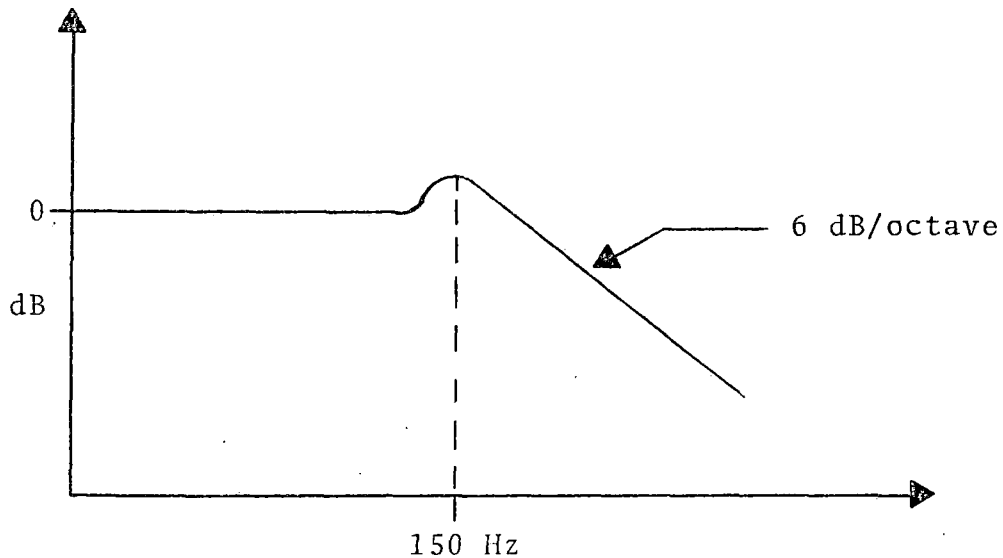
Figure 2-4. Mount Amplitude Response

Each accelerometer was mounted in a mechanical isolator to provide a congruent phase angle between all the signals and to insure high reliability during the 10,000-mile revenue service tests (see Section 2.4.2). This also provided a convenient means of mounting and aligning the accelerometers. Each accelerometer was securely bolted to the inner cup of the isolator; the outer cup was then bolted to brackets welded to the car. These brackets were aligned to provide orthogonal mounting to within ±one degree. The isolator was then enclosed with a dust and water proof plastic cover to complete the environmental protection of each accelerometer. A complete accelerometer unit is shown in Figure 2-5.

2.1.3 ACCELEROMETER LOCATIONS

Accelerometers were mounted on the loads, carbodies and axles of the test cars to obtain complete data for each of the mass elements. The carbody was instrumented with 17 accelerometers as illustrated in Figure 2-6. Three axles per flatcar were
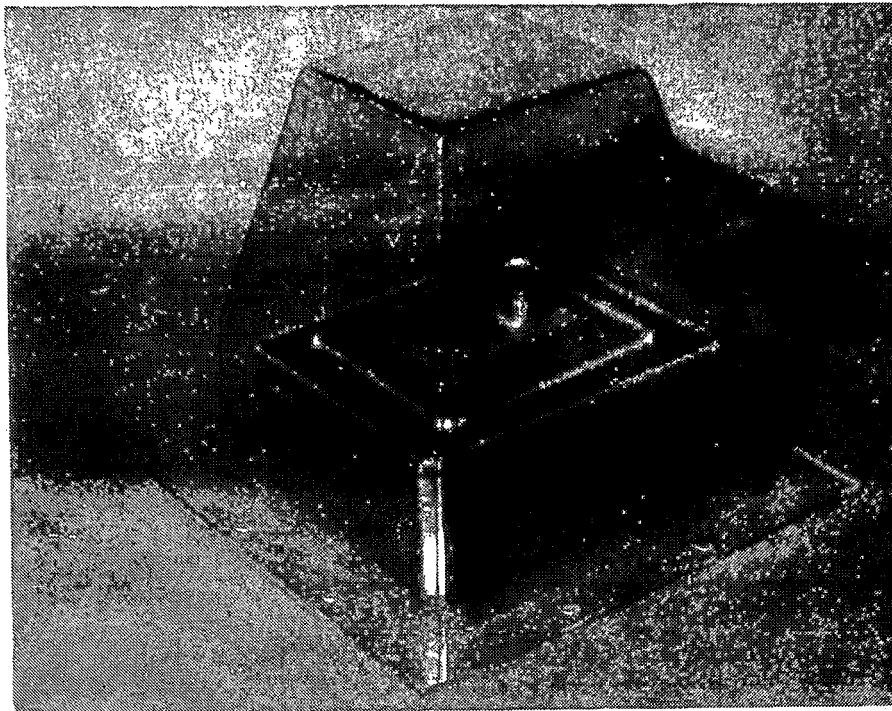
Figure 2-5. Typical Accelerometer Mounting

Figure 2-6. Carbody Accelerometers
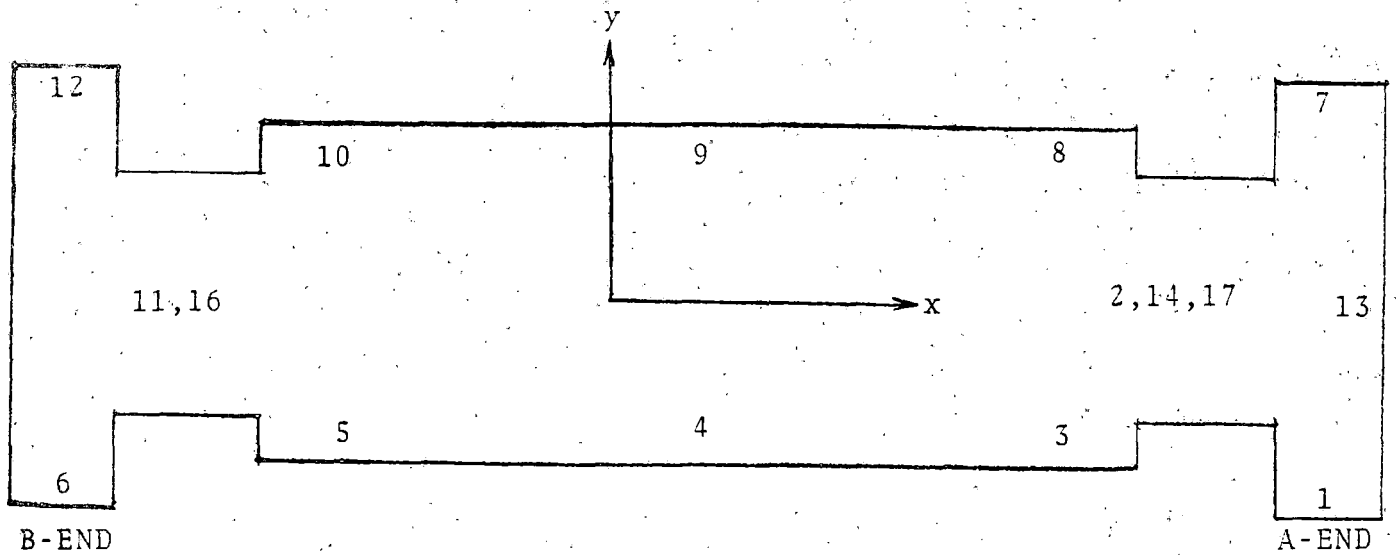
Accelerometer	Direction
1 - 12	Vertical
13 - 16	Lateral
17	Longitudinal

instrumented with five accelerometers each as shown in Figure
2-7 and the loads were instrumented with eight accelerometers
each, as shown in Figure 2-8. Thus, a completely instrumented
car with two containers or trailers carried 48 accelerometers.
Tests conducted during the latter part of the program required
only 35 accelerometers, since the half-laden configuration was
employed exclusively and only two axles were instrumented.
The accelerometer locations are specified in Appendix A.

Since each accelerometer has a sensitive axis with a positive
and negative direction, and since a Cartesian coordinate system
with the center of each flatcar as the origin, was established
to simplify the data analysis, all the accelerometers were
mounted so that the positive direction of their sensitive
axis corresponded with the positive direction of each axis
of the coordinate system. The only exception was the longi-
tudinal accelerometers on the axles which were mounted asym-
metrically. The resulting polarity inversion was corrected
during processing.

2.1.4 INSTRUMENTATION SYSTEM

Figure 2-9 is a schematic representation of the instrumentation
system. The transducers on each car were hardwired via cables
and connectors to a weatherproof junction box (J-box) (Figure
2-10) on that car. The consolidated signals were conducted
through individually shielded conductor pairs to the Data
Acquisition Vehicle, T-5, which contained the analog signal
conditioning and digital data acquisition system. Figure
2-11 is a simplified block diagram of the signal flow.
Figure 2-12 is a more detailed description of a typical
data channel.

The excitation voltage (±15 VDC) was transmitted through a
cable from T-5 to the transducer. The output signal from
the transducer was transmitted back to T-5 via the shielded
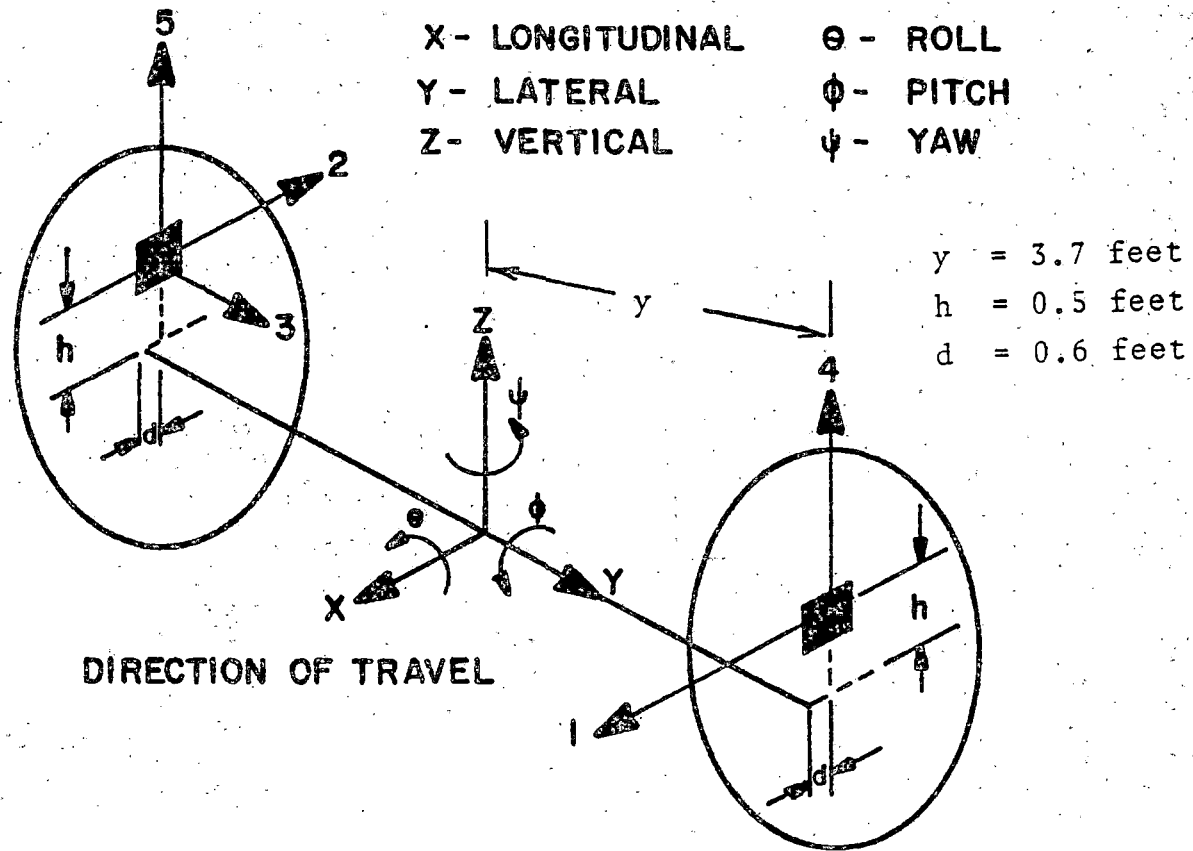
Figure 2-7. Axle Transducer Locations

(a) Trailer
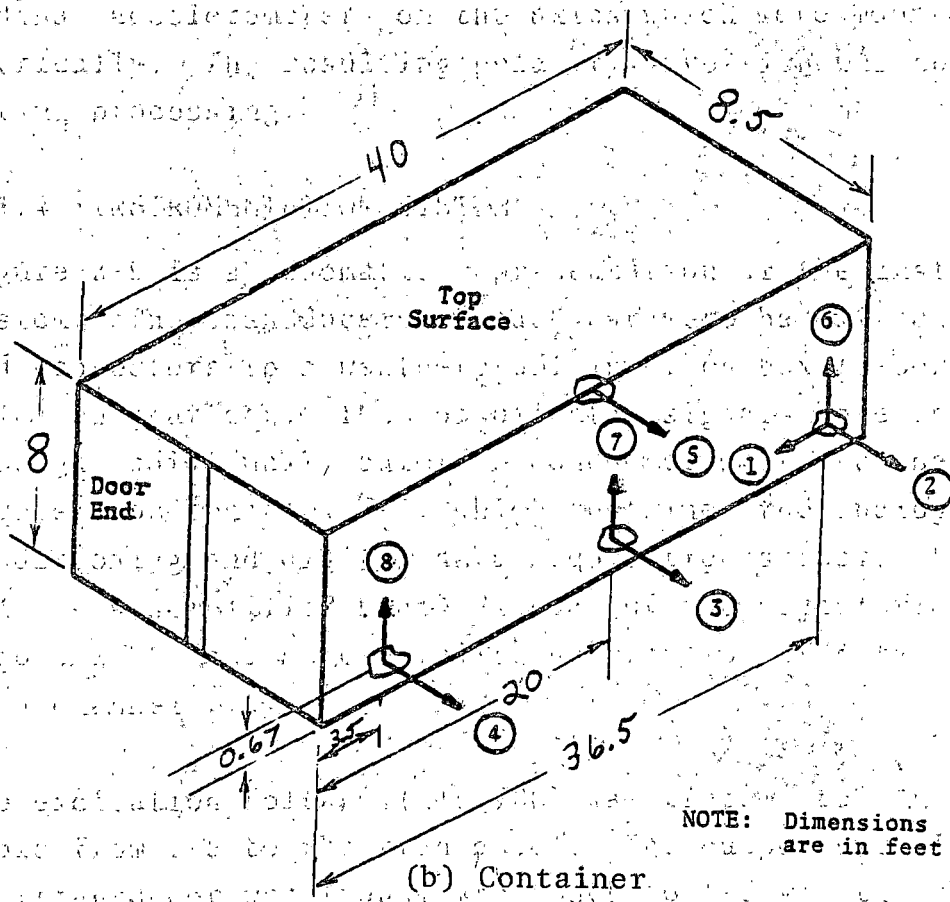
NOTE: Dimensions are in feet

(b) Container

NOTE: Dimensions are in feet

Figure 2-8. Load Accelerometer Locations

SHIELDED CABLES

CONTAINER WITH 8 ACCELEROMETERS

TRAILER WITH 8 ACCELEROMETERS

CONTAINER OR TRAILER WITH 8 ACCELEROMETERS

J-BOX

J-BOX

J-BOX

TLDX-62 FLATCAR WITH 32 ACCELEROMETERS

TTAX FLATCAR WITH 32 ACCELEROMETERS

TLDX-61 FLATCAR WITH 32 ACCELEROMETERS AND ALD

DATA ACQUISITION VEHICLE (T-5)

SPEED
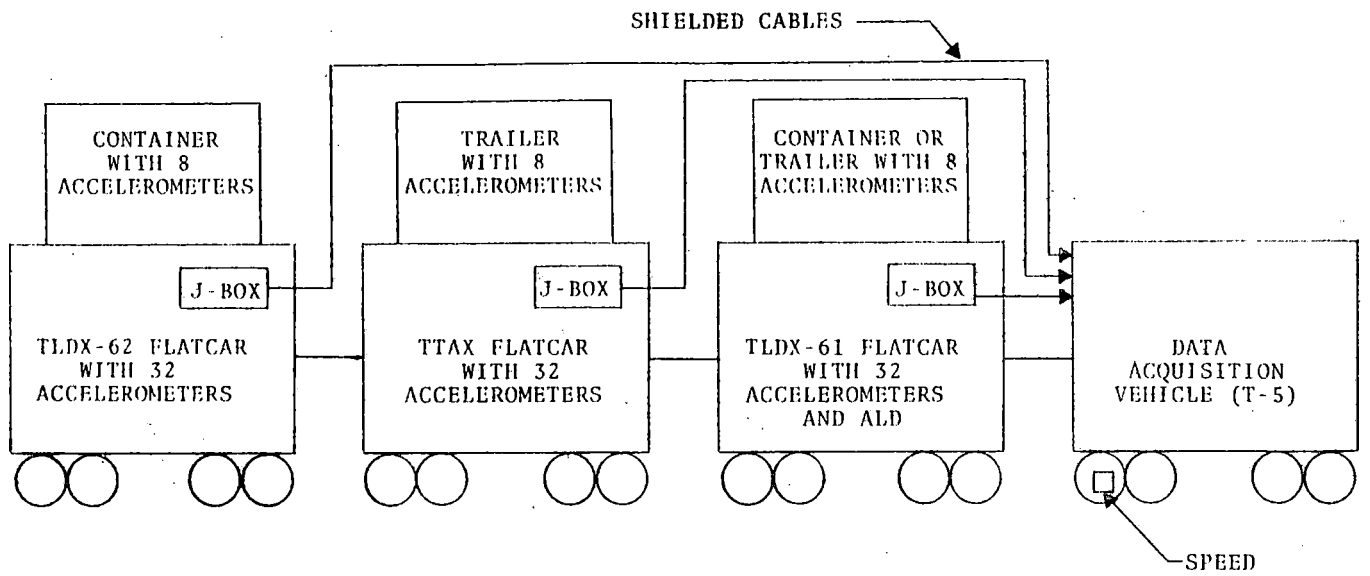
Figure 2-9.   Schematic Representation of
Data Measurement System
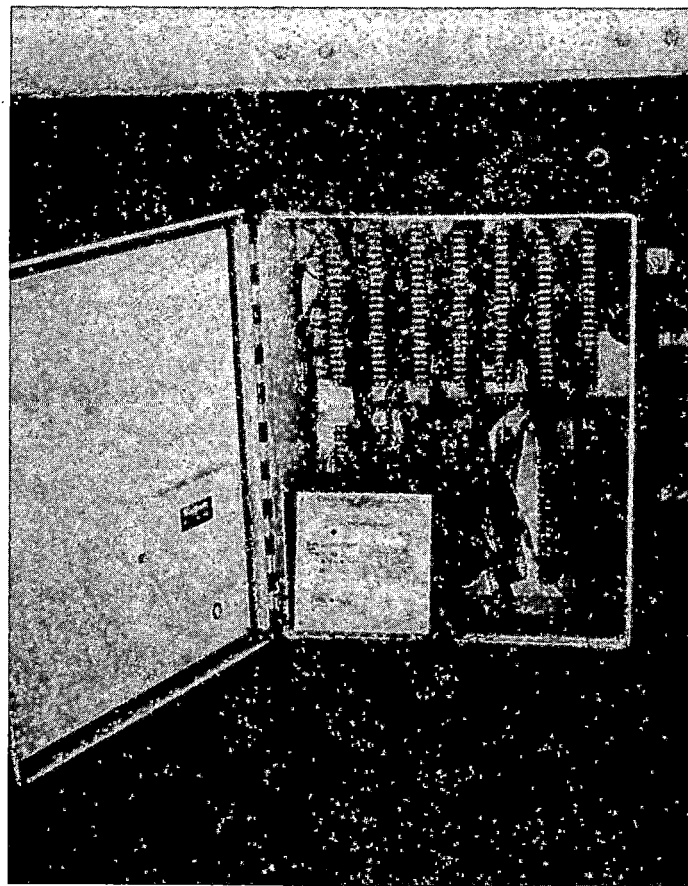
Figure 2-10.   Junction Box (J-Box) and Associated Cabling

2-10
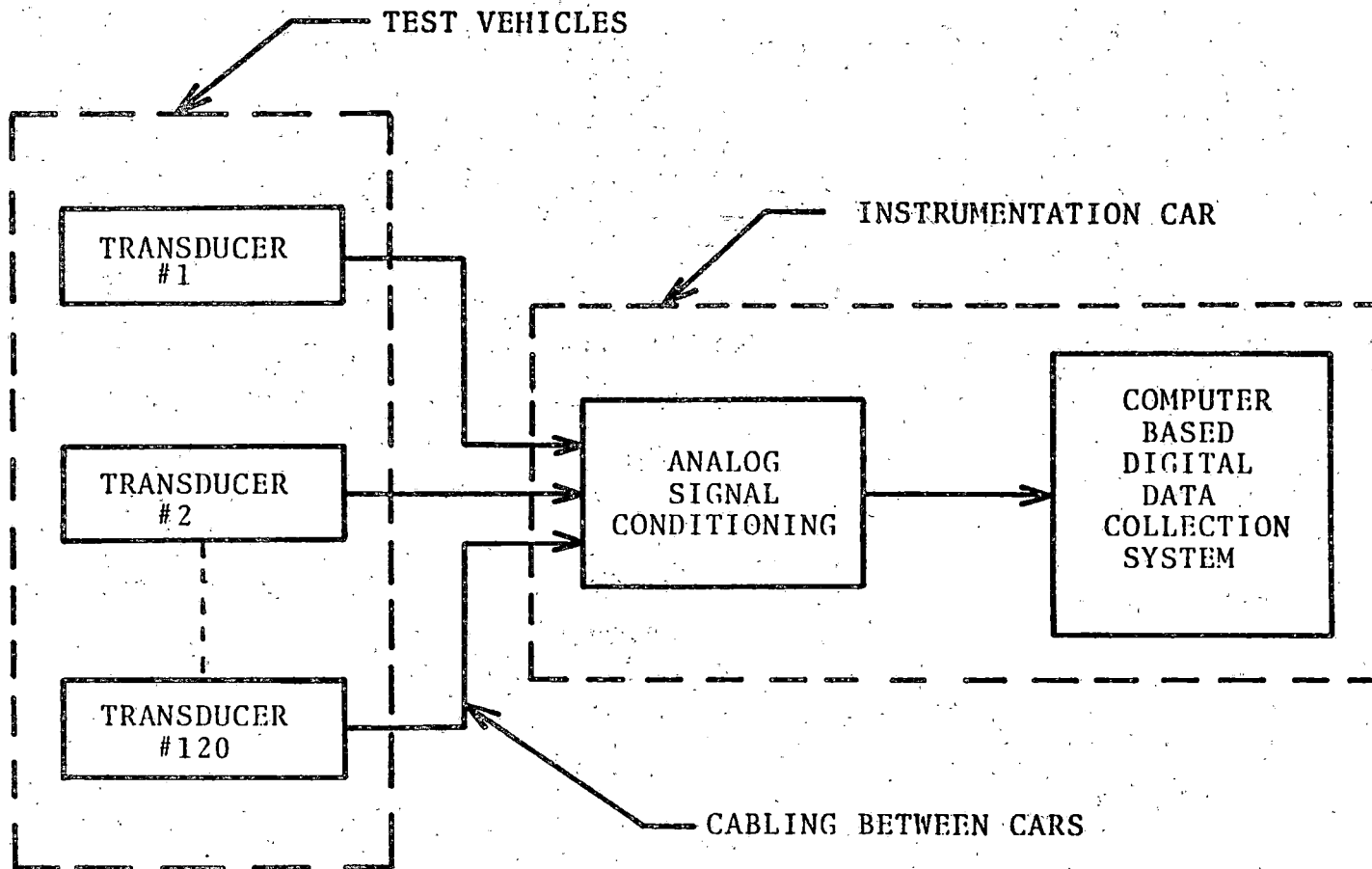
Figure 2-11. Simplified Block Representation of Data Measurement System
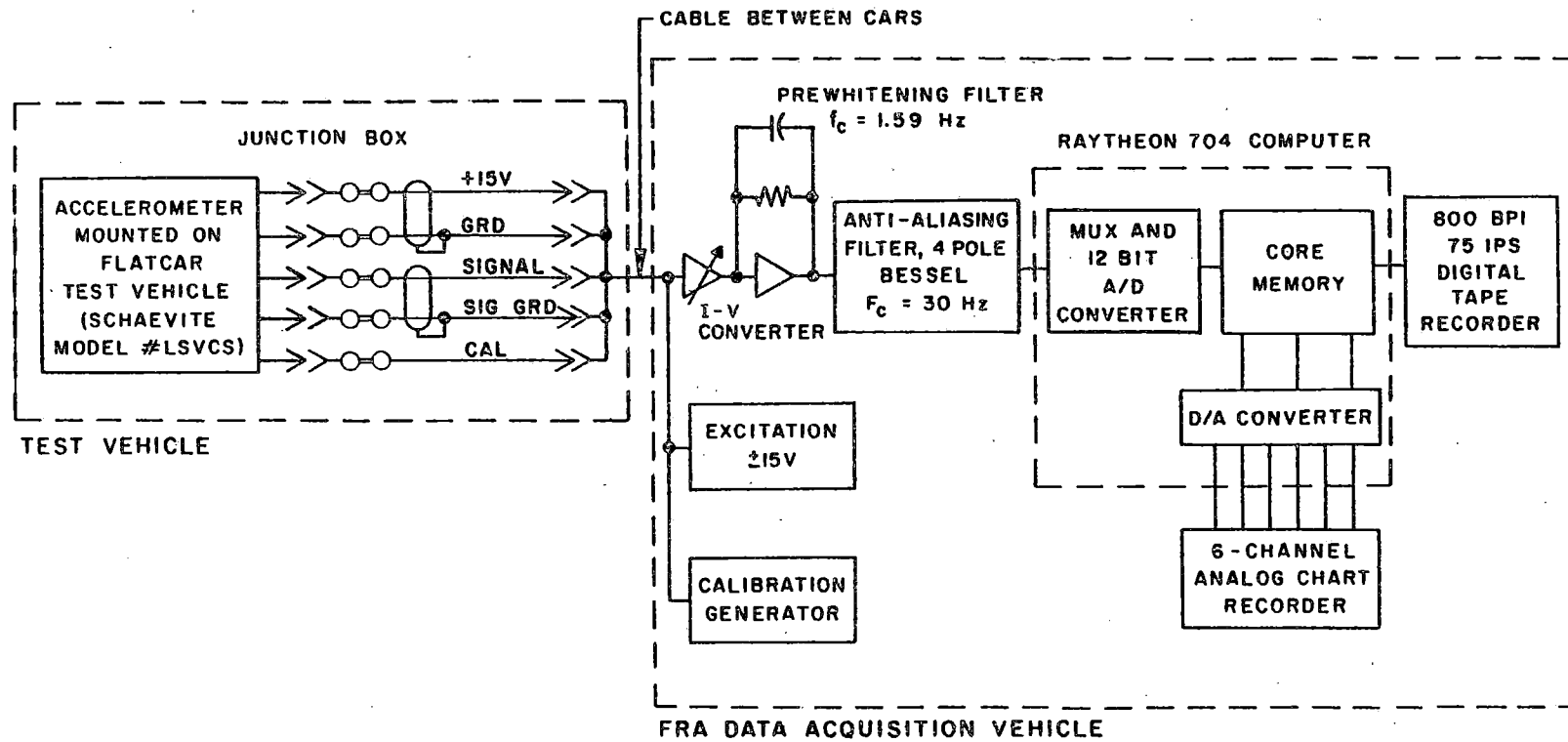
Figure 2-12. Typical Measurement Channel

pairs. At this point, the transducer signal is in the form
of a signal current to eliminate line resistance effects.
The signal current was then converted to a signal voltage
in a current/voltage (I/V) converter onboard T-5.

The output of the current/voltage converter was subjected to
a prewhitening filter which provided a DC gain of 20 but
which attenuated the signals above 1.6 Hz at a rate of 6 dB
per octave. The filter was necessary because acceleration
signals showed an increase with frequency in the range of
interest, from 0 to 30 Hz in spite of the attenuation from
the mechanical isolators. The 6 dB/octave attenuation of
the filter eliminated this increase and resulted in an
amplitude versus frequency response distribution which was
more nearly rectangular, or white. The filter response is
illustrated in Figure 2-13.

The prewhitening filter output drives an antialiasing filter
which insures that digital heterodyning of the signal will
not occur when the signal is digitized. The filter is a
four-pole, low pass, Bessel filter with a cutoff frequency
of 30 Hz. The Bessel filter is used in order to maintain
linear phase shift over the passband to make subsequent
calculations simpler.
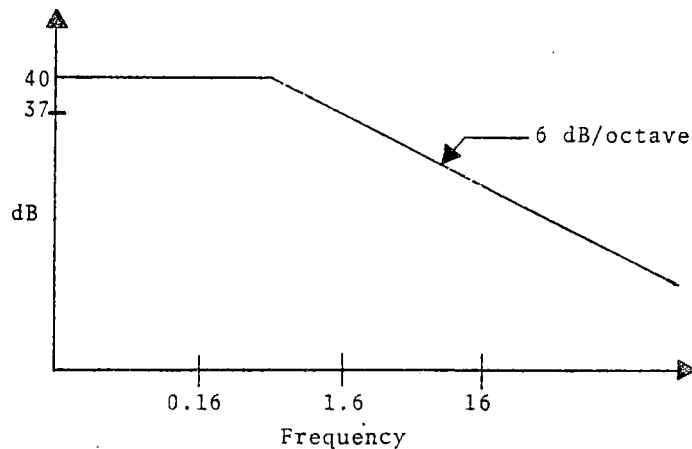
Figure 2-13. Prewhitening Filter Response

The 120 signal inputs are connected to an analog multiplexer which sequentially chooses a channel to be digitized by the 12-bit analog to digital converter. The multiplexer and A/D converter are part of a Raytheon 704 computer which controls the conversion and storage process. After the analog signals are digitized at a rate of 128 times per second per channel, the digital words are stored and formatted in the memory of the computer. The formatted data are then recorded on digital magnetic tape to be processed off-line.

To allow real time monitoring of data channels and to check for computer malfunctions, selected channels of digital data were passed through a digital to analog (D/A) converter and displayed on an analog strip chart recorder, up to six channels at a time. Selection of a given combination of channels was under operator control through the computer.

2.1.5 CALIBRATION PROCEDURES

Prior to installation on the test flatcars, all of the approximately 120 accelerometers used in the test were individually calibrated on a swept frequency shaker table in the Transportation Test Center Metrology Lab. The resulting calibration data were given to ENSCO for individual unit verification and were filed at the TTC Metrology Lab for future reference.

Prior to any testing, each individual accelerometer was calibrated to determine its static scale factor and output polarity, and to verify interconnection wiring between the transducer and data acquisition system. This calibration was performed by measuring the accelerometer output at a rest position and then by rotating it through 180° to impose +1, 0 and -1 g on the accelerometer. The change in output voltage as the accelerometer is rotated at the output of the signal conditioning circuitry divided by a change of 2 g's (+1 g - (-1 g)) produced the scale factor in volts/g for

each accelerometer. Because each accelerometer output was taken in the current mode and the internal impedance varied ±10 percent, the corresponding output of each accelerometer varied accordingly. On the initial test, the gain of each signal conditioner was adjusted to provide a nearly exact scale factor of 3.5 V/g at the A/D input for the 30 g accelerometers and 4.0 V/g for the 5 g accelerometers. A written record of each channel sensitivity was maintained.

Since turnover calibration of the accelerometer requires the removal of the accelerometer from the test vehicle and is quite time consuming, an electrical method of calibration, which can be performed quickly, was devised and performed prior to each test. The calibration method depends on transmitting an accurately known current to the accelerometer force-balance coil from the data acquisition vehicle via the signal cable. The current applies the equivalent of a given acceleration to the accelerometer and causes it to produce an output signal proportional to the simulated acceleration input. Both DC step functions and a sine wave were applied.

The pretest calibration consisted of the following sequence:

1. In close coordination with personnel in the Data Acquisition Vehicle, T-5, a technician located the calibration input terminals of a given accelerometer in the function box on the test vehicle. The technician connected a portable, floated, constant current, 10 Hz source, capable of generating an approximate half-scale signal to the calibration terminals of the accelerometer.

2. Personnel in T-5 connected an analog strip chart recorder to the appropriate channel to record the 10 Hz calibration signal, and verified that the accelerometer was operable and connected to the appropriate channel.

3. Upon completion of Steps 1 and 2, the cali-
    bration technique depicted in Figure 2-14
    was used to automatically inject the following
    series of calibration signals:

a. Zero

b. 10 Hz signal at approximately full-scale

c. Constant signal at positive 1/2-scale

d. Constant signal at positive full-scale

e. Zero

f. 10 Hz signal at approximately full-scale

g. Constant signal at negative 1/2-scale

h. Constant signal at negative full-scale

Note the effects of the low-pass filtering or the steady-state
sinusoid response and the step response. This calibration
sequence was recorded by the digital data acquisition system
for use in post-test data analysis.

2.2 LOADS

The lading for the flatcars consisted of standard intermodal
trailers and containers mounted on the appropriate car as
specified by test plans. The containers and trailers were
either empty or loaded with 2,000 pound bales of paper.

2.2.1 TRAILERS

Four 40-foot Fruehauf Z Vans (Figure 2-15) were obtained
for use in the test sequence. The serial numbers are:
SFTZ 202519, SFTZ 202699, SFTZ 202710 and SFTZ 202751.
All four trailers had been manufactured in August or
September of 1974, and all four were Model No. FBZ9-F2-40.

The trailers were fitted with worn, retread tires of various
manufacture (including Firestone, Goodyear, Uniroyal, OHTSU)
which were inflated to 75-85 psi cold.
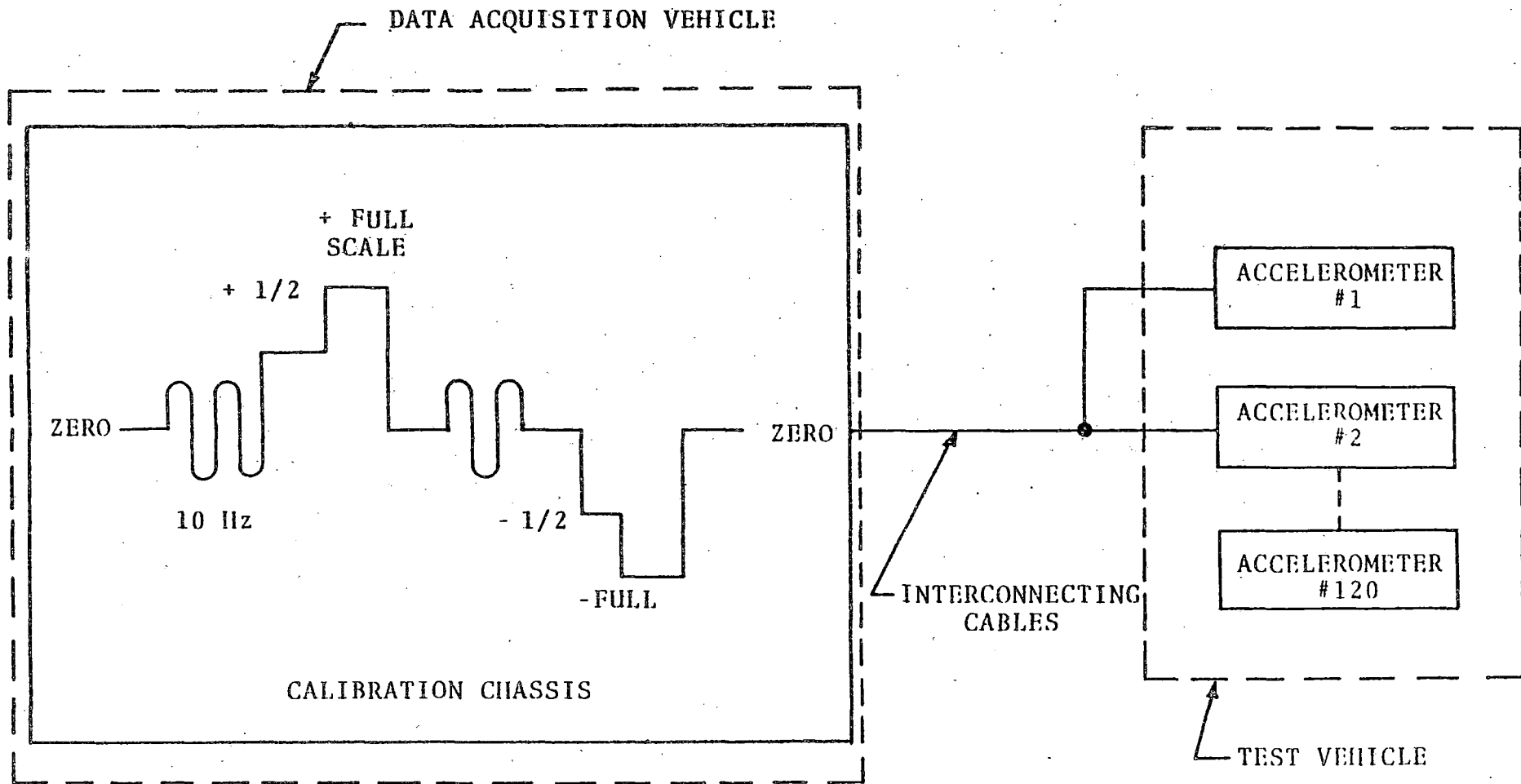
Figure 2-14.   Calibration System
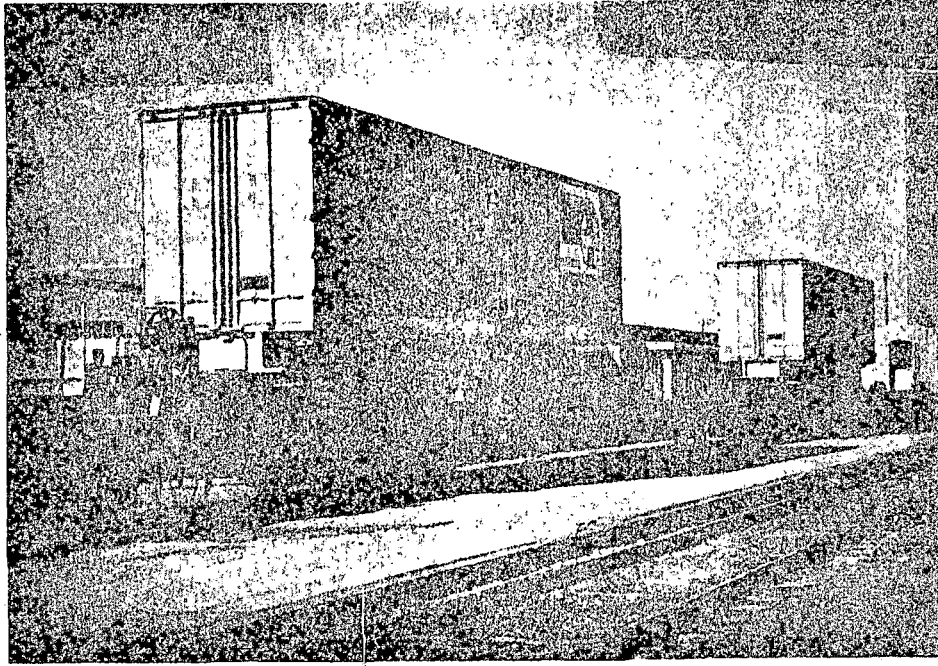
Figure 2.15. Forty-Foot Trailer

Empty trailer weight was 12,400 pounds and when loaded with paper bales, the gross weight was 44,500 pounds. The trailers were rated for a gross weight of 68,000 pounds.

Each trailer has 15 mounting locations, six inches apart, for the bogie (trailer wheel and suspension). For three of the trailers, the bogie was mounted in the fifth position from the rear. For one (SFTZ 202699), the bogie was mounted in the fourth from the front.

2.2.2 CONTAINERS

The containers (Figure 2-16) were Fruehauf Model KAX-40TRA, (Serial Nos. XTRV 871264, 871595, 874756 and 877189) designed for general cargo service. The containers were constructed of a steel frame with aluminum walls and a wooden floor. Each container was 8.5 x 8 x 40 feet, and weighed 6,450 pounds empty. When required for the test, they were loaded with 32,000 pounds of baled paper. The maximum capacity for each container was 64,000 pounds.
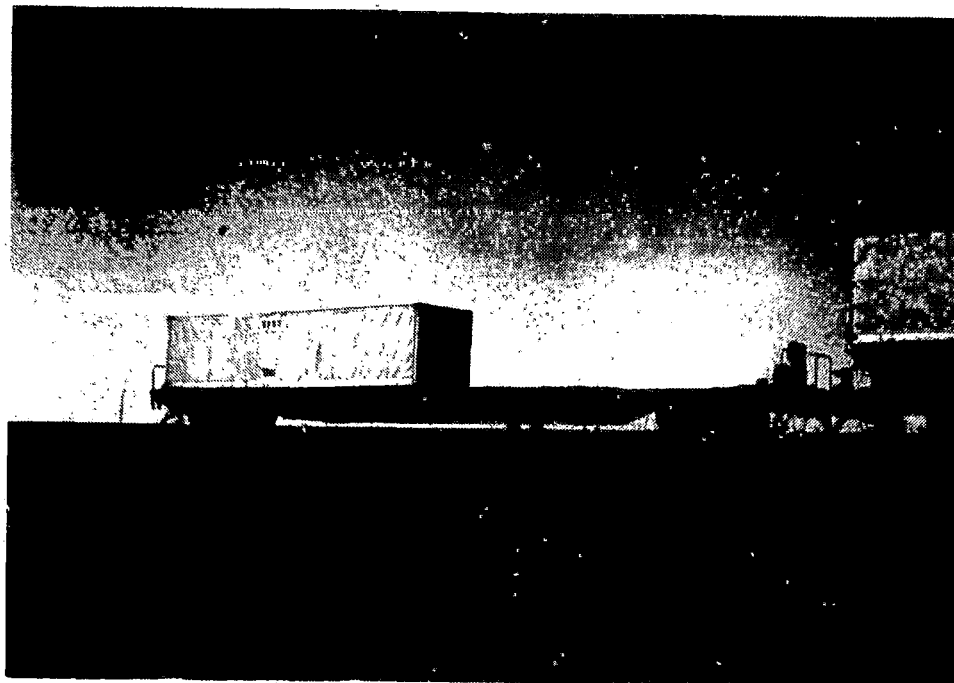
Figure 2.16. Standard 40-Foot Container

2.3 TEST CONSIST

Testing was conducted with a four-car consist comprised of the three instrumented flatcars and the FRA Data Acquisition Vehicle, T-5. Figure 2-17 schematically represents a typical test consist. The test vehicles were operated empty or loaded with trailers or containers as stipulated by the test plan for each test.

2.3.1 FLATCARS

Tests were conducted using three different flatcars; one conventional general purpose flatcar and two lightweight prototype flatcars (shown in Figure 2-18). Accelerations on similar load configurations were found to be comparable for the different types of flatcars.

The conventional flatcar (TTAX 973799) owned and operated by Trailer Train weighs approximately 69,000 pounds including trucks. The car is 90 feet long (over strikers) and 9 feet wide with the deck 2 feet, 5-1/2 inches above the rail. There

are two collapsible kingpin pedestals, one at the car center
and one at the B-end*. The TTAX is capabile of transporting
two trailers, two 40-foot containers, or one of each. The
trucks used in this study were 70-ton American Steel Foundary
(ASF) ride control trucks spaced 66 feet center-to-center.

One lightweight flatcar (TLDX-61) was configured to transport
only trailers and the other (TLDX-62) was configured to trans-
port only containers. These cars weigh approximately 59,000
pounds and 49,000 pounds empty, respectively. The length
over the strikers is 84 feet, the width is 9 feet, and the deck
is 3 feet 5-1/2 inches above the rail. The trucks under these
cars were also the 70-ton ASF ride control trucks spaced 63
feet center-to-center.

2.3.2 DATA ACQUISITION VEHICLE

In order to obtain measurements of the three flatcars' dynamic
performance under both actual operating and controlled condi-
tions, the FRA Data Acquisition Vehicle, T-5, was used to
collect data and provide test support. T-5 is self-contained
for periods of one to two weeks and can support a crew of
four. The support systems are powered by two 50 kW diesel
generators and include, in addition to the data acquisition
system, all necessary amenities such as sleeping quarters,
kitchen facilities and shower. These support systems were
particularly important in the Over-the-Road test series
(Section 2.4.2).

The data acquisition system onboard T-5 is capable of accomo-
dating up to 120 channels of electrical analog signals gen-
erated by any of today's state-of-the-art transducers. The
overall system is comprised of an analog and a digital

---

*The end at which the hand brake is located is referred to
as the B-end. The other end is the A-end. All tests were
performed with the A-end leading.
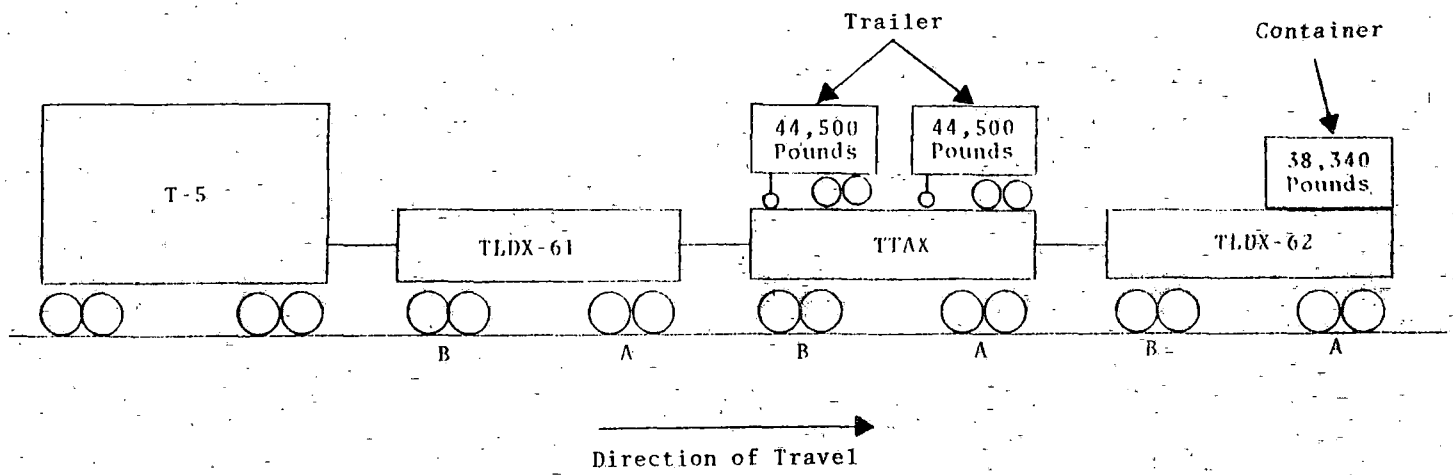
Figure 2.17. Schematic Representation of Typical Test Consist
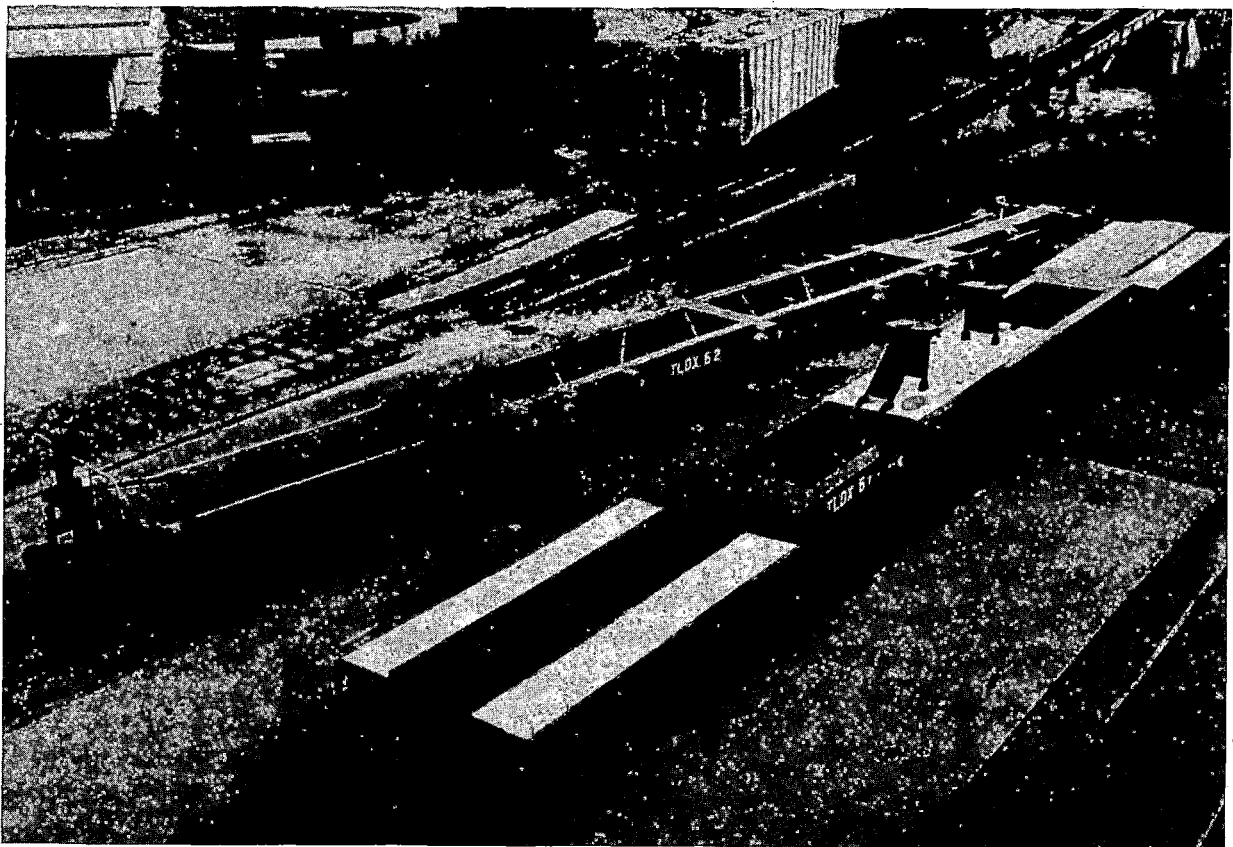
Figure 2.18. Lightweight Flatcar TLDX-61 and TLDX-62

subsystem. The analog signals are input to the analog
subsystem which provides power to the transducers and con-
ditions the incoming signals by filtering, amplifying, etc.
The digital subsystem is centered around and controlled by
a Raytheon 704 Central Processing Unit, a 12 K mini-computer.
The digital subsystem digitizes the data, carries out some
limited processing and records the data on magnetic tape.
In addition, six data channels can be reconverted to analog
format and displayed in real-time on a strip chart recorder.
The computer is also used in off-line processing and is
capable of performing data searches, editing and copying.

2.4 TEST PROCEDURE

The objectives of the test program required two types of
tests to obtain the necessary data: a series of controlled
Ride Vibration Tests (RVT) and a set of in-service Over-the-
Road Tests (OTR). Prior to these tests, safety and functional
checkout tests were run. The test chronology is listed in
Table 2-2.

The RVT series consisted of three tests conducted after a
specified number of miles had been accumulated to provide
data on the effects of wear. The first RVT, carried out at
zero (nominal) miles of service on the flatcars, was designed
both to establish a data base for wear measurements and to
acquire the data necessary for calculation of the mode shape
functions, required for modal analysis, which were assumed
not to change significantly with wear since they are princi-
pally functions of the internal structure configuration.
The second and third RVT's, carried out at 50,000 and 125,000
miles of service, were designed to acquire data on the
effects of wear on the flatcars.

TABLE 2-2

TEST CHRONOLOGY

Test	Dates	Accumulated Mileage
Functional Checkout	May - July 1976	0 (Nominal)
RVT #1	August - September 1976	0 (Nominal)
OTR	December 1976 - February 1977	10,000
RVT #2	September 1977	50,000
RVT #3	November 1978	125,000

The OTR tests were all conducted at approximately 10,000 miles of wear, at the time indicated in Table 2-3. These tests were designed to measure the performance of the test cars under actual revenue service conditions. In contrast to the RVT's, the test consist was connected to the trailing end of a revenue freight train.

2.4.1 RIDE VIBRATION

The three Ride Vibration Tests (RVT) were conducted in a special test train configuration over two test zones on the Atchison, Topeka and Santa Fe (AT&SF) Railroad 13 miles east of La Junta, CO. The general location of these zones is shown in Figures 2-19 and 2-20. The zones represent two different track classes to provide a wider range of data. Each zone was marked by Automatic Location Device (ALD) targets, which were metal strips nailed to ties at pre-determined locations. A magnetic sensor onboard TLDX-61 detected the targets and transmitted a signal to T-5 where the signal was recorded in conjunction with the data.
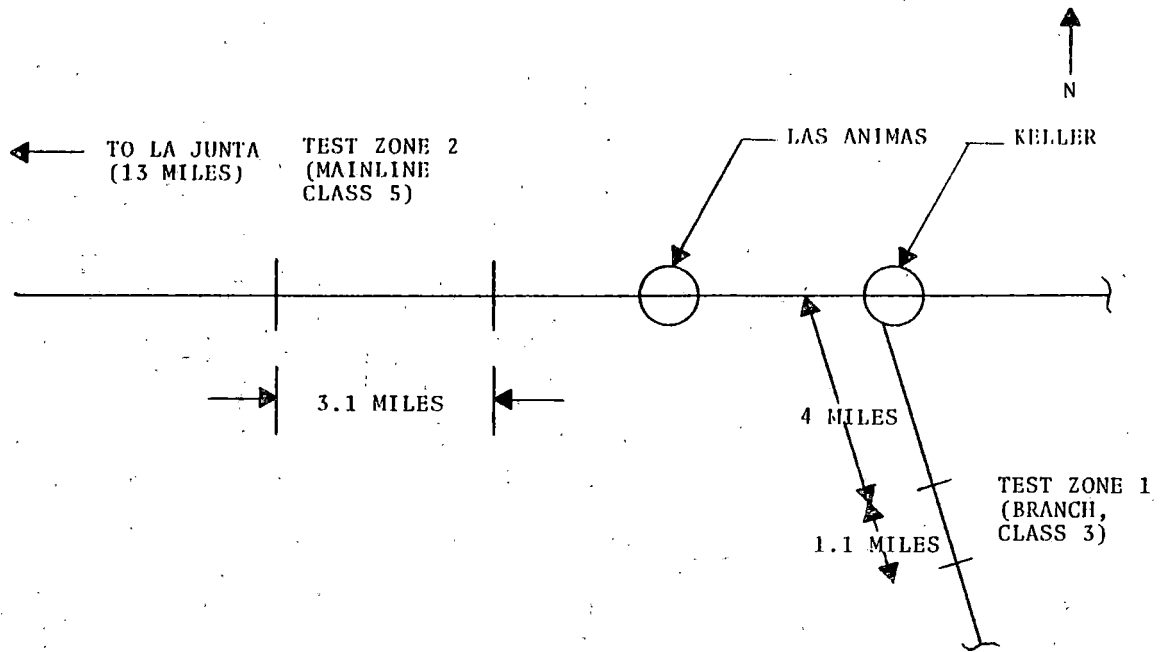
Figure 2-19. General Location of Test Zones
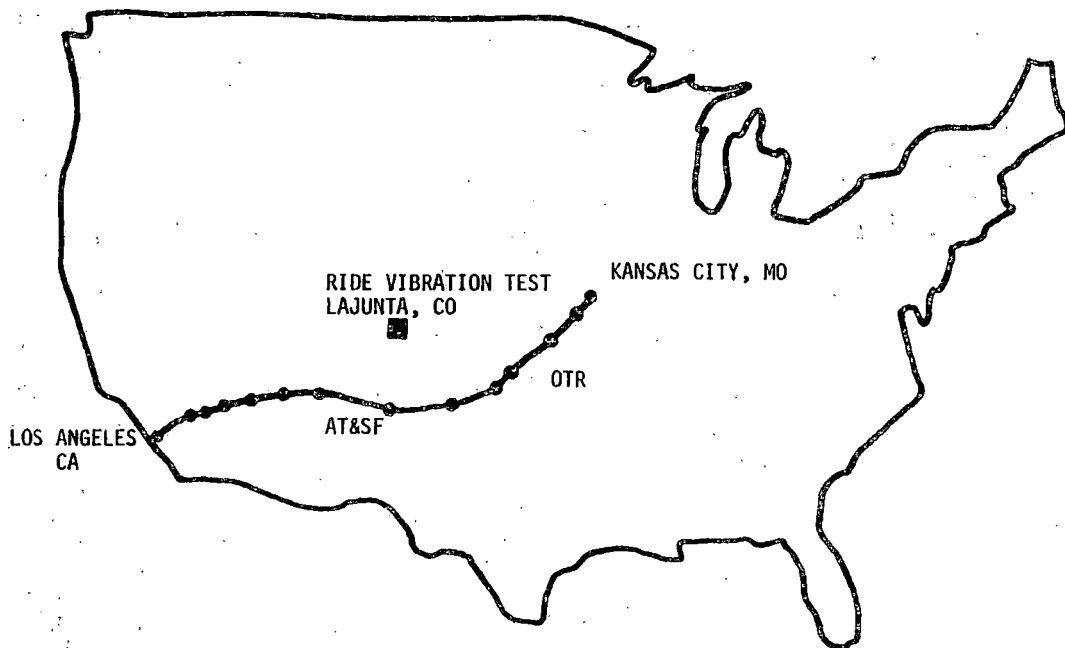
Figure 2-20. Test Zone Locations

Test Zone 1 was in the First District, Colorado Division and consisted of 5,808 feet (1.1 miles) of Class 3 tangent track beginning at Milepost (MP) 234 and extending 528 feet beyond MP 233 south of Keller, CO on the Boise City line (see Figure 2-21). The ALD target locations and mileposts are also indicated in Figure 2-21. This zone was composed of 90 pound rail with bolted joints on wood ties. Between the second and third RVT's, this zone was significantly upgraded* although the Class 3 rating was not changed.

Test Zone 2 consisted of Class 5 tangent track beginning 4,224 feet west of MP 541 and extending to a point 528 feet west of MP 537 on the mainline track in the same district and division as Test Zone 1 (see Figure 2-22). The total length of the test zone was 16,368 feet (3.1 miles). This was mainline track, composed of 119 pound rail with bolted joints on wood ties.

The tests consisted of a series of passes through each zone at different speeds and different load configurations. On the beginning of each day, a calibration and track conditioning run was made, to verify the proper functioning of the ALD system. Calibration also followed each day's test runs.

The test runs through each zone were made over a range of speeds with the maximum speed equal to the legal maximum for that class track. The speed was held constant through the test zone for each target speed. The five target speeds for each zone are listed in Table 2-3.

---

*The subgrade and ballast had been completely reconditioned for welded rail to be laid in the near future. The rail was still bolted at the time of the third RVT but all ties had been replaced and spiked. The joints appeared to have been redone as well.

MP 234 — ALD-1 BEGINNING TEST ZONE #1

528'

ALD-2

5,808'

528'

ALD-3

N

MP 233

— MILEPOST

— ALD TARGET NAILED TO TIES

528'

ALD-11 END TEST ZONE #1

Figure 2-21. Test Zone 1

MP 54I

4224'

ALD-1 BEGIN TEST ZONE
        #2

N

528'

528'

16,368'

MP 540

ALD-31 END TEST ZONE
         # 2

528'

MP 537

a — MILEPOST

⊏▭⊐ —ALD TARGET
      NAILED TO TIES
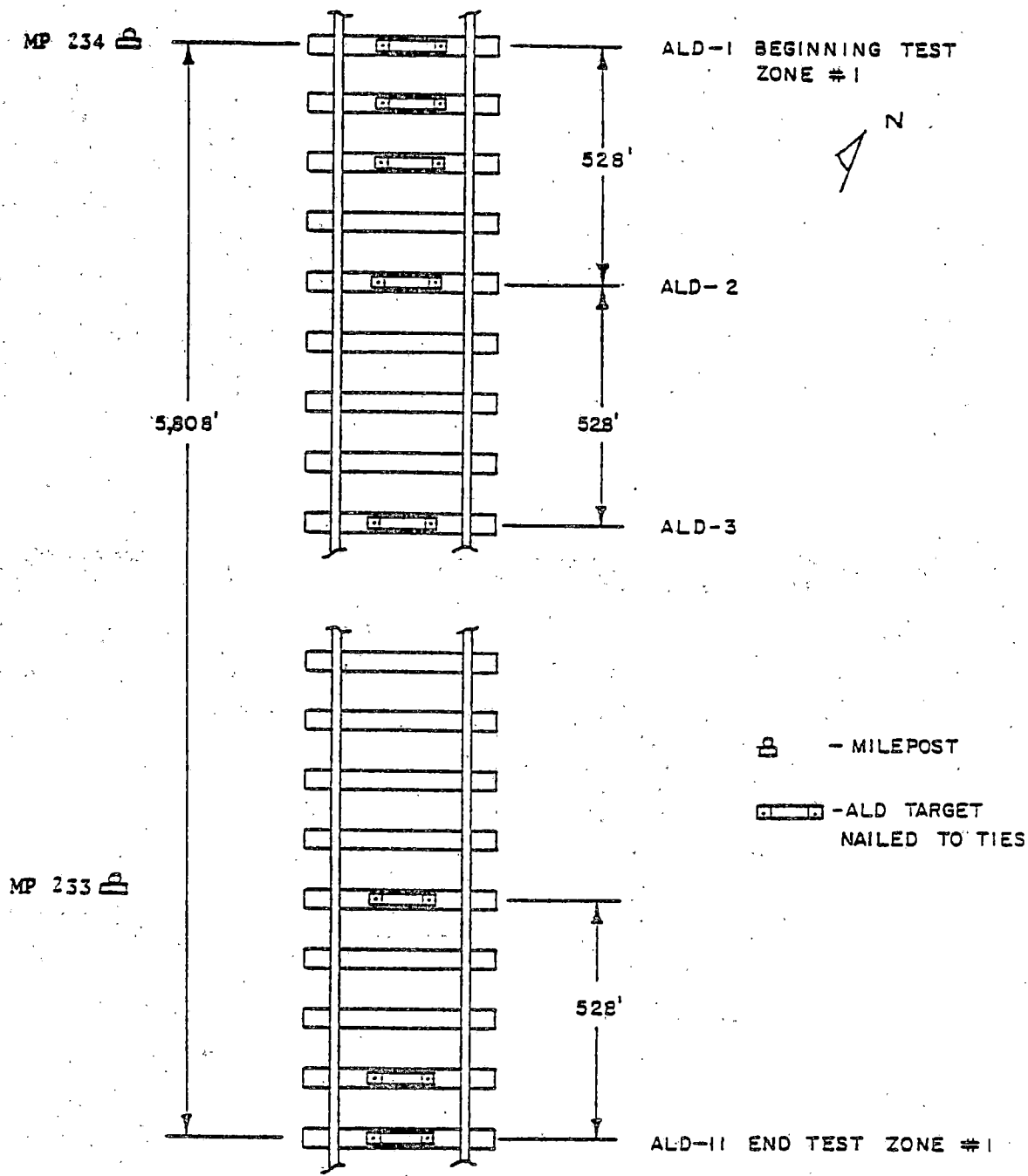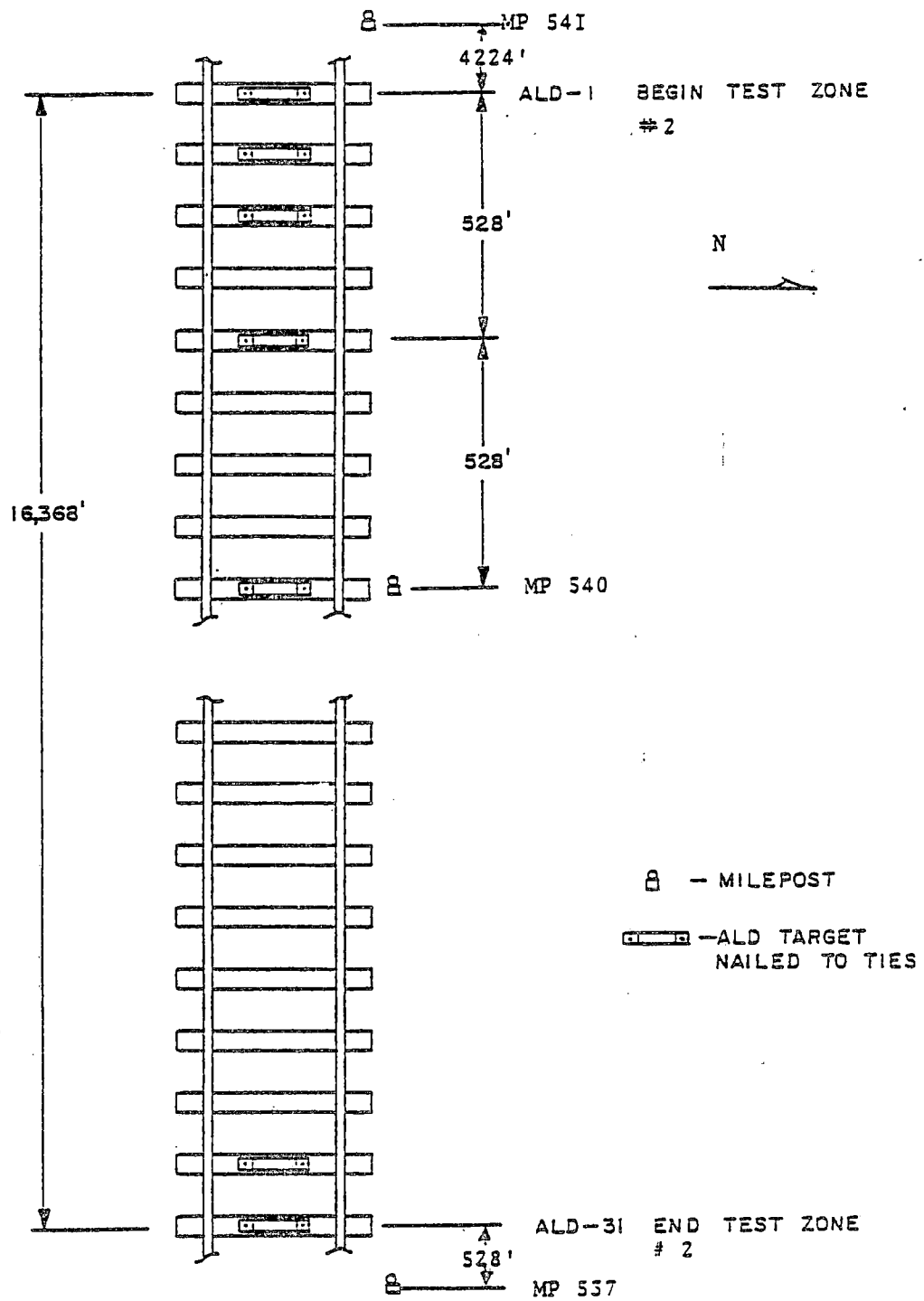
Figure 2-22. Test Zone 2

The load configurations for the flatcars included two, one and no containers or trailers mounted on the flatcars, in various combinations. Five configurations covering a full range of possibilities were used for the first RVT. These are illustrated in Figure 2-23 a through e. Following analysis of the data from the first RVT, only one configuration was chosen to be used for the rest of the RVT tests; because, except for empty flatcars which are not of interest, the most severe vibrations were observed for the load configurations listed in Table 2-4. More extensive data on the various configurations were obtained from the OTR tests (Sections 2.4.2) which were conducted between the first and second RVT's.

Following the first RVT, instrumentation was removed from the A axles. The axle instrumentation configuration for the second and third RVT's is listed in Table 2-5.

The instrumentation was reduced based on the evident redundancy of axle behavior simplifying the subsequent tests and eliminating unnecessary data.

TABLE 2-3

TEST SPEEDS

Test Zone	Target Speeds (mph)
1	10, 15, 20, 30, 40
2	40, 50, 60, 70, 79
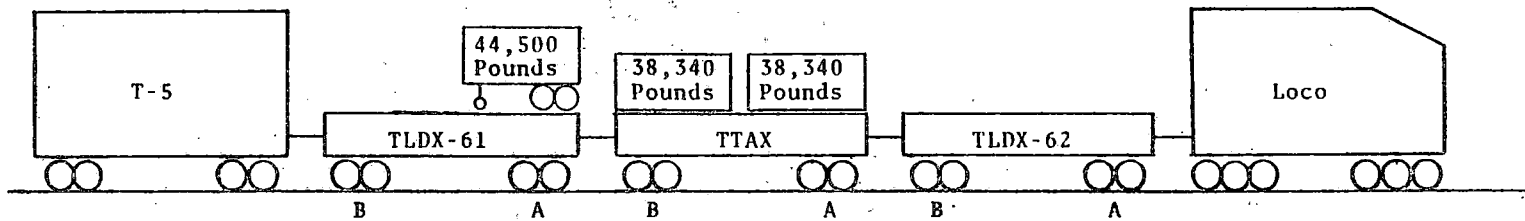
(a)   Test #LWFC-1, 21 August 1976
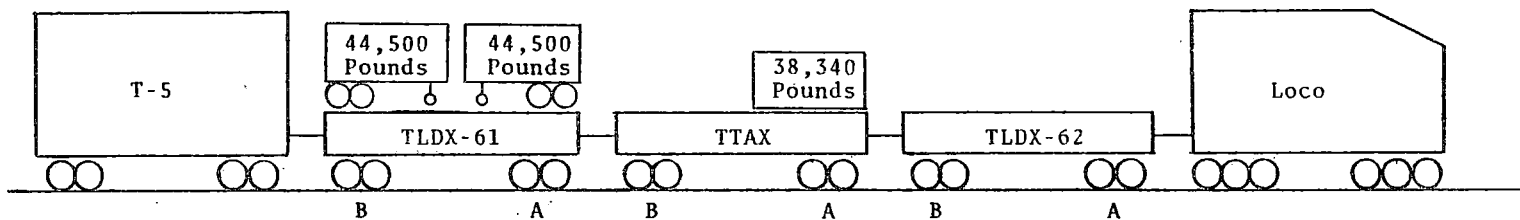
(b)   Test #LWFC-2, 19 August 1976
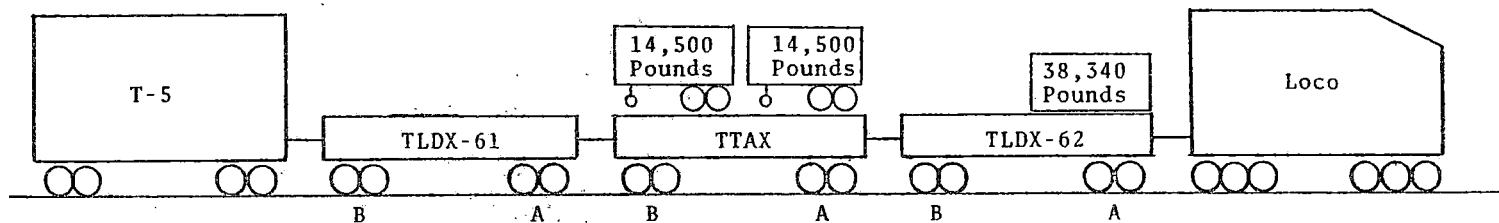
(c)   Test #LWFC-3, 23 August 1976

Figure 2-23.   Five Configurations for the First RVT
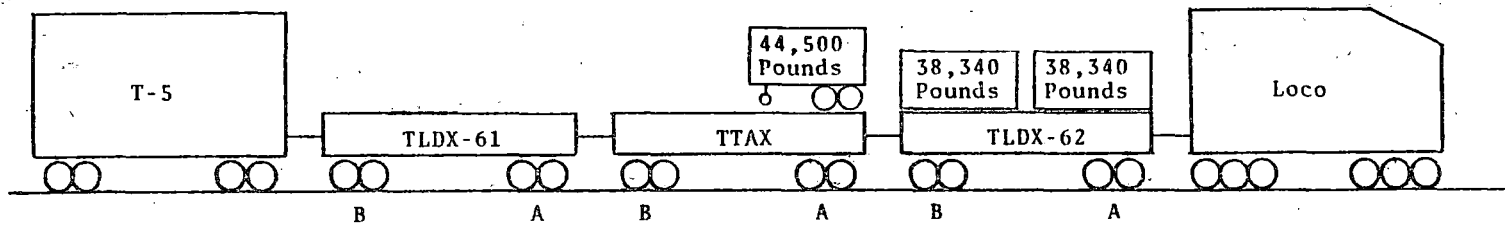
(d) Test #LWFC-4, 26 August 1976
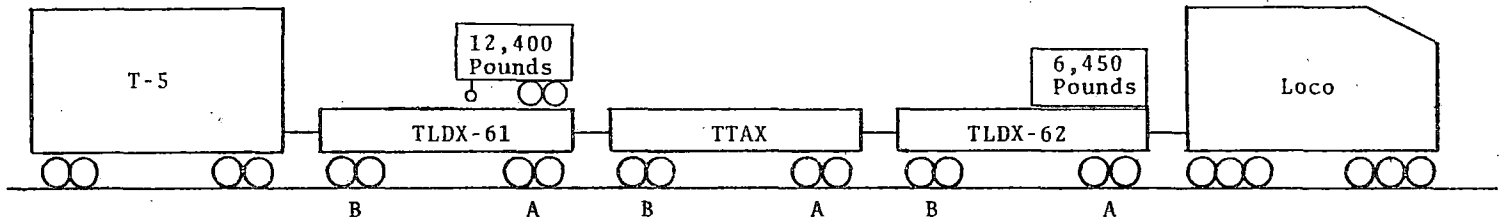
(e) Test #LWFC-5, 27 March 1976

Figure 2-23. Five Configurations for the First RVT
(Continued)

TABLE 2-4

FINAL TEST CONFIGURATION

Flatcar	Load
TLDX-61	1 Loaded Trailer
TTAX	1 Loaded Trailer
TLDX-62	1 Loaded Container

TABLE 2-5

INSTRUMENTED AXLES

Car	Instrumented Axles
TLDX-61	AA and B
TTAX	AA and B
TLDX-62	AA and BB

AA   A   B   BB
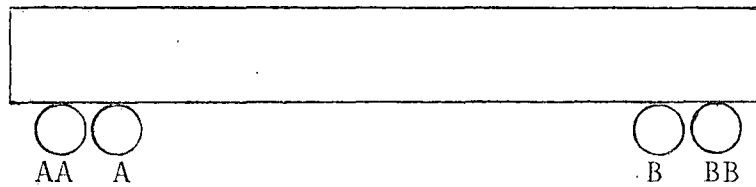
2.4.2 OVER-THE-ROAD TESTS

The in-service or OTR tests were designed to measure the vibrational environment of containers and trailers under typical revenue service conditions. The load configurations for the OTR tests were similar to those of the first RVT, covering a wide range of possibilities. The structure of the consist and the load combinations used are outlined in Table 2-6. The sequence in which the tests were conducted is shown in Table 2-7.

The first test started in Los Angeles, CA and proceeded to Kansas City, KS. At Kansas City, the load configuration was changed and a system calibration which served as a post-test calibration for the first test and a pre-test calibration for the second test was performed. The calibration included mechanical and electrical checks using a shaker table. The second configuration was tested on the return trip from Kansas City to Los Angeles; the remaining tests followed this pattern and required a total of three round trips.

Twelve test zones were selected on the AT&SF route between Los Angeles and Kansas City to represent a full range of track conditions. These zones and a description of the zone location and track conditions are listed in Table 2-8.

The data were acquired while the test cars were coupled to the trailing end of a revenue freight train and hauled through the test zones. Zone identification was based on visual observation of milepost signs. In addition, no control of the train speed or handling was possible or desired.

TABLE 2-6

LOAD COMBINATIONS

| AT&SF Train | TLDX-62 | TTAX 799 | TLDX-61 | T-5 | Cab |

A   B A   B A   B
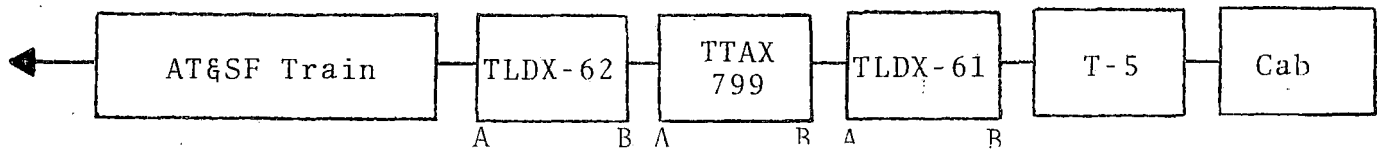
Configurations	Instrumented Cars/Loads		
	TLDX-62	TTAX-799	TLDX-61
LWFC-6		1LT	1LT
LWFC-7	1LC	1LC	
LWFC-8	2LC	2LC	
LWFC-9		2LT	2LT
LWFC-10		1ET	1ET
LWFC-11	1EC	1EC	

Notes: LT = Loaded trailer
        ET = Empty trailer
        LC = Loaded container
        EC = Empty container

With only one container/trailer, the load was on the A-end.

TABLE 2-7

CHRONOLOGY OF TESTS

Dates	Route	Configuration
16-18 December 1976	LA-KC	LWFC-6
21-23 December 1976	KC-LA	LWFC-7
23-25 January 1977	KC-LA	LWFC-8
1-3 February 1977	LA-KC	LWFC-10
6-8 February 1977	KC-LA	LWFC-9
12-14 February 1977	LA-KC	LWFC-11

TABLE 2-8

SPECIAL TEST ZONES

Division	MP	Location	Grade	Curvature	Rail	Remarks
1. Los Angeles	735-725	Newberry	.4% Westbound	Tangent	Welded	Double
2. Los Angeles	716-706	Pisgah	1% Eastbound	Two 2° Several Smaller	Welded	Double
3. Los Angeles	656-646	Cadiz	Changes from .4% Westbound to .7% Eastbound	Mostly Tangent	Welded	Concrete Ties 651-650 Double
4. Albuquerque	527-517	Harris	1.42% Eastbound	Numerous to 6°	Welded	Double
5. Albuquerque	412-402	Eagle Nest	Changes from 1° Westbound to 1% Eastbound	Several Long 1°	Welded	Double
6. Albuquerque	231-221	Pinta	To .6% Eastbound	Few Short 1°	North Jointed and South Welded	Double
7. New Mexico	888-878	Becker	To 1.2% East-bound	One 1°	Welded	Single
8. Plains	620-610	Black	Relatively Flat	Tangent	Welded	Single
9. Plains	408-398	Fargo	Relatively Flat	Tangent	Welded	Single
10. Plains	320-310	Loder	Relatively Flat	Tangent	Welded	Single
11. Middle	168-158	Aikman	.4% Eastbound	Mostly Tangent	Welded	Single
12. Eastern	25-15	Craig	.6% Westbound	Numerous 2°	Welded 15-20 Jointed 20-25	Double

3.0 DATA REDUCTION

The acceleration data were processed off-line to present the
results in a form and format that would fulfill the program
objectives. The processing consisted of three basic procedures.
First, the raw data were inspected to insure the validity of
the measurements. Second, in a separate data stream, the
linear accelerations were transformed into a set of global
accelerations which describe the motion as a whole. These
are referred to as mode accelerations. The theory and prac-
tical aspects of this analytical technique are described in
detail in Volume I of this report (Reference 1). The third
step is the presentation of the mode acceleration time
histories in an output format which can be readily interpreted.

3.1 DATA PREPARATION AND VALIDATION

Prior to data processing, the raw data were inspected to
verify that the data were apparently valid measurements of
railcar dynamic behavior. In addition, preliminary data
processing transformed the data to the format necessary for
the analytical processing system. In order of occurrance,
the data were:

- Transformed from a packed format to a
  16-bit word length and converted to
  floating point.

- Scaled to dimensional units with the
  mean value or bias removed.

- Reproduced as analog plots and vali-
  dated by visual examination.

3.1.1 TAPE FORMAT AND UNPACKING

The acceleration data collected by the T-5 Data Acquisition
Vehicle were recorded in digital form on magnetic tape. Each
tape contained one or more data files which contained the data
collected from one pass through one test zone. Each data file
consisted of a header and a number of data records correspond-
ing to the length of the test zone and the sample rate of the
120 data channels containing the digitized acceleration data
for a particular test zone.

The data file header consisted of 85 sixteen-bit words. These
words contained the:

- File number
- Tape number
- Number of channels
- Sample rate
- Number of scans per record
- Date
- Consist configuration
- Run number
- Additional general information which
  may have been added at the time of
  the test.

The data records contained 2,973 sixteen-bit words. The
data were digitized in twelve bits, and, to increase real-
time processing efficiency, the data were recorded on the
tape as illustrated in Figure 3-1. The twelve bits of the
first datum were recorded in the first twelve bits of the
first word. The second datum was recorded beginning with
the last four bits of the first word and continuing into
the first eight bits of the second word. In this manner,
it was possible to record exactly four data values in three
words on the tape.

4 Bits	4 Bits	4 Bits	4 Bits
1	1	1	2
2	2	3	3
3	4	4	4
5	5	5	6
6	6	-	-
-	n	n	n

Figure 3-1. Sample Data Records

3.1.2 REMOVAL OF MEAN AND SCALING

Data from each accelerometer were individually averaged on a record-by-record basis. The mean value for each record was then subtracted from each data sample in that record, and the resulting data were recorded for further processing. This procedure resulted in a slight discontinuity between adjacent records, but the difference was normally negligible.

The data were scaled on the basis of calibration information obtained at the time of the tests, and in effect, the data were converted from voltage measurements to engineering units.

3.1.3 ANALOG REPRODUCTION AND VALIDATION

The data were analog reproduced in strip chart format for visual correlation and comparison with the strip charts produced during the tests. A principal objective of this step was the subjective determination that the data were valid representations of the tests. An example of the analog reproductions is illustrated in Figure 3-2.

CHANNEL DEFINITION

CHANNEL NUMBER		DESCRIPTION	ENGINEERING UNITS PER COUNT	CHANNEL RANGE	UNITS PER MINOR DIVISION
1 - 34	TTAX TRUCK LATERAL - AA END		0.0013950	0.30	0.040
2 - 26	TTAX TRUCK LATERAL / A END		0.0013350	0.30	0.040
3 - 29	TTAX TRUCK LATERAL - B END		0.0013950	0.30	0.040
4 - 4	TLDX61 TRUCK LATERAL - AA END		0.0013950	0.30	0.040
5 - 76	TLDX61 TRUCK LATERAL - A END		0.0013950	0.30	0.040
6 -109	TLDX61 TRUCK LATERAL - B END		0.0027900	0.30	0.040

FILE 03 TAPE 22 NC= 0124 SP= 0128 NS= 003089 JULY 76 LWFC REALCO RUN

TAPE 22 - FILE 3 - TRUCK LATERALS
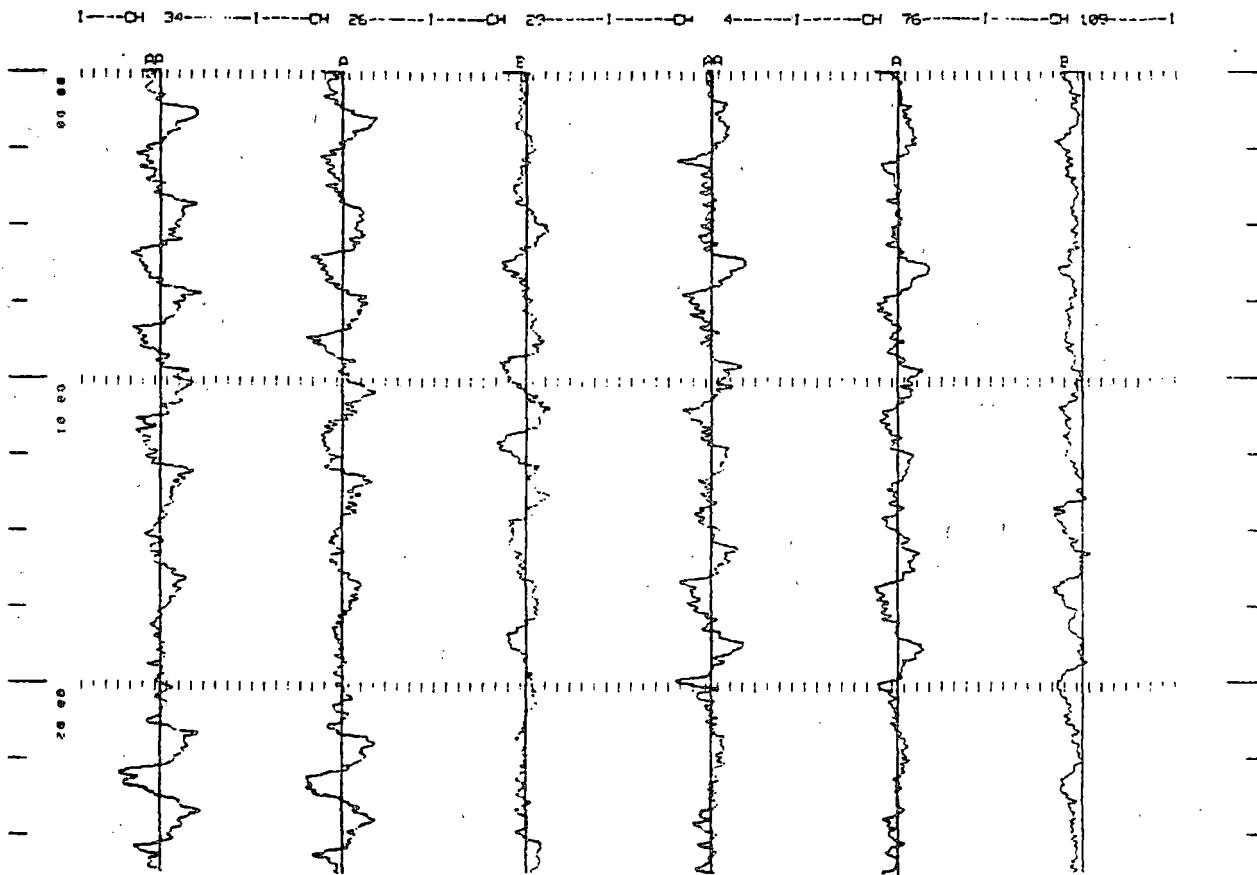
Figure 3-2. Sample Analog Printout

3.2 MODAL TRANSFORMATION

The evaluation of the complex vibrational environment of a railcar requires a large number of measurements to obtain a comprehensive picture. The vast amount of such data can cloud the true picture, and for analytical purposes, it is better to combine the measurements in some rational manner to obtain a representation which is easier to visualize. For this reason, the data from the lightweight flatcar test program were transformed from local acceleration values to components of vibrational modes. That is, the dynamic behavior of a railcar was represented in terms of free-body modal components.

The modal components are composed of a set of mode shape functions each describing a rigid or elastic mode and a set of time dependent modal amplitudes describing the motion of the test vehicles in terms of the mode shape functions. The general problem was to solve for the modal components, given a set of local acceleration measurements. An abbreviated description of this transformation follows; a complete description is available in Volume I of this report.

The modal components consisted of six rigid body modes and as many as four elastic body modes. The rigid motions, illustrated in Figure 3-3, include translation along each of the three axes and rotation about each of the three axes. The elastic modes, shown in Figure 3-4, include two bending modes and two torsional modes.

Each elastic mode shape was approximated by a truncated series or polynomial. These polynomials are listed in Table 3-1. The subscripted coefficients are referred to as the mode shape coefficients. They embody the elastic characteristics of the flatcars and, theoretically are constant for varying test parameters.

3-5
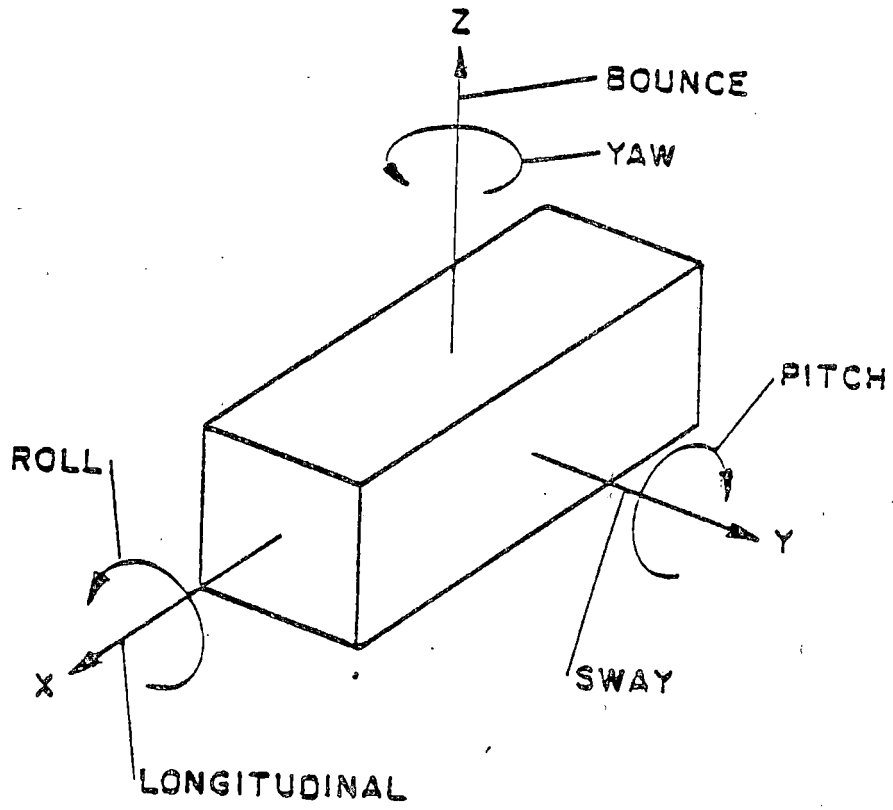
Figure 3-3. Rigid Body Modes
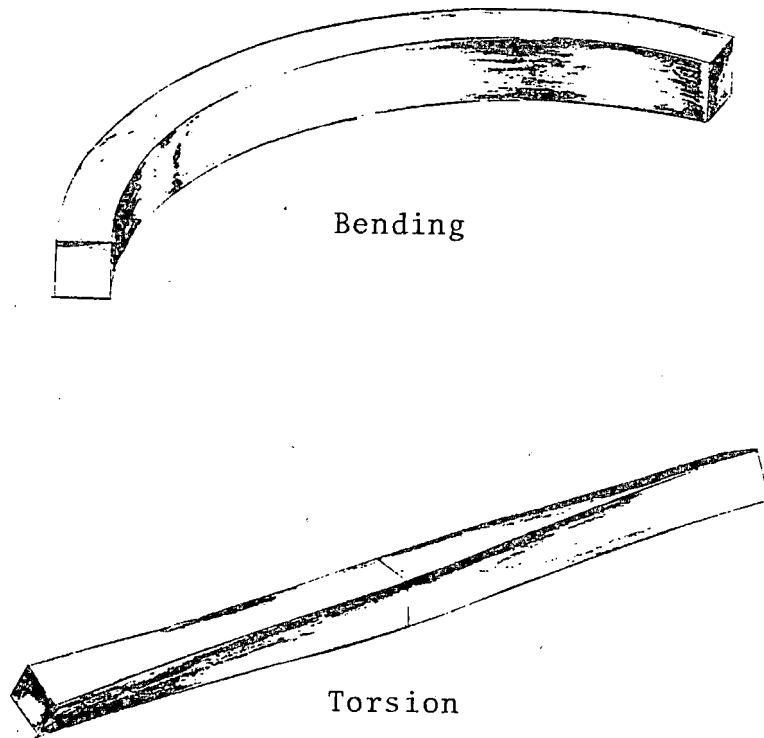
Bending

Torsion

Figure 3-4. Elastic Body Modes

TABLE 3-1

ELASTIC MODE POLYNOMIALS

Mode	Equation
First Bending	$B_{yz1}(x) = 1 + b_2 x^2 + b_4 x^4$
Second Bending	$B_{yz2}(x) = x + b_3 x^3$
First Torsion	$T_{x1}(x) = x + c_3 x^3$
Second Torsion	$T_{x2}(x) = 1 + c_2 x^2$

Four elastic modes were used to model the flatcar dynamic response. For the loads and the axles, only a limited number of modes were expected to contribute significantly to linear acceleration. The modes selected for each case are listed in Table 3-2. Because the carbody displays the greatest dynamic complexity, the equations developed henceforth will be in reference to the carbody.

TABLE 3-2

ELASTIC MODES FOR EACH CASE

Case	Mode
Carbody	First bending about the y-axis Second bending about the y-axis First torsion about the x-axis Second torsion about the x-axis
Loads	First bending about the z-axis
Axle	None

The overall dynamic behavior of the carbody can be expressed as the sum of the rigid and elastic mode contributions. The elastic contributions are the product of the mode shape functions and time-dependent modal amplitude coefficients. The equations for carbody accelerations are

$$\ddot{x}(y,z,t) = \ddot{x}_o(t) + \ddot{\phi}_o(t)z - \ddot{\psi}_o(t)y \tag{1}$$

$$\ddot{y}(x,z,t) = \ddot{y}_o(t) - \ddot{\theta}_o(t)z + \ddot{\psi}_o(t)x \tag{2}$$

$$- \tau_{x1}(t)(x + c_3x^3) - \tau_{x2}(t)(1 + c_2x^2)$$

$$\ddot{z}(x,y,t) = \ddot{z}_o(t) + \ddot{\theta}_o(t)y - \ddot{\phi}_o(t)x \tag{3}$$

$$+ \beta_{yz1}(t)(1 + b_2x^2 + b_4x^4)$$

$$+ \beta_{yz2}(t)(x + b_3x^3) + \tau_{x1}(t)(x + c_3x^3)y$$

$$+ \tau_{x2}(t)(1 + c_2x^2)y$$

where $\ddot{x}$, $\ddot{y}$, and $\ddot{z}$ represent the modeled accelerations, $\ddot{x}_o$, $\ddot{y}_o$ and $\ddot{z}_o$ represent translational model accelerations, and $\ddot{\theta}_o$, $\ddot{\phi}_o$ and $\ddot{\psi}_o$ represent rotational model accelerations about the x, y and z axes, respectively. The functions $\beta_i(t)$ and $\tau_i(t)$ represent the amplitudes of the elastic modal coordinates.

Each equation represents a presupposed form of a linear acceleration which can be rewritten collecting terms with like powers of x, y and z. Resulting in a set of equations which are multivariate polynomials. For example, rewriting Equation (3) results in the following expression:

$$\ddot{z}(x,y,t) = A_0(t) + A_1(t)x + A_2(t)x^2 + A_3(t)x^3$$

$$+ A_4(t)x^4 + A_5(t)xy + A_6(t)x^2y$$

$$+ A_7(t)x^3y + A_8(t)y \tag{4}$$

in which $A_0(t) \equiv \ddot{z}_0(t) + \beta_{yz1}(t)$

$$A_1(t) \equiv \beta_{yz2}(t) - \ddot{\phi}_0(t)$$

$$A_2(t) \equiv \beta_{yz1}(t)b_2$$

$$A_3(t) \equiv \beta_{yz2}(t)b_3$$

$$A_4(t) \equiv \beta_{yz1}(t)b_4$$

$$A_5(t) \equiv \tau_{y1}(t)$$

$$A_6(t) \equiv \tau_{x2}(t)c_2$$

$$A_7(t) \equiv \tau_{x1}(t)c_3$$

$$A_8(t) \equiv \ddot{\theta}_0(t) + \tau_{x2}(t) .$$

A unique equation of the form of Equation (4) can be derived
for each measured acceleration. In order to determine the
values of the mode accelerations, a number of measurements
must be made to produce a sufficiently large set of equations.
As discussed in Reference 1, the modal analysis technique
relies on a redundant set of measurements to determine, in
a statistical sense, the best set of modes necessary to
completely model the dynamic behavior of an elastic body.

Briefly, the solution may be outlined as follows. The set of equations resulting from N number of measurements, written in matrix form as

$$\{Z\} = [X]\{A\}, \tag{5}$$

where the Z-vector, $\{Z\}$, is the set of measured accelerations, the X-matrix, $[X]$, is the transducer location matrix (note that elements of the X-matrix are in general sums of $x_i^n x_j^m$), and the A-vector, $\{A\}$, is the vector of A coefficients such as those defined in Equation (4). The X-matrix is general rectangular; therefore, it is necessary to first multiply by the transpose of the X-matrix denoted $[X]^T$.

$$[X]^T\{Z\} = [X]^T[X]\{A\} \tag{6}$$

Letting $\quad [Q] \equiv [X]^T[X],$

where by definition Q is a square matrix and where the inverse, $[Q]^{-1}$, exists as long as the determinant $|Q|$ is non zero, Equation (6) becomes

$$[Q]\{A\} = [X]^T\{Z\} \tag{7}$$

Thus, $\quad \{A\} = [Q]^{-1}[X]^T\{Z\}$. $\tag{8}$

Defining $\quad [H] \equiv [Q]^{-1}[X]^T,$

$$\{A\} = [H]\{Z\} . \tag{9}$$

Thus, the H-matrix, which consists of known transducer locations, transforms the set of measured linear accelerations, the Z-vector, to mode accelerations or combinations of the same*. For example, A_o, as defined in Equation (4) is the sum of bounce, $\ddot{z}_o$, and bending, β_{yz1}.

---

*Before the transformation was made, the data were first inverse filtered to remove the effects of the dynamic filter (1.6 Hz) discussed in Section 2.1.4.

When a component of the Λ-vector is defined by a combination of mode accelerations, the Λ-component must be uncoupled to provide information on each mode acceleration. To uncouple the rigid and elastic components, equations must be derived from the conditions of vehicle dynamic equilibrium. That is, the rigid body inertial forces must balance the externally applied forces and moments, and the net forces and moments associated with elastic deformations must equal zero. The resulting equations are:

$$\ddot{z}_0(t) = A_0(t) + \frac{M_1}{M_0} A_2(t) + \frac{M_2}{M_0} \dot{A}_4(t) \tag{10}$$

$$\ddot{\phi}_0(t) = A_1(t) - \frac{M_2}{M_1} A_3(t) \tag{11}$$

$$\ddot{\theta}_0(t) = A_8(t) + \frac{H_1}{H_0} A_6(t) \tag{12}$$

$$\text{where} \qquad M_n \equiv \int_{-L/2}^{L/2} x^{2n} \rho(x) dx \qquad n = 0,1,2 \tag{13}$$

$$H_s \equiv \int_{-L/2}^{L/2} x^s J(x) dx \qquad s = 0,1 \tag{14}$$

A_i is a multivariate polynomial coefficient, $J(x)$ and $\rho(x)$ represent the polar moment of matrix distribution and the mass distribution, respectively, for the mass component in question, and L is the total length of the vehicle in the direction being considered.

Furthermore, from the definitions of the multivariate poly-
nomial coefficients, expressions for the mode shape coeffi-
cients are derived. The expression for the mode shape
coefficient is a ratio of power and cross spectral densities,
i.e.,

$$a_i = \frac{G_{A_i \alpha_i}}{G_{\alpha_i \alpha_i}} \qquad (13)$$

where a_i is a mode shape coefficient, A_i is the multivariate
polynomial coefficient in question, α_i is the associated
modal coordinate (β or τ), $G_{A_i \alpha_i}$ is the cross spectral
density (CSD) and $G_{\alpha_i \alpha_i}$ is the power spectral density (PSD).

Once the mode shape functions and modal amplitudes are known,
a straight forward calculation of the theoretical or modeled
local accelerations can be made using Equations (1) through
(3). The resulting local accelerations can then be compared
with the measured accelerations to obtain an estimate of the
accuracy of the modal representation.

3.3 OUTPUT FORMATS

The transformation of linear acceleration to modal accelera-
tion is a transformation of one set of time series to another.
Although modal accelerations are readily visualized, it is
necessary to summarize each time series in a form that is
also readily understood. For this purpose, three data output
formats were chosen. In the frequency domain, the power
spectral density (PSD) was used; in the time domain, the
probability density function was used; and as a hybrid
output, an octave root mean square history was used pro-
viding some time and frequency domain information simultaneously.

3.3.1 POWER SPECTRAL DENSITIES

PSD's are a conversion of data from the time domain to the frequency domain. Time domain data are based on measurements taken at a 128 Hz sample rate. The data are processed in blocks of 512 samples, representing a four-second time interval. Each block is Fourier Transformed, and the PSD is then calculated from the Fourier Transform and its complex conjugate. This PSD consists of frequency increments of 1/4 Hz, the limiting value allowable for a four-second time interval.

The PSD's for each block are stacked, or summed, until all complete four-second blocks have been transformed as shown in Figure 3-5. The total sum of the PSD is then averaged by dividing by the number of PSD's calculated, and the resulting average PSD is plotted as shown in Figure 3-6. The horizontal axis represents the frequency domain between zero and 30 Hz, and the vertical axis represents the engineering units appropriate for the mode displayed; the units are either gravities (1 g - 32.2 ft/sec^2) or radians/second/second. The vertical axis is adjusted so that the maximum value of the PSD equals the maximum value of the axis in units of acceleration squared/Herz (Hz).

3.3.2 PROBABILITY DENSITY FUNCTION

The modal acceleration data are presented in a percent occurrance format to display the degree to which the data are normally distributed. The procedures are outlined in Figure 3-7.

Based on the maximum amplitude range of the data, the range is divided into 200 bins of equal amplitude increments. The data are taken in four-second blocks for convenience, each sample amplitude is evaluated and a count entered in the bin representing that amplitude. When the entire set of four-
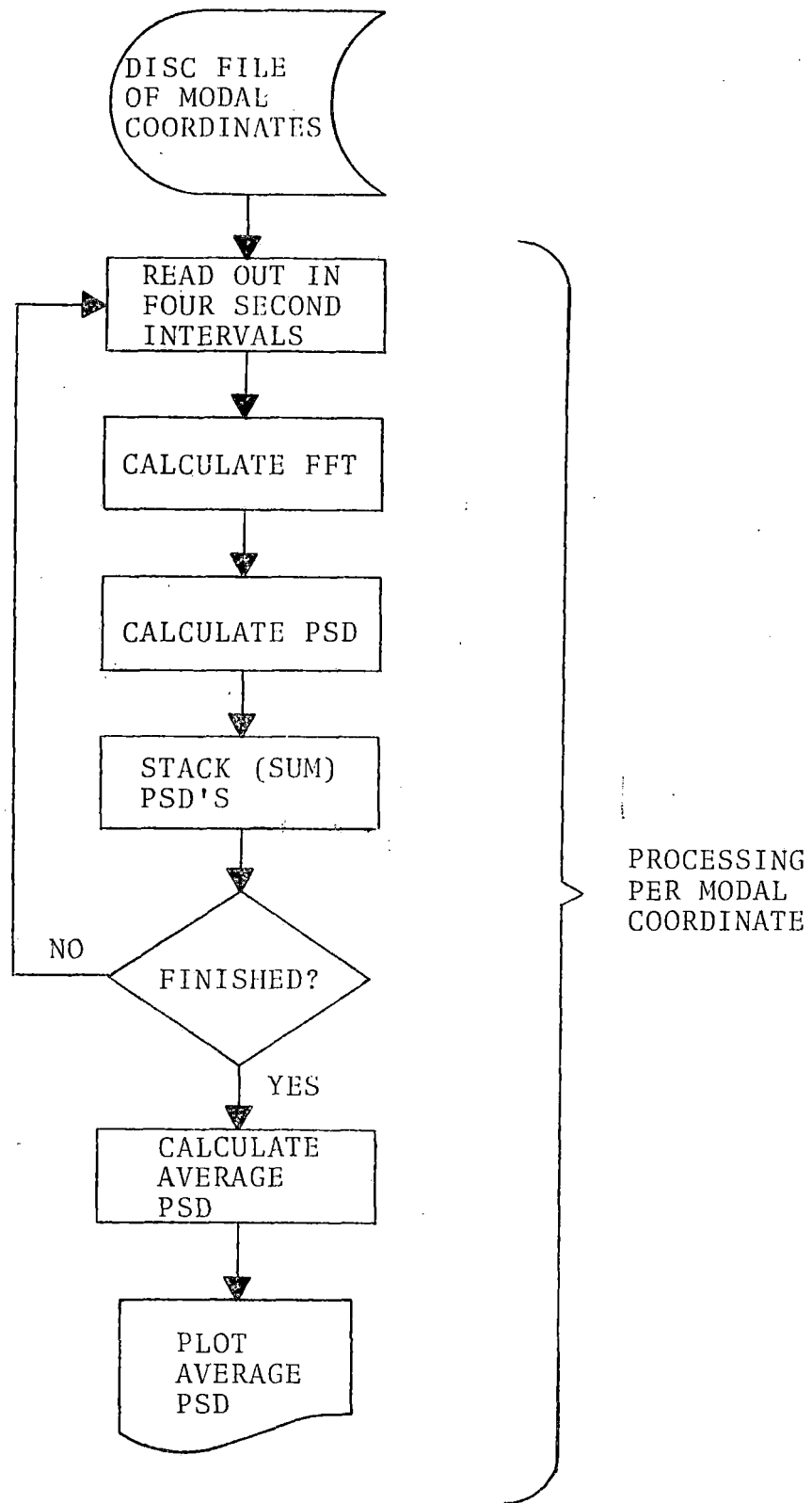
Figure 3-5. PSD Processing

B- LOAD
TTAX   ZONE 8   LWFC 8   2LC

YMIN =   .00000E 00   YMAX =   .35844E-03   X-AXIS SCALE   .19866E 02 REAL DATA POINTS PER INCH
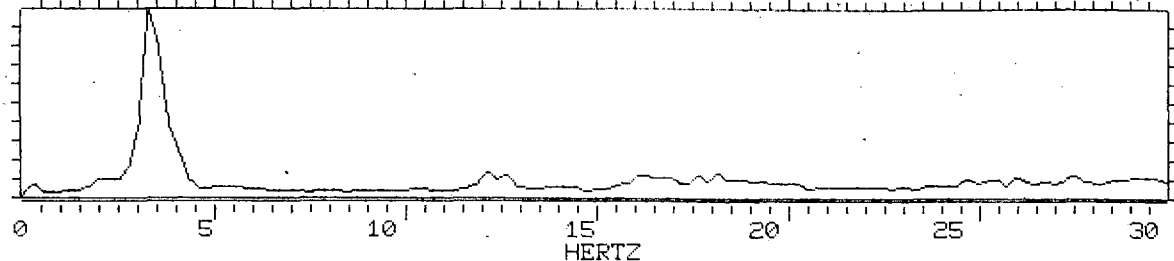
LONGITUDINAL MODE
TOTAL POWER IN THE 0-30HZ BAND   .8483E-03
G'S MEAN SQUARE
ROOT MEAN SQUARE   .2913E-01

YMIN =   .00000E 00   YMAX =   .12037E-02   X-AXIS SCALE   .19866E 02 REAL DATA POINTS PER INCH
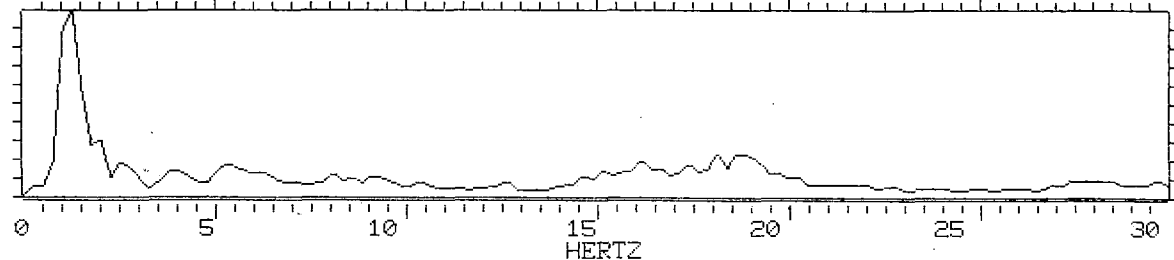
SWAY MODE
TOTAL POWER IN THE 0-30HZ BAND   .3611E-02
G'S MEAN SQUARE
ROOT MEAN SQUARE   .6009E-01

YMIN =   .00000E 00   YMAX =   .58593E-02   X-AXIS SCALE   .19866E 02 REAL DATA POINTS PER INCH
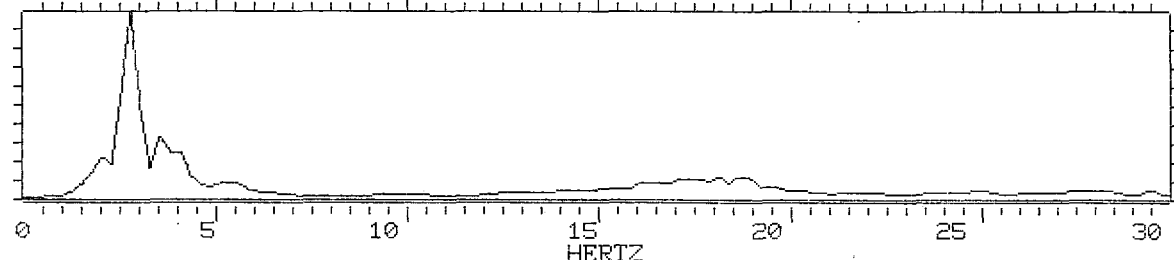
BOUNCE MODE
TOTAL POWER IN THE 0-30HZ BAND   .1078E-01
G'S MEAN SQUARE
ROOT MEAN SQUARE   .1038E 00

Figure 3-6.   Sample PSD Plots of Modal Coordinates
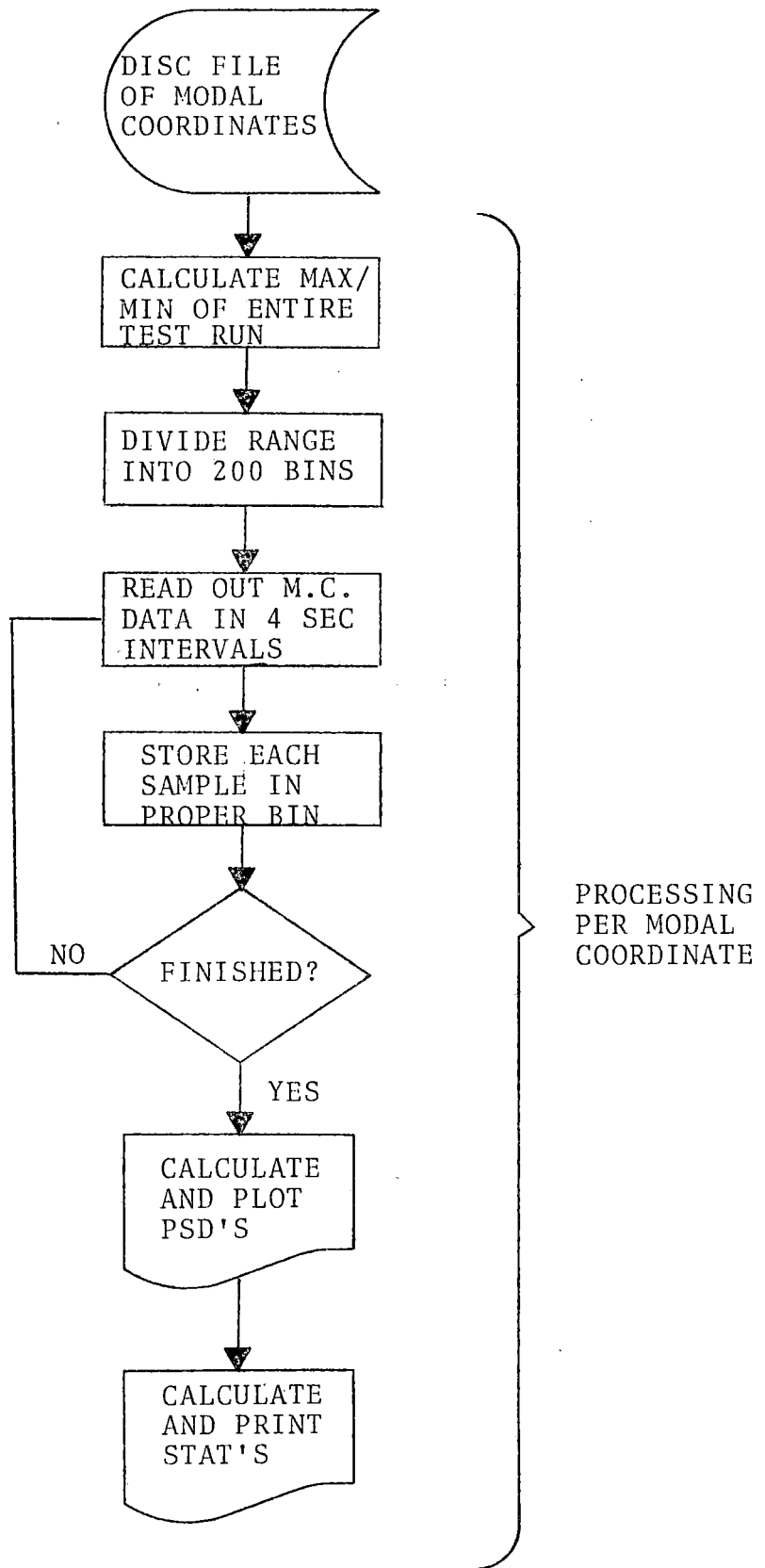
Figure 3-7. Probability Density Processing

second blocks has been exhuasted, the values in the bins are transformed to a probability density (e.g., a data base of 100 values) and plotted as a probability density function as shown in Figure 3-8.

The standard deviation and the 95 percent and 99 percent levels of the probability density function are also calculated. Each level measures the percent of time that the corresponding accelerations have values lower than indicated. The indicated values are listed as shown in Figure 3-9.

3.3.3 OCTAVE RMS HISTORY

The frequency band from zero to 30 Hz was divided into four regions or octaves, as illustrated in Figure 3-10. The acceleration behavior in each mode is calculated separately for each octave and compared to the overall behavior for that mode. The calculations are illustrated in Figure 3-11.

PSD values are generated for each four-second block of acceleration data. Each PSD is divided into four octave regions with center frequencies at 2, 4, 8 and 16 Hz; the rms values are calculated for each octave. In addition, the rms value for the entire frequency band is calculated.

Thus, each four-second block is transformed to a set of five rms values. These values are then plotted in sequence, as time functions. An example is shown in Figure 3-12. In this figure, the vertical axis represents the range of rms values encountered in the processing of the PSD's. The horizontal axis represents the time, in seconds, encompassed by the processed acceleration data. The five numbered plots in the graph represent the five rms values calculated as described above. The plot numbered "5" represents the rms values for the entire frequency range from 0 to 30 Hz, and the plots

YMIN = .00000E 00   YMAX = .33864E 01   X-AXIS SCALE   .49875E 02 REAL DATA POINTS PER INCH

-0.220   -0.110   0.000   0.110   0.220
                                   CH   1
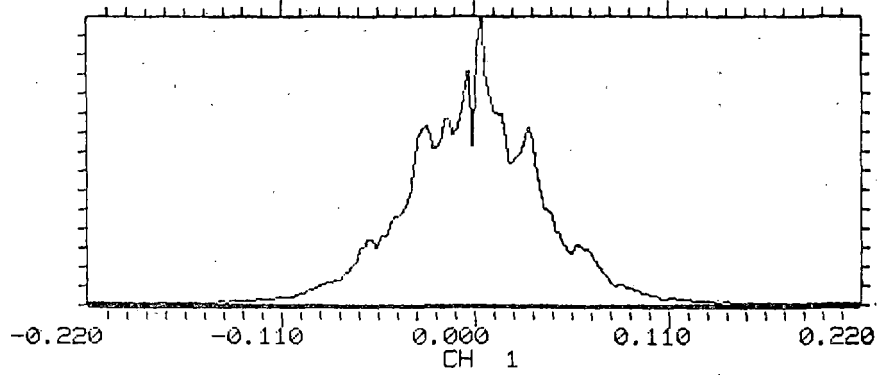
YMIN = .00000E 00   YMAX = .36951E 01   X-AXIS SCALE   .49875E 02 REAL DATA POINTS PER INCH

-0.295   -0.147   0.000   0.147   0.295
                                   CH   2
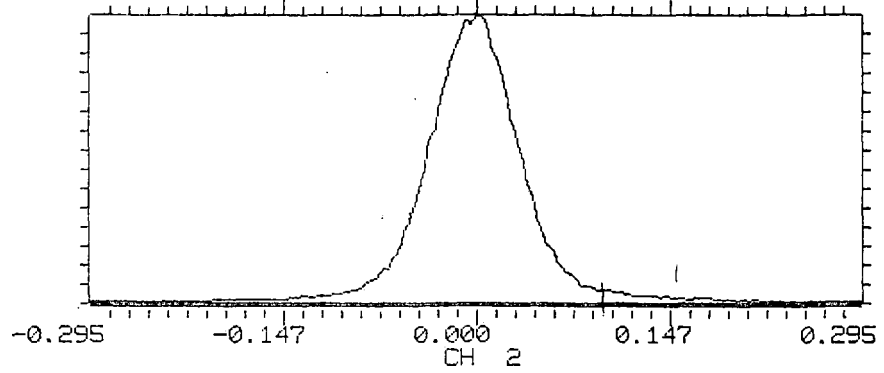
YMIN = .00000E 00   YMAX = .28722E 01   X-AXIS SCALE   .49875E 02 REAL DATA POINTS PER INCH

-0.433   -0.217   0.000   0.217   0.433
                                   CH   3
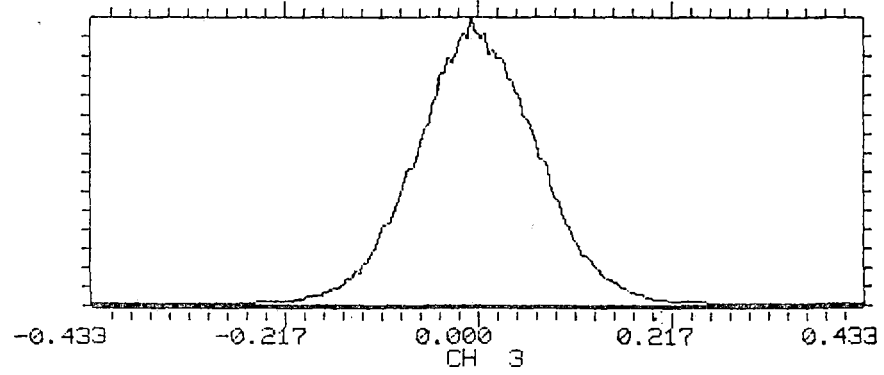
Figure 3-8.   Sample Probability Density Plots of Modal Coordinates

```
                    V I B R A T I O N  A N A L Y S I S  S U M M A R Y
            TTAX              ZONE 8            LWFC 8            2LC


                              CH  6         CH  7         CH  8         CH  9         CH 10

STANDARD DEVIATION            0.047         0.092         0.183         2.678         0.178

95 PER CENT LEVEL             0.090         0.182         0.365         5.311         0.352

99 PER CENT LEVEL             0.133         0.240         0.483         7.501         0.484

RMS                           0.047         0.092         0.183         2.678         0.178




              T I M E  P R O C E S S E D    300.00    S E C O N D S
```

Figure 3-9.   Sample Vibration Analysis Summary Sheet
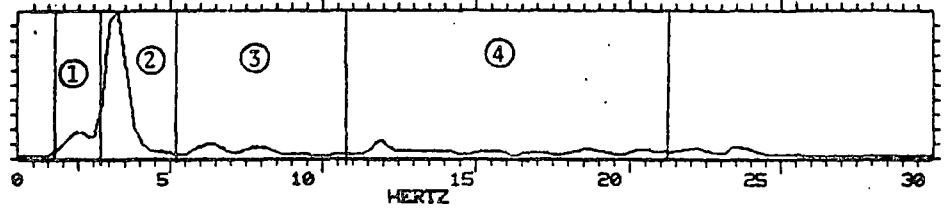
BOUNCE MODE

TOTAL POWER IN 30 HERTZ BAND   .539006E-02   G'S MEAN SQUARE
                                .734170E-01   RMS

Figure 3-10.   Frequency Band Octaves

numbered "1" through "4" represent the correspondingly numbered
octaves in Figure 3-10.   Note that plot "2", which is closest
to the overall rms plot, represents the octave with the bulk
of the power in the PSD.   Finally, the test velocity is plotted
in Figure 3-13 for correlation with the variations in the rms
values.
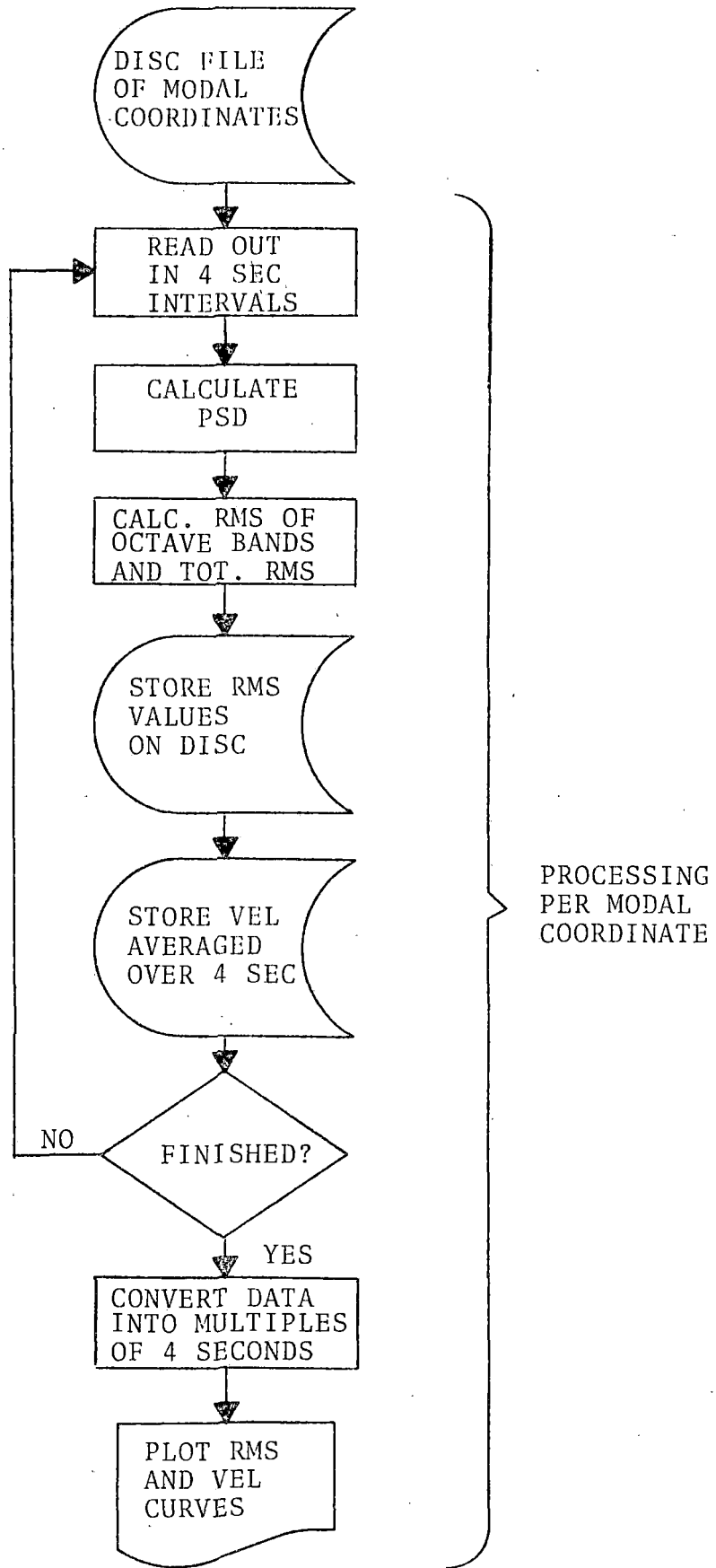
Figure 3-11.   Octave Band RMS Processing
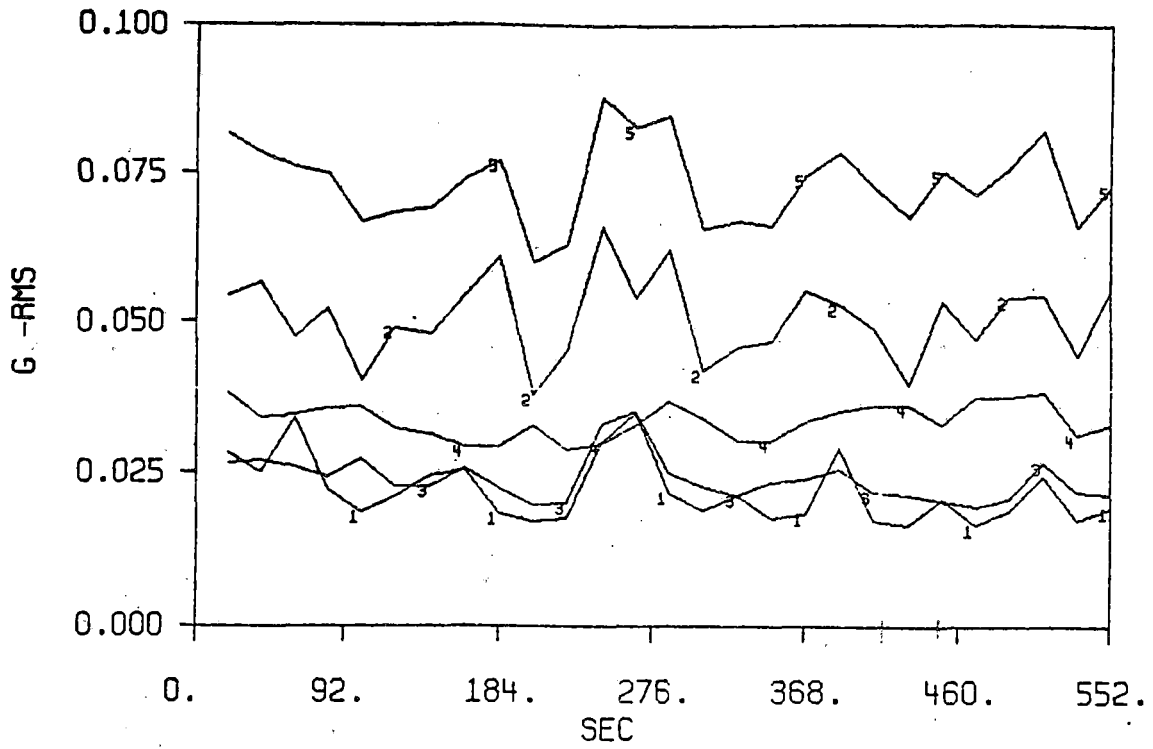
Figure 3-12.   RMS Values for Each Octave
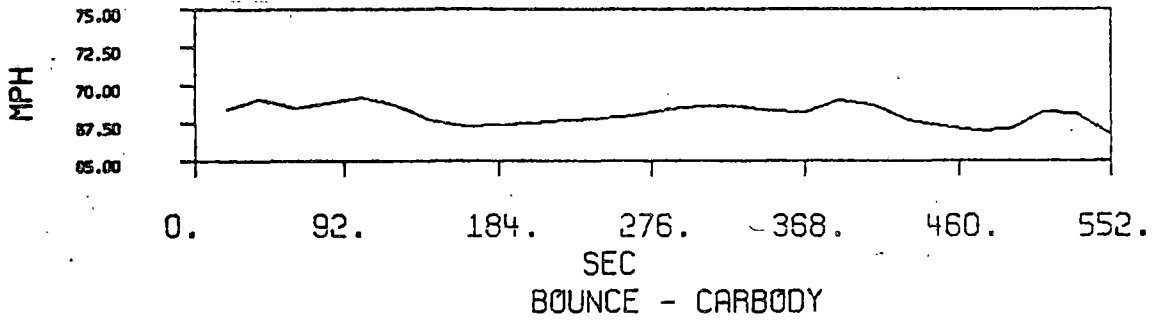
Figure 3-13.   Test Velocity

4.0 COMPARISON OF DYNAMIC BEHAVIOR

The processed acceleration data collected during the two years and 125,000 miles of the Lightweight Flatcar Test Program provide a comprehensive profile of the vibrational environment for a flatcar. The processed data are modal acceleration values representing the variations of behavior of a flatcar from the variation of one or more of the seven parameters or test conditions. These parameters and test conditions are:

- Car Type
- Mass element or subsystem (axle, carbody, load)
- Lading configuration
- Speed
- Test zone
- Accumulated mileage
- Test environment

The processed data which most simply summarize the dynamic behavior of the three flatcars are the modal rms accelerations from the Ride Vibration Tests (RVT). However, a detailed analysis of the RVT data showed that a full and accurate understanding of the rms accelerations was crucially dependent on an examination of the power spectral densities (PSD's) for each mode. The PSD plots are included in the appendices.

The results of the data analysis are presented in the following sections by mass element, in the order: axles, carbody and load, with a descrption of the key features in the analysis of the PSD's and references to specific information which indicates similarities and differences in the behavior of the test flatcars. Because vibration levels were found to be generally largest for the half-laden configuration,

the analysis is centered on this configuration, with an
examination of the other configurations to verify the con-
clusions drawn from the half-laden configuration. For
similar reasons, the analysis of axle data is focused on
the rearmost (BB) axle.

4.1 AXLES

The bounce and roll modes for the axles were expected to
clearly reflect the effects of rail joints. This effect is
a function of speed, and the vibrational frequency corres-
ponding to this input may be expressed as $f = nV/39$, where
V is the velocity of the flatcar in feet per second, n is
either 1 or 2 depending on the mode of interest, and 39 is
the standard number of feet between rail joints. A concen-
tration of vibrational energy corresponding to rail joint
input was observed at the predicted frequenices for each
speed in the axle PSD's of both bounce and roll. The effect
of this particularly strong input was also observed to a
lesser degree in the PSD's for the other modes.

The frequency corresponding to the 39-foot rail input was
more dominant in the higher speed Class 5 track. The vibra-
tional input from the Class 3 track contained sufficient
input from rail irregularities that the energy associated
with rail joints was often not the only dominant energy
source. Examples of Class 3 and Class 5 PSD's are shown
in Figure 4-1.

Despite the input from the irregularities of the Class 3
track, the accelerometer signals from the 30 g accelerometers
at the lower speeds (under 30 mph) were often of such a low
level that they became lost in system noise, particularly at
higher frequencies where the prewhitening filter had a larger
effect. Consequently, the processed data had white noise
characteristics at higher frequencies, and when this data

YMIN =   .00000E 00   YMAX =   .78036E-02
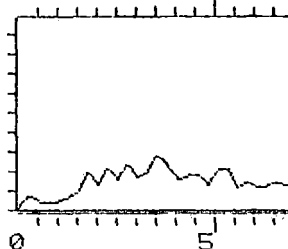
POWER IN BAND (0 - 30) =   0.06216 (GS-MS)
                    RMS =   0.24931

(a)

YMIN =   .00000E 00   YMAX =   .11214E-01
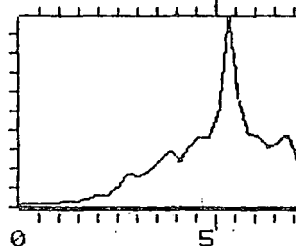
POWER IN BAND (0 - 30) =   0.06925 (GS-MS)
                    RMS =   0.26315

(b)

Figure 4-1.   Comparison

X-AXIS SCALE   .19866E 02 REAL DATA POINTS PER INCH

BOUNCE MODE
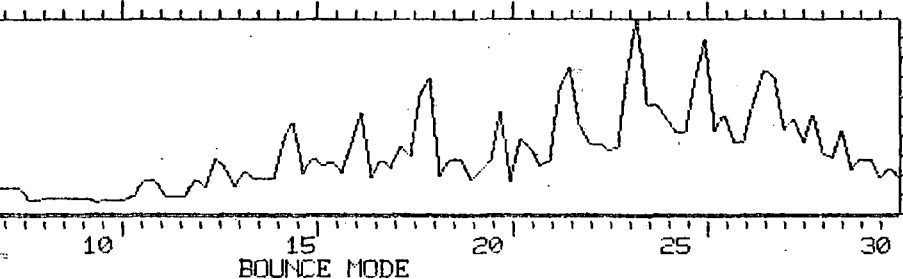
Class 3 PSD

X-AXIS SCALE   .19866E 02 REAL DATA POINTS PER INCH

BOUNCE MODE
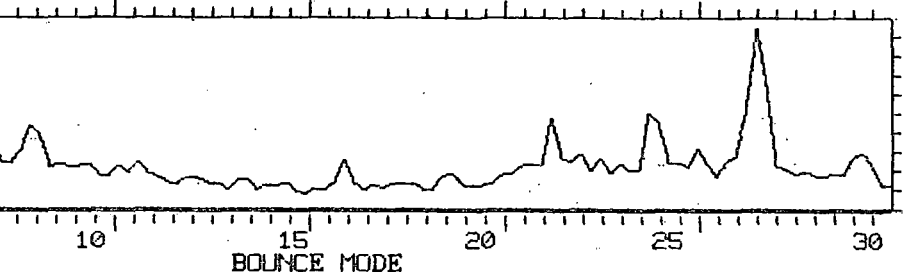
Class 5 PSD

of Class 3 and Class 5 PSD's

was inverse filtered, the resulting PSD had an appearance similar to that shown in Figure 4-2. In this particular example, the PSD is considered valid only to about 5 or 6 Hz, and the rms value, although reasonably small, is nonetheless questionable.

The PSD's for bounce were very similar for all three cars and for both front and rear trucks as expected. In addition to the rail joint frequency which reached a maximum of 6 Hz at 79 mph, a set of three smaller peaks in the 15 to 30 Hz range were observed. These peaks are also speed dependent and are presumed to be characteristic of the ASF truck suspension system.

An exception to the regularity of the bounce PSD was observed for the BB-axle of TLDX-61 in Zone 2 of RVT 1. A source of high energy input was observed beginning at 14 Hz at 40 mph and varying linearly with speed to 26 Hz and 79 mph. The frequencies associated with this anomaly appear to be associated with wheel rotation, and since the truck was essentially new, the energy is assumed to be caused by some manufacturing defect. The anomaly appears in every mode and seems to be associated with a defect more complex than an out-of-round wheel. The anomaly may have been caused by an intermittent dragging brake.

A second anomaly was observed in the bounce PSD's for TLDX-62 during the third RVT. In this case, there was sufficient energy in the higher frequencies to make the rail joint input virtually undetectable. Further, as speed was increased, the energy reached frequencies above 30 Hz, and the rail joint energy re-appeared in its usual dominant magnitude. This sequence of PSD's is shown in Figure 4-3. This phenomenon, most likely due to a flat spot on the wheel or a bad bearing, had a marked effect on the rms values as shown in Table 4-1.

4-4

BB- AXLE
TLDX 62   TAPE 52   FILE 1   20 MPH   RVT1   LNFC 3A

YMIN = .00000E 00   YMAX = .59135E 00   X-AXIS SCALE   .19866E 02 REAL DATA POINTS PER INCH

0   5   10   15   20   25   30
ROLL MODE
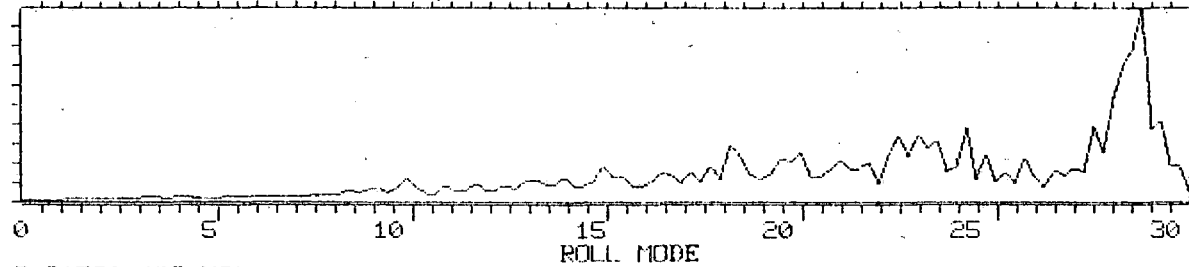
POWER IN BAND (0 - 30) =   2.21790 (GS-MS)
              RMS =   1.46926

YMIN = .00000E 00   YMAX = .18172E-01   X-AXIS SCALE   .19866E 02 REAL DATA POINTS PER INCH

0   5   10   15   20   25   30
YAW MODE
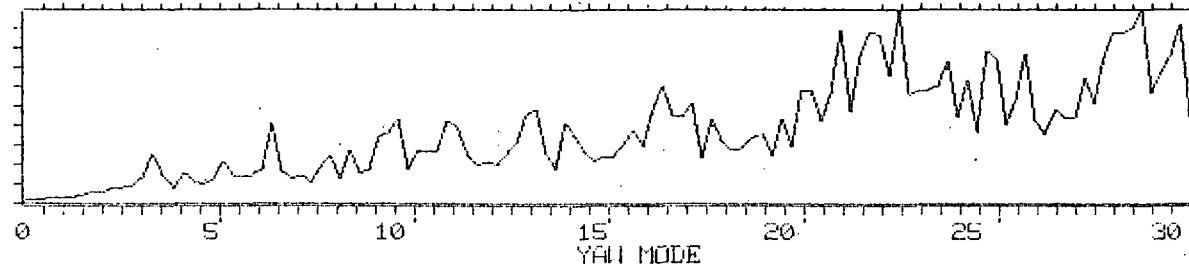
POWER IN BAND (0 - 30) =   0.20007 (GS-MS)
              RMS =   0.44729

:RW,8
:OT
03/22/79   01:00:00
:XX

Figure 4-2.   An Example of Inverse Filtered White Noise

BOUNCE MODE

POWER IN BAND (0 - 30) = 0.08597 (GS-MS)
                   RMS = 0.29321

(a)   40 mph

YMIN = .00000E 00   YMAX = .10686E 00   X-AXIS SCALE   .19866E 02 REAL DATA POINTS PER INCH

BOUNCE MODE

POWER IN BAND (0 - 30) = 0.07621 (GS-MS)
                   RMS = 0.27607

(b)   50 mph

YMIN = .00000E 00   YMAX = .66976E-02   X-AXIS SCALE   .19866E 02 REAL DATA POINTS PER INCH

BOUNCE MODE

POWER IN BAND (0 - 30) = 0.04052 (GS-MS)
                   RMS = 0.20128

(c)   60 mph

YMIN = .00000E 00   YMAX = .13619E-01   X-AXIS SCALE   .19866E 02 REAL DATA POINTS PER INCH

BOUNCE MODE

POWER IN BAND (0 - 30) = 0.06964 (GS-MS)
                   RMS = 0.26390

(d)   70 mph

Figure 4-3.   Anomaly in Bounce Mode for BB-Axle of TLDX-62

Listed in Table 4-1 are the bounce rms accelerations for the three test cars during the third RVT. For the TLDX-61 and the TTAX, a steady increase is observed for each zone, but for the TLDX-62, the pattern is disrupted. This is due to the large amount of energy input from the anomaly. This input is speed dependent and passes beyond the frequency band over which the rms value was computed. Thus, the rms values for the TLDX-62 are significantly above the norm for speeds below the value at which the anomaly passes above 30 Hz, approximately 60 mph.

TABLE 4-1

BB AXLE BOUNCE RMS VALUE FOR RVT 3

Zone	Speed (mph)	TLDX-62	TTAX	TLDX-61
1	10	0.20	0.05	0.07
	15	0.25	0.07	0.11
	20	0.23	0.09	0.15
	30	0.29	0.15	0.17
	40	0.35	0.19	0.22
2	40	0.29	0.10	0.12
	50	0.28	0.13	0.15
	60	0.21	0.18	0.20
	70	0.26	0.23	0.25
	79	0.30	0.26	0.30

The rms levels for axle accelerations were observed to increase roughly as the square of speed as best demonstrated by the bounce mode. This occurs because the acceleration is proportional to the second derivative of the rail profile with the constant of proportionality being equal to the square of the speed as shown in the following equation.

$$a = \frac{d^2 s}{dt^2} = \frac{d^2 s}{dx^2} \left(\frac{dx}{dt}\right)^2 = \frac{d^2 s}{dx^2} V^2$$

where   a is the acceleration

s is vertical distance

t is time

x is horizontal distance

V is speed

This relationship should be kept in mind when analyzing carbody and load accelerations with respect to the suspension.

The PSD's for the longitudinal mode generally indicated random accelerations with no consistently clear dominant frequency. This was expected since input to this mode comes largely from the locomotive and is in part a function of test procedures and train handling. In the first RVT, the data for any given speed came from several separate test runs. In the second and third RVT's, there was only one test run for each speed making it more reasonable to compare the longitudinal rms values for these two RVT's. The rms values for the TLDX-62 were observed to be consistently higher than for either of the other cars. This is attributed to the position of TLDX-62 in the test consist. It was coupled directly to the locomotive and was receiving direct input from the locomotive and from operator effects. These rms values are listed in Table 4-2.

TABLE 4-2

AXLE RMS VALUES FOR LONGITUDINAL MODE

Zone	Speed (mph)	TLDX-62	TTAX	TLDX-61
1	10	0.018	0.019	0.019
	15	0.033	0.027	0.028
	20	0.040	0.033	0.033
	30	0.053	0.051	0.050
	40	0.066	0.064	0.065
2	40	0.037	0.030	0.033
	50	0.044	0.036	0.042
	60	0.057	0.051	0.052
	70	0.086	0.059	0.065
	79	0.096	0.070	0.071

Speed dependence was normally evident in the dominant frequencies in the bounce and roll modes and also in the yaw and sway (lateral) modes. One exception appeared in the dominant frequency for the yaw mode for the TTAX, which was seen to increase with speed up to a maximum of 2.25 Hz at 60 mph, Above that, it remained at 2.25 Hz, although there was no upper limit on the dominant frequency for the other flatcars. This may be an effect of the greater weight of the TTAX, possibly producing significantly greater frictional resistance to truck rotation. This phenomenon is particularly interesting because the limiting speed of 60 mph is the speed at which hunting is generally observed to begin and the TTAX is more prone to hunting than either the TLDX-61 or TLDX-62. Further investigation of this correlation may be warranted.

Thus far, the analysis has been limited to the BB axle (rear). This axle was chosen because previous work had indicated that the dynamic behavior of the BB-axle was more severe than the behavior of the front axles. Data from the AA axles were examined to verify this and to check for any unusual behavioral patterns. The AA-axle was found to behave similarly to the BB-axle.

The most significant differences between the AA- and BB- axles were observed for sway and yaw. At speeds of 60 mph and higher, sway and yaw rms accelerations increased significantly faster for the BB-axle than for the AA-axle. Thus, whatever relationship held between the front and rear axles at lower speeds changed such that BB sway or yaw clearly exceeded AA sway or yaw, at times by a factor of three.

One additional exception to the axle relationship was observed in the longitudinal mode for the TLDX-62. In this instance, the rms acceleration for the AA-axle exceeded that of the BB- axle. This can be attributed, as noted earlier, to the direct coupling of the car to the locomotive.

4.2 CARBODY

The natural frequencies of the carbody bounce mode were found to be independent of speed and related to the relative mass of the flatcars. For an undamped spring-mass system, which crudely approximates a flatcar, the resonant frequency is directly proportional to $\sqrt{k/m}$, where k is the spring constant and m is the mass. Since the trucks were identical, the springs were identical, therefore, k does not vary and the resonant frequency is a function of mass only. A larger mass will result in a lower resonant frequency as shown in Table 4-3. Remember that TLDX-62 is lighter than TLDX-61 because of the absence of trailer mounting hardware and that the frequencies determined from the PSD's are only resolvable to 0.25 Hz.

TABLE 4-3
CARBODY RESONANT FREQUENICES IN HERTZ

	TTAX	TLDX-61	TLDX-62
Half Laden	2.75	3.00	3.50
Unloaded	3.75	4.00	5.00

RMS accelerations for the bounce mode were consistely larger for the lighter cars, by 20 to 50 percent on the average. At lower speeds, the rms values were seen to increase linearly with speed, as expected for a damped spring-mass system. At speeds above 40 mph, the suspension acts as a filter and tends to reduce the effect of rail joint inputs which are the principal input. Thus, at higher speeds, the bounce rms accelerations were observed to level off and occassionally drop in value.

At low speeds, the carbody bounce PSD's reflect only accelerations at the natural frequency, while at higher speeds, the frequency corresponding to rail joint input appears at significant power levels. The appearance of rail joint input occurs over relatively small speed increases. This is due to an increase in vertical activity and to a resonance effect of the input frequency with the natural frequency of the suspension system. The speeds at which this level is reached were highest for the TLDX-62, the lightest car.

The carbody sway PSD's displayed rail joint inputs at low speeds and were consistely speed dependent. The only unusual frequency behavior was the appearance of energy in the third harmonic of the rail joint input at midrange speeds, usually from 40 to 60 mph. In several instances, the sway rms values varied from the normal linear increase producing an apparent non-linear relationship with speed and in some cases,

the variance reached a peak value at a speed below 79 mph. This non-linearity and the rms peaks occurred between 50 and 70 mph which may correspond to periods of hunting. This is substantiated by the presence of rms peaks for yaw at the same speeds. These speeds are shown in Table 4-4.

The yaw mode was least affected by rail-joint inputs which were not clearly seen until speeds of 30 to 50 mph had been reached, and in one case (TLDX-61) this input was not seen until 70 mph had been reached. The flatcars did not respond in any particular order to rail joint excitation.

Carbody roll accelerations were affected by rail joint inputs at 20 mph for the TTAX and TLDX-61, and at 30 mph for the TLDX-62. The response at this level appeared as an unusually well-defined peak in the PSD at the rail joint frequency (3 Hz). However, due to crosstalk from the elastic modes, the rms values for roll are not truly indicative of the energy or displacement of the peak. Instead, the actual values of the relevant peak in the PSD must be considered. These peaks coincide with the phenomenon commonly referred

TABLE 4-4

SWAY AND YAW RMS ACCELERATION PEAKS

	TTAX		TLDX-61		TLDX-62	
	Sway (mph)	Yaw (mph)	Sway (mph)	Yaw (mph)	Sway (mph)	Yaw (mph)
RVT 1	None	None	None	None	None	None
RVT 2	60	60	50*	50*	70*	70*
RVT 3	50	50	70	-	-	50

NOTE: "*" indicates that there was only an unusually sudden rms increase, but not enough to produce a peak.

to as rock and roll. This is the situation in which the
rocking back and forth from rail joints coincides in frequency
with the natural frequency of the railcar, and severe roll
results from sustained operation at this speed. The higher
speed for TLDX-62 is a result of the rigidly-mounted load
which changes the polar moment of inertia.

At speeds just above the resonant speed, the contribution of
the rail joint decreased to a negligible level. However,
at higher speeds, the rail joint frequency reappeared and
became dominant while the rms values increased with speed.
The reappearance became well-defined at 70 mph for the TLDX-62
and at 60 mph for the other flatcars. Again, this difference
is attributed to the load configuration.

Thus far, the differences or similarities between the flatcars
have been attributed to the rigid-body modes which are af-
fected by either the interaction of the carbody and its
suspension system or of the carbody and the load. Now the
discussion will turn towards similarities or differences that
can be attributed to the elastic-body modes which are affected
by the structural differences of the flatcars.

After a complete analysis of the rather large data base
created by the LWFC Program, certain limitations arose in the
analysis and discussion of elastic-body modes. One such limi-
tation dealt with the coupling problem. Although the compo-
site of the modes selected did adequately model the measured
accelerations some difficulties were encountered in decoupling
(Section 3.2) of the elastic and rigid-body modes. In some
cases, illustrated in Figures 4-4 and 4-5, the decoupling was
incomplete resulting in crosstalk. In Figures 4-4 and 4-5,
rigid-body pitch mode which occurs at lower frequencies
(~5 Hz), and elastic-body second bending, which occurs at
higher frequencies (~12 Hz), were not properly decoupled.

YMAX = .12457E-01   X-AXIS SCALE   .19866E 02 REAL DATA POINTS PER INCH

HERTZ

POWER IN SECOND BENDING MODE

YMAX = .26171E-02   X-AXIS SCALE   .19866E 02 REAL DATA POINTS PER INCH

HERTZ

POWER IN PITCH MODE
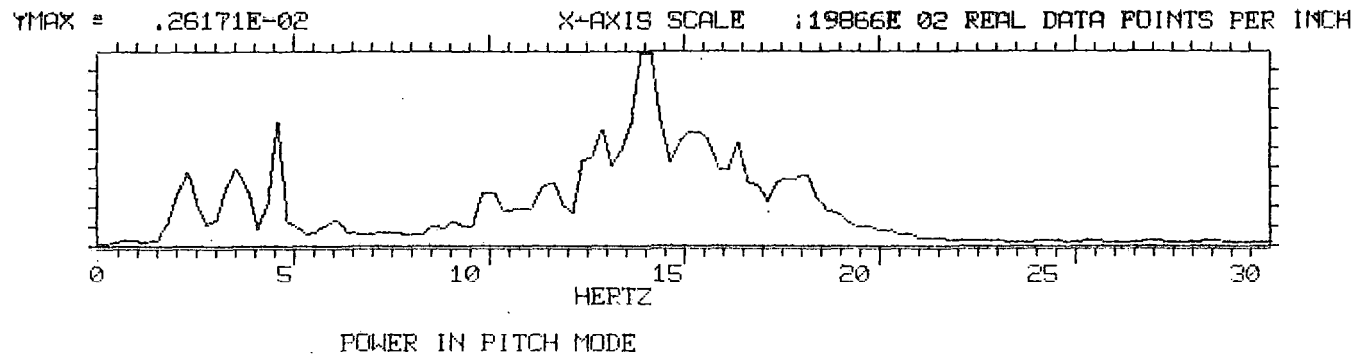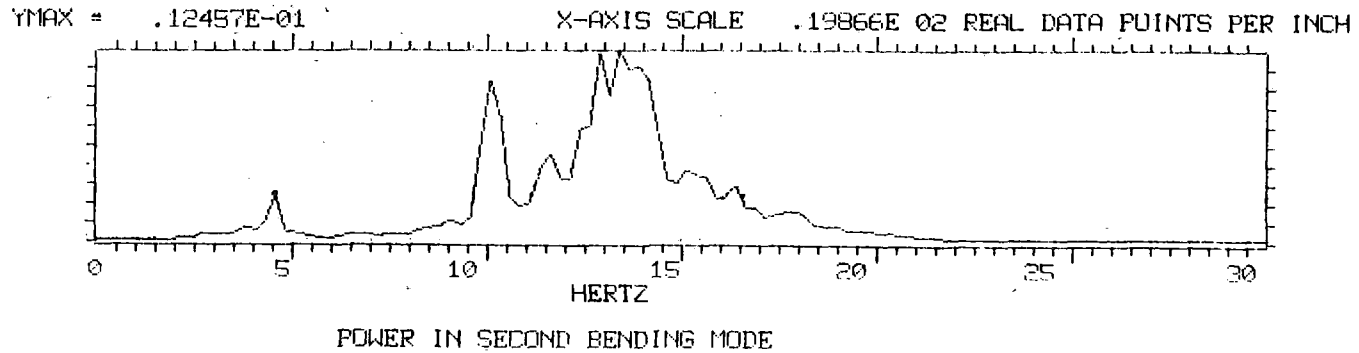
TOTAL POWER IN 30 HERTZ BAND   .130101E-01   (RAD/SEC/SEC) MEAN SQUARE
                                .114062E 00   RMS

Figure 4-4.   Crosstalk from Elastic to Rigid Body Modes

YMAX = .11107E-01   X-AXIS SCALE   .19866E 02 REAL DATA POINTS PER INCH

POWER IN SECOND BENDING MODE

YMAX = .15582E-01   X-AXIS SCALE   .19866E 02 REAL DATA POINTS PER INCH

POWER IN PITCH MODE
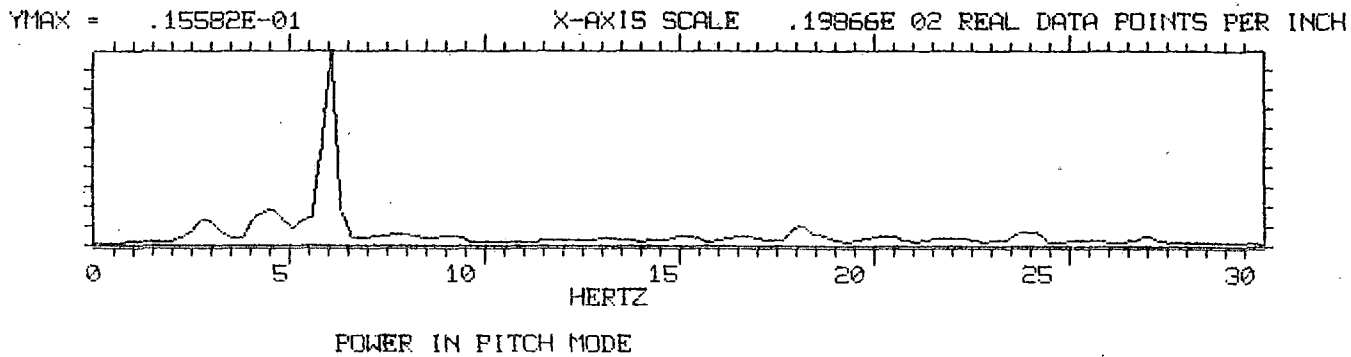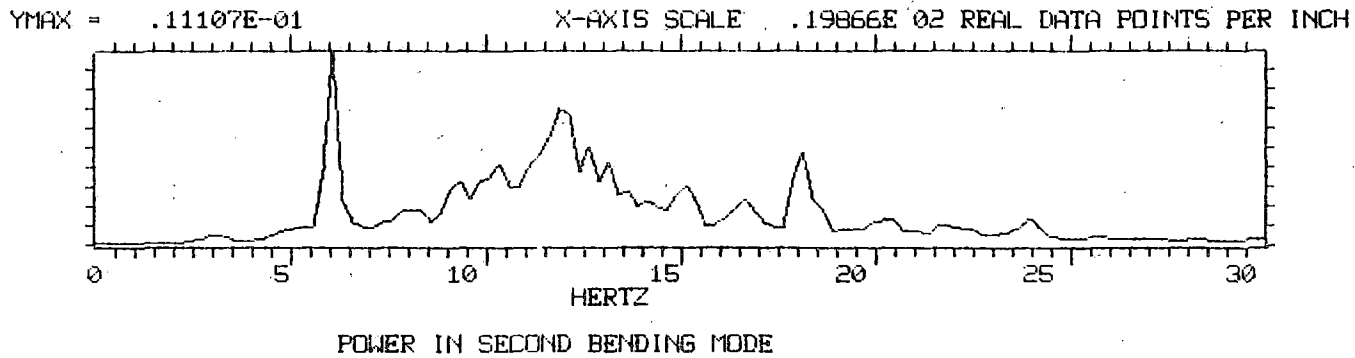
TOTAL POWER IN 30 HERTZ BAND   .197392E-01   (RAD/SEC/SEC) MEAN SQUARE
                                  .140496E 00   RMS

Figure 4-5.   Crosstalk from Rigid to Elastic Body Mode

Crosstalk may occur for several reasons, but the primary cause is related to the expression of the mode shape. That is, the binomial expression (Table 3-1) used to depict the second bending mode was inadequate. The bending and torsion modes of these flatcars were more complex, due to abrupt changes in structure along the length of the car, than the modes described by the limited power series. An example of this was observed in the relatively large differences between the measured and modeled accelerations at locations near the bolster or center plate of the car. None the less, several important observations can be made based on the elastic-body behavior of these flatcars.

The first and second bending modes are characterized by consistent PSD signatures with dominant frequencies largely independent of speed. The first bending mode for the TTAX was characterized by two concentrations of energy in the lower and upper regions of the frequency range. The lower frequency was in the expected frequency range for the first bending mode. The upper concentration could not satisfactorily be attributed to high frequency errors or to crosstalk; therefore, it is considered to represent vibration in the third bending mode. This conclusion is consistent with the dominant frequency values for the first and second modes, as listed in Table 4-5. In addition, it is mathematically reasonable since the third mode, like the first, would be represented by an even polynomial, i.e., a polynomial with only even powers of the variable. Thus, the mode shape polynomial for first bending is functioning as a crude approximation for third bending. This phenomenon appeared only for the TTAX which indicates a somewhat more rigid design than the lightweight flatcars. In some instances what appeared as the third mode for the TLDX-61 or TLDX-62 was found to be crosstalk. This is evidently a phenomenon associated with the structural characteristics of the flatcars.

TABLE 4-5

CARBODY TORSION FREQUENCIES IN HERTZ

	TTAX	TLDX-61	TLDX-62
1st Torsion	7 - 10	9 - 11	8 - 10
2nd Trosion	14 - 15	18 - 21	16 - 20 - 21
3rd Torsion	21 - 25	-	-

The dominant frequencies in the first and second torsion
PSD's for the TTAX varied over a considerable range, roughly
averaging around 8 and 16 Hz, respectively. These frequencies
are notably lower than the dominant frequencies for first and
second torsion for the two lightweight flatcars which
averaged about 10 Hz for first torsion and 20 Hz for second
torsion. The higher frequencies for the lightweight flatcars
is attributed to their stiffer torsional design. In addition,
the dominant frequencies for the lightweight flatcars were
more constant for varying speed; this may also be attributed
to their stiffness.

4.3 LOADS

The dynamic characteristics for the containers and trailers
were totally different, since the trailers were suspended at
one end while the containers were rigidly mounted. The con-
tainers very closely reflected the carbody behavior; the
trailers behaved largely in response to the dynamic charac-
teristics of their own suspension systems.

Trailer behavior in rigid modes illustrates the interaction
between the natural vibration frequencies and rail joint
response. The natural frequency is a function of spring
characteristics and trailer mass, and thus it remains con-
stant at all test speeds. By contrast, rail joint response

is a direct function of speed and is related to the regular
39-foot intervals of the rail joints. For a speed of 40
mph a rail joint will be reached every 2/3-second, and thus
the impact of rail joints will be measured at a rate of
3/2 or 1.5 Hz. This impact will appear in the PSD as a
spike or peak at 1.5 Hz. For modes which are based on the
relative input from both rails, rail joint input will occur
every 19-1/2 feet since the rail joints are staggered. Thus,
the impact will occur every 1/3-second and be measured at a
frequency of 3 Hz. At higher (or lower) speeds, rail joint
impact will occur at a faster (or slower) rate and thus will
be measured at a higher (or lower) frequency. Thus, the
peak corresponding to rail joint input will appear to move
up or down the PSD spectrum as speed is changed.

Figure 4-6(a) illustrates the two peaks corresponding to
rail joint input and natural spring/mass frequency. The
lower peak, at 0.5 Hz, corresponds to rail joint input,
and the peak at 1 to 1.25 Hz corresponds to the natural
frequency in sway for the trailer in question. The rail
joint input for 10 mph is exactly 0.75 Hz; however, due to
approximations in calculating the PSD's and the 0.25 Hz
bins that compose the PSD's, this input is shown at 0.5 Hz
instead of 0.75 Hz.

Due to damping in the trailer suspension system, it acts as
a second order filter for inputs from the carbody. The fil-
tering effect can be seen by observing the progression of
the rail joint peak through the PSD spectrum as speed is
increased. In Figure 4-6(b) it can be seen that the rail
joint peak has increased in frequency. Examination of the
YMAX values indicates an increase of nearly an order of
magnitude. This is partly the result of the increase in
speed and partly the result of the frequency range of the
input which is magnified by the truck suspension. This
range of magnification is illustrated in Figure 4-7.

4-18
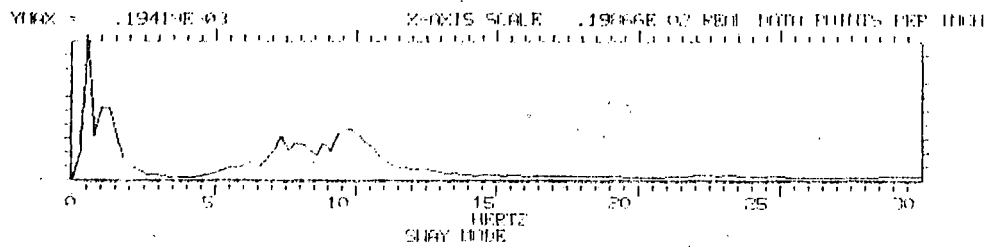
(a)   10 mph
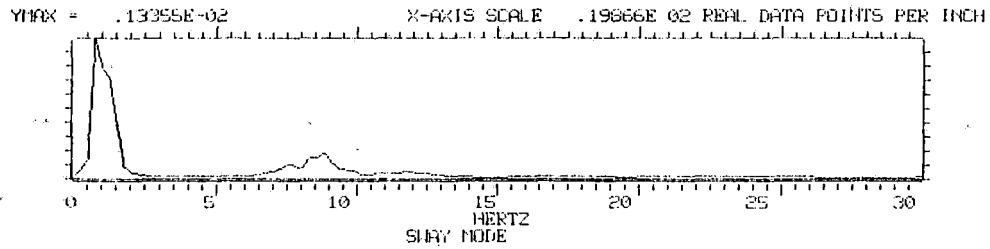
(b)   15 mph
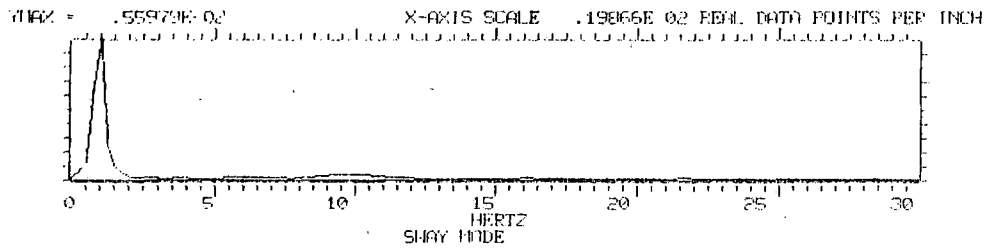
(c)   20 mph
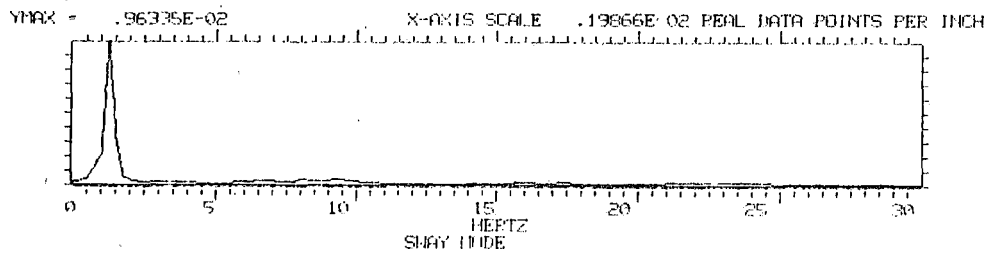
(d)   30 mph
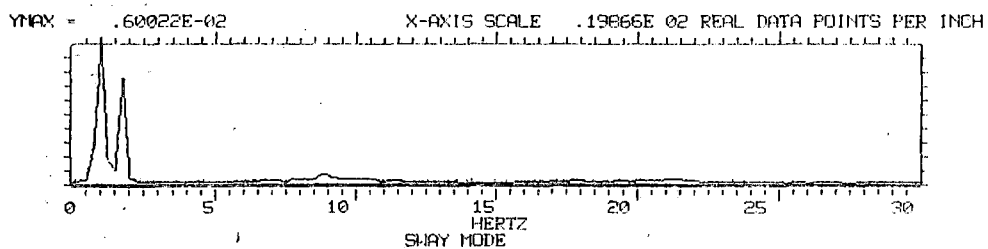
(e)   40 mph

Figure 4-6.   Apparent Effect of Track Input
on Resonant Frequency

4-19
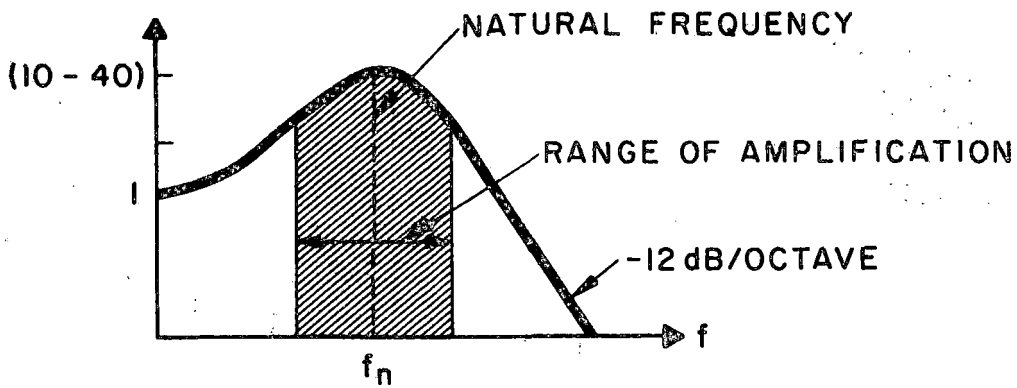
Figure 4-7.   Idealized Truck Suspension Response

Figure 4-6(c and d) shows the merging of the natural frequency peak and the rail joint peak. In Figure 4-6, the natural frequency appears to change with speed. This, however, is not the case. The natural frequency is not speed dependent, while the rail joint input does change with speed, and, since the rail joint input is amplified by the truck suspension, it overshadows the natural frequency peak. Producing one large peak (Figure 4-6(d) and Figure 4-8) that moves with speed.

Finally in Figure 4-6(e) the energy corresponding to rail joint input can be seen as a separate peak at a higher frequency. This peak is smaller in size because the higher frequency is now being attenauted by the trailer suspension instead of being magnified.
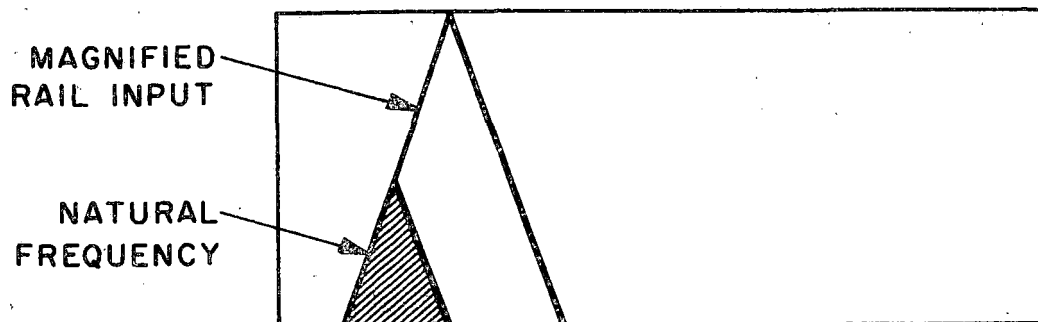
Figure 4-8.   Example of Rail Joint Input Overshadowing
the Natural Frequency

The attenuation of the rail joint input peak begins after it has passed the resonant frequency and increases with an increase in speed. This is caused by the trailer suspension which is behaving like a second order low-pass filter with a corner frequency corresponding to its natural resonant frequency. Thus, inputs to the trailer at frequencies above the natural frequency are attenuated which increases with higher frequencies. Associated with this effect, is the general absence of high frequency information in the trailer PSD's. The natural frequencies for the trailers in each mode are listed in Table 4-6.

With the exception of lateral bending, the PSD's for trailers mounted on the TTAX and TLDX-61 were remarkably similar at all speeds. In addition, rms values were comparable in the modes. Lateral bending differed between the TTAX and TLDX-61 for the trailer. On the TLDX-61 the accelerations were generally in the neighborhood of 12-15 Hz (which is believed to be a natural frequency for the trailers), while accelerations for the TTAX-mounted trailer were around 5-10 Hz. This variation is thought to be related to the differences in elastic stiffness between the TTAX and TLDX-61 carbodies.

TABLE 4-6

TRAILER RESONANT FREQUENCIES

	Resonant Frequency (Hz)
Longitudinal	3.0
Sway	1.0
Bounce	3.0
Roll	3.0 - 5.0
Pitch	3.5
Yaw	3.0
Bending	9.0 - 13.0

The trailer PSD's were compared to the corresponding carbody
PSD's to determine the effect of carbody inputs on the load.
Most trailer modes derived their input from the corresponding
carbody mode with three clear exceptions. First, trailer
pitch was seen to be related to carbody bending (first
bending mode only). This can be seen by examining the
frequency content of the load and carbody PSD's shown in
Figure 4-9. Second, lateral bending of trailers was seen
to relate primarily to carbody yaw. Finally, trailer yaw
was seen to receive significant inputs from both yaw and
longitudinal accelerations of the carbody.

An important phenomenon observed in connection with carbody
input to trailer accelerations is the effect of the trailer
on the carbody. This effect, which may be aptly described
as feedback, is believed to play an important role in the
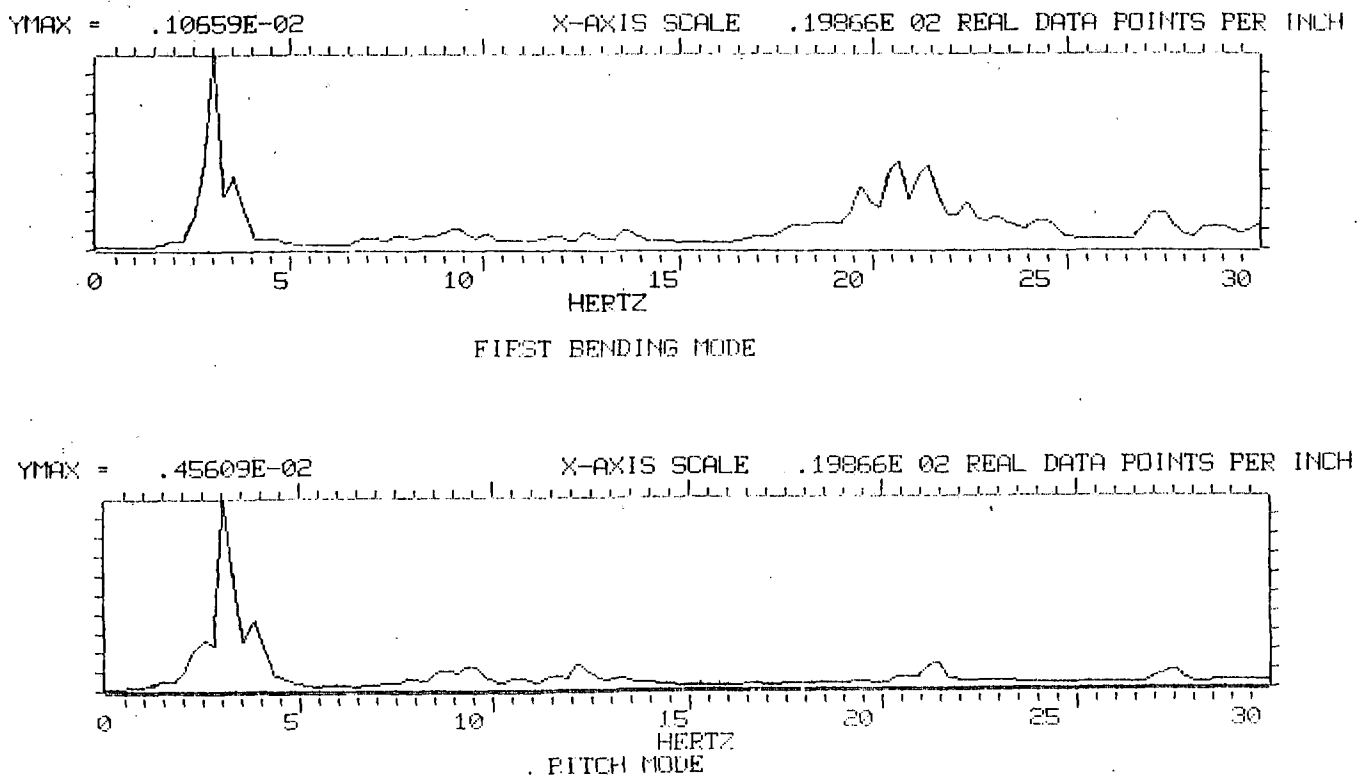
Figure 4-9. Effects of Carbody Bending on Trailer Pitch

area of crosstalk between carbody modes. Feedback is a
relatively limited phenomenon for the trailer configurations,
because of the filtering effects of the trailer suspensions.
However, for rigidly mounted containers, the effect is much
more pronounced. In this situation, two otherwise unrelated
carbody modes may contribute to one container mode, which
may then feedback the effect equally to the two carbody
modes. This effect is illustrated in Figure 4-10. The
upper and lower PSD's correspond to two unrelated carbody
modes, and the center PSD corresponds to a container mode.
The solid lines indicate the apparent contributions of the
carbody to the container accelerations, and the broken line
indicates the feedback from the container. This theory is
substantiated by examination of the PSD's for unladen car-
bodies where the crosstalk is markedly reduced.

Feedback from containers is more pronounced than feedback
from trailers because, as was previously mentioned, the
containers are rigidly mounted to the carbodies with no
suspension system to attenuate the inputs. Thus, carbody
container interactions are subject to virtually every com-
plexity of the physical geometry of carbody motion. The
carbody modes which contribute to container mode accelerations
are listed in Table 4-7. The explanation in geometric terms
is relatively straightforward, as illustrated in Figure 4-11,
where the motion of the carbody and container in pitch is
shown. The carbody center remains unmoved, but the container
center will contain elements of both bounce (vertical) and
longitudinal motion. Thus, carbody pitch can be visualized
as a contributor to bounce, longitudinal and pitch modes for
the container. The real effect, however, will depend sig-
nificantly on the displacement within a mode, because dis-
placement is magnified by the geometry of the carbody/load
system. In addition to the carbody/load relationship, the
container possesses a significant mass, therefore, it is

YMAX = .31549E-03   X-AXIS SCALE   .19866E 02 REAL DATA POINTS PER INCH

0   5   10   15   20   25   30
HERTZ
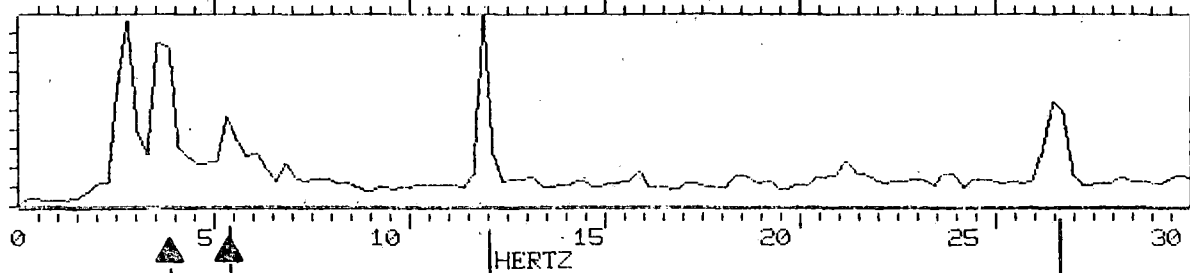
Carbody Longitudinal Mode

YMAX = .53914E-03   X-AXIS SCALE   .19866E 02 REAL DATA POINTS PER INCH

0   5   10   15   20   25   30
HERTZ
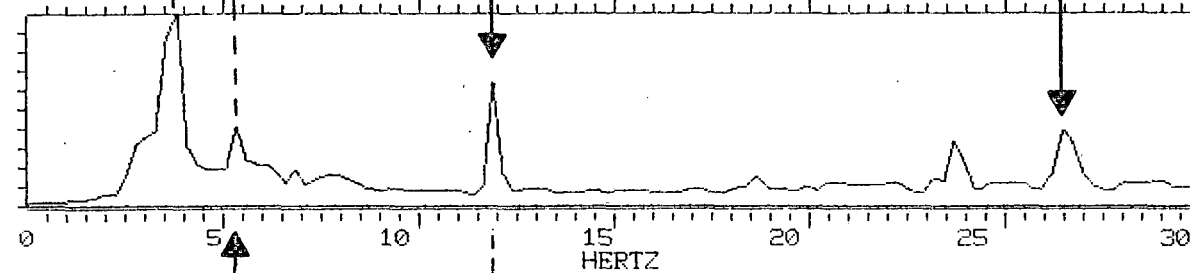
Load Longitudinal Mode

YMAX = .41472E-02   X-AXIS SCALE   .19866E 02 REAL DATA POINTS PER INCH

0   5   10   15   20   25   30
HERTZ
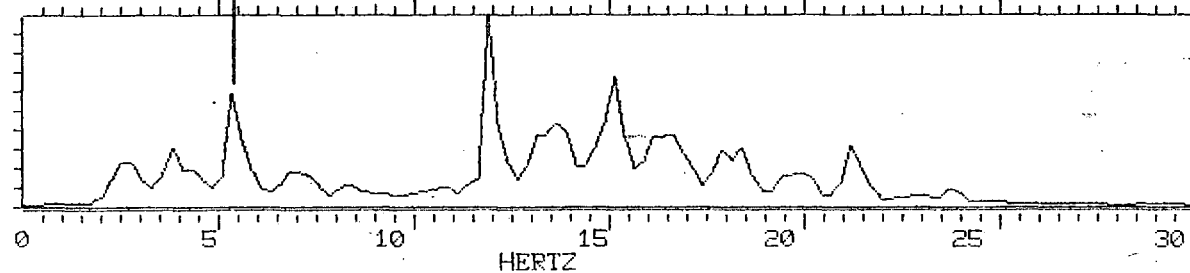
Carbody Pitch Mode

Figure 4-10.   Feedback Between Load and Carbody

TABLE 4-7

INFLUENCE ON CONTAINER MODES

Load Mode	Principal Carbody Contribution	Other Sources
Longitudinal	Longitudinal	--
Sway	Sway	Yaw
Bounce	Roll	Bounce, Pitch, First Bending
Roll	Roll	--
Pitch	First Bending	Pitch
Yaw	Yaw	--
Lateral Bending	Yaw	--
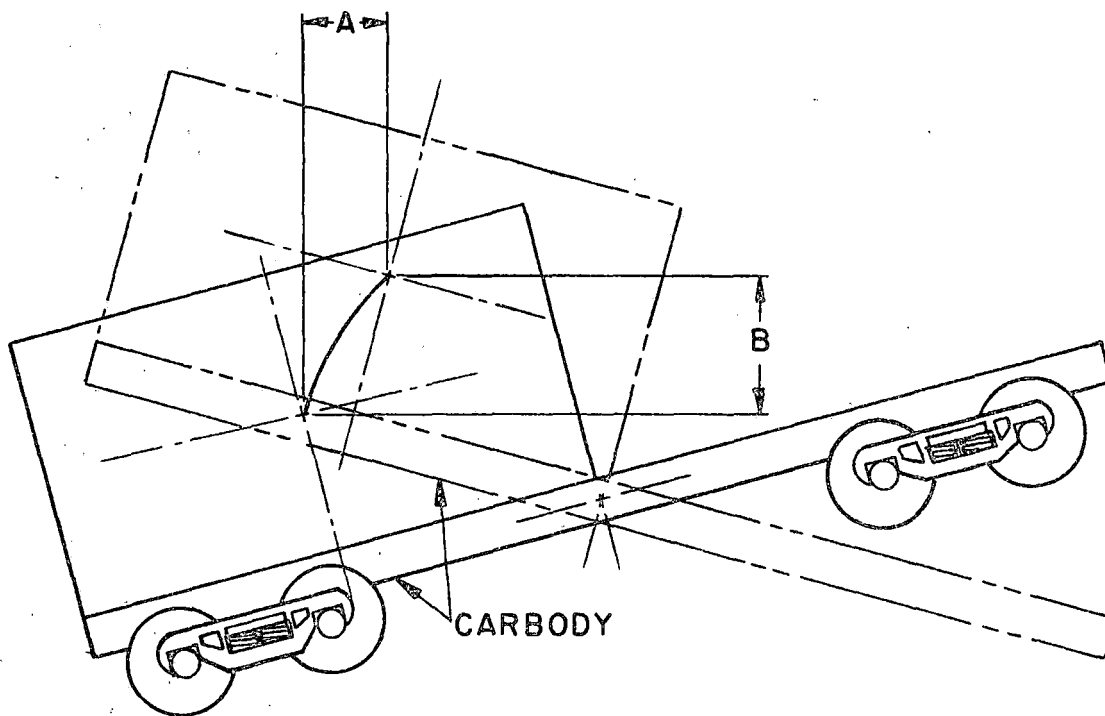
A: LONGITUDINAL DISPLACEMENT
B: VERTICAL DISPLACEMENT (BOUNCE)

Figure 4-11. Motion of Carbody and Rigidly-Mounted Container in Pitch Mode

reasonable to expect that its motion will cause the carbody center to move. That is, there may be a feedback contribution to carbody sway from the momentum of the container. From these observations, it is quite appropriate that the axle/carbody/load system be referred to as a single system.

5.0 MILEAGE ACCUMULATION EFFECTS

The objectives of the Lightweight Flatcar Program include the assessment of the mileage effects on the dynamic performance of the flatcars. For this purpose, the Ride Vibration Test (RVT) was performed three times at different amounts of accumulated mileage. The three RVT's were performed at 0 (nominal), 50,000 and 125,000 miles of revenue service accumulated over a period of more than two years. To determine the effects of accumulated mileage, the PSD's from the three RVT's were examined for the half-laden configuration (the configuration with the most severe acceleration). The details of the results are presented in this chapter by mass element, in the order: axles, carbody and loads.

5.1 AXLES

Axle behavior remained essentially constant throughout the test series. The modes with vertical orientations were particularly unchanged as expected since the wheel was tracing the rail profile. There were isolated increases in rms accelerations for the lateral modes at high speeds, but there was no consistency or evidence to relate these isolated increases with vehicle wear. These isolated occurrances are attributed to hunting, which was observed randomly in the later RVT's.

The accelerations on the PSD's for the axle data from the Class 3 test zone were sufficiently random, thus no noteworthy peaks at speeds below 40 mph corresponding to the rail joint input were produced. This effect held for the first and second RVT's, but for the third RVT, a dominating energy peak was observed at the rail joint frequency. This disparity is the result of track maintenance and improvement which was carried out in the low speed test zone between the second and third RVT's.

An anomaly was observed in the PSD for the TLDX-61 from the
first RVT. A high frequency source of energy dominated the
power spectrum at low speeds, and at higher speeds the input
frequency rose above 30 Hz resulting in a more normal PSD
signature. This anomaly was attributed to some manufacturing
or assembly defect associated with wheel rotation. The PSD's
for the second and third RVT's were examined to determine
whether this effect disappeared as the truck acquired wear.
The PSD's from the second RVT do suggest that this effect had
been smoothed out through wear. However, the third RVT was
performed on track which had been upgraded, thus, with the
reduced overall input to the axles, the anomaly was again
evident. It is, therefore, apparent, that wear reduces the
excitation but does not eliminate it.

5.2 CARBODY

The carbody mass element is the most important indicator of
wear effects for two reasons. First, input to carbody
dynamics is directly through the truck components which
wear the most, whereas input to the axles is directly from
the track. Second, input to the loads is filtered by the
carbody and, in the case of trailers, by a second suspension
system. Analysis of the data verified that the most signi-
ficant mileage effects were displayed by the carbody PSD's.

The analysis of the carbody data began with the expectation
that evidence would be found indicating increasing rms
accelerations with wear. Like axles, a clear correlation
between wear and rms values was not observed. In most
instances, however, there were increases through the speed
range. In a few cases, there was a reversal of the expected
relationship between rms accelerations and accumulated mileage.
There are a number of factors which may have contributed to
these consistencies, including

- Periodic maintenance, which is known to have occurred at least once.

- Test Zone 1 upgrade, between the second and third RVT's.

- Wheels turned due to spalling.

Thus, although a trend of increasing rms values is suggested, there is no conclusive support in the data.

There were, however, two significant effects discovered which were clearly attributable to wear. One effect was the change in the speed at which the bounce mode first displayed considerable response to rail joint input. That is, a change in the speed at which the input forces overcome the stiction (static friction force) between the columb damping devices. These speeds are listed in Table 5-1.

The data indicates that as mileage is accumulated, the critical speed (the speed at which the stiction is overcome) is reduced. This can reasonably be attributed to the breaking in of the moving parts in the truck suspension. In addition, the lightest car, the TLDX-62, consistently responded at the highest critical speed. This may be attributed to the design of the truck suspensions which were designed for the heaviest car, the TTAX.

TABLE 5-1

BOUNCE RESPONSE SPEEDS (IN MPH)

Test	TTAX	TLDX-61	TLDX-62
RVT 1	30 - 40	30 - 40	40
RVT 2	30+	30+	40
RVT 3	20	20	30

Another major effect of wear is the apparent increase in
tendency of the system to resonate. That is, although wear
did not produce a consistent increase in rms values, the
play in the suspension system increased the likelihood of
resonance. For example, consider the data in Table 5-3;
when the flatcars were new there was no evidence of resonant
activity in either sway or yaw. As mileage accumualted, the
resonant activity increased at low speeds in most cases.
This indicates that with greater wear, the system resonates
more easily, that is, resonant activity may occur at the
lower energy levels associated with lower speeds. The
associated rms levels are listed in Table 5-2. Observe
that for numerous cases in the second and third RVT's there
are either peak rms values at speeds less than 79 mph, or
there are sudden non-linear increases with speed in the
rms patterns. However, neither of these occurrences is
observed for RVT 1, when the trucks were new.

5.3 LOADS

Trailer PSD's and rms values displayed remarkable consistency
throughout the test series which is most likely related to
the double filtering effect of the carbody and trailer sus-
pension systems. The rms values displayed no significant
or regular increases with wear; the variations can be
attributed to variations in test conditions, since several
trailer modes are significantly affected by inputs in the
longitudinal mode. (The longitudinal mode directly reflects
any variations in the operation of the locomotive during the
tests.)

The absence of high frequency energy in the trailer PSD's
due to suspension filtering remained the dominant charac-
teristic. The natural frequencies were unchanged by wear.

TABLE 5-2
CARBODY RMS SWAY AND YAW ACCELERATION

Speed	Sway			Yaw		
	RVT 1	RVT 2	RVT 3	RVT 1	RVT 2	RVT 3
TTAX						
40	0.026	0.028	0.029	0.032	0.034	0.058
50	-	0.058	0.056	-	0.067	0.072
60	-	0.096	0.049	-	0.103	0.086
70	-	0.089	0.066	-	0.087	0.110
79	0.066	0.117	0.081	0.070	0.102	0.120
TLDX-61						
40	0.034	0.036	0.038	0.044	0.045	0.049
50	0.042	0.061	0.054	0.054	0.076	0.083
60	0.051	0.070	0.077	0.063	0.088	0.108
70	0.065	0.086	0.137	0.077	0.094	0.137
79	0.081	0.097	0.135	0.089	0.102	0.167
TLDX-62						
40	0.026	0.029	0.033	0.029	0.029	0.033
50	0.033	0.034	0.049	0.039	0.046	0.072
60	0.040	0.056	-	0.051	0.079	0.060
70	0.050	0.111	0.112	0.066	0.170	0.158
79	0.068	0.129	0.122	0.098	0.198	0.184

In contrast, the container PSD's showed the effects of
accumulated mileage since they reflect carbody behavior.
The interaction of container and carbody modes was presented
in Section 4.3. The pattern of interaction was unchanged
throughout the test series. As noted in Section 5.2, one
of the major observations in carbody mileage effects was
the increase of activity with wear which was indicative of
resonant-type behavior which appeared as a sudden non-linear
increase in rms acceleration at some point in the progression
of the test speed. These same increases were also observed
in container behavior. An example of this relationship is
presented in Table 5-3, where rms acceleration values for
container bounce are presented for the Class 5 test zone.
The data for the third RVT shows the most severe deviation
from linearity.

TABLE 5-3

CONTAINER RESPONSE TO MILEAGE EFFECTS

Speed (mph)	RVT 1	RVT 2	RVT 3
Container Bounce			
40	0.08	0.09	0.12
50	0.11	0.11	0.14
60	0.13	0.14	0.15
70	-	0.21	0.26
79	0.19	0.27	0.30
Carbody Roll			
40	0.28	0.31	0.36
50	0.31	0.37	0.44
60	0.35	0.43	-
70	0.39	0.70	0.92
79	0.44	0.93	1.11

Container bounce was observed, on the basis of PSD signature, to derive most of its energy from carbody roll. This relation was seen to hold true throughout the test series and as such carbody roll rms accelerations were expected to exhibit the same characteristics as container bounce, as shown in Table 5-3 where the increase in rms acceleration with speed becomes non-linear as mileage is accumulated.

6.0   INFLUENCE OF LOAD CONFIGURATION

An evaluation of the effects of load configuration on flatcar behavior was based on data from the first Ride Vibration Test (RVT) and the Over-the-Road Test (OTR). These data provide comparative information on the new flatcars and on the flatcars after approximately 10,000 miles of accumulated wear.

6.1   RVT DATA

6.1.1   LOADS

Analysis of the data from the first RVT was preceded by converting modal accelerations to a common unit. The angular accelerations, measured in radians per second per second, were converted to g's so that a comparative analysis of the relative contributions of all of the modes could be made.

Conversion of the angular accelerations to g's required calculation of the mode shape function and an analysis for each specific location of interest on the load or carbody. The linear accelerations associated with the rotational and elastic modes are functions of location in the system, whereas the accelerations due to translational contributions are, by definition, constant.

After the measurements were converted to the same units, the load accelerations were calculated for the location and condition resulting in the maximum accelerations. The far corner of the load at the maximum allowable speed was found to have the largest acceleration. This is believed to represent the worst case for the vibrational environment and to provide an estimate of the upper limit of the vibrational environment.

Table 6-1 summarizes the range in which the data for an
extreme corner of the A-end load on a fully loaded flatcar.
The bounce ($\ddot{z}_o$) and roll ($\ddot{\theta}_o$) modes appear to be the largest
contributors to load acceleration. The higher levels of
acceleration are associated with containers, because of the
absence of the filtering effect of a suspension system. In
tabulating the data, the differences between the conventional
and lightweight flatcars was observed to be quite small.

For comparison, similar data are presented in Table 6-2 for
the corner near the center of the flatcar of the A-load. At
this location, several of the modes are significantly smaller
in magnitude then at the far end of the load and none of the
modes are larger than the extreme outer corner.

Table 6-3 contains data for the B-end load. The vibrational
environment for a load is seen to be generally independent of
its position on the flatcar. Containers showed particularly

TABLE 6-1

A-END LOAD ACCELERATIONS ON A FULLY LOADED
FLATCAR AT AN EXTREME CORNER (79 MPH)

Mode	Acceleration (g)
$\ddot{x}_o$	0.04 - 0.06
$\ddot{y}_o$	0.08 - 0.09
$\ddot{z}_o$	0.13 - 0.17
$\ddot{\theta}_*$	0.12 - 0.16
$\ddot{\phi}_*$	0.13
$\ddot{\psi}_*$	0.07 - 0.10
β_{zyl*}	0.06 - 0.11

*This subscript indicates conversion to linear acceleration.
Angular accelerations are multiplied by the appropriate
distance from the center of mass to the point of interest
to convert them into linear accelerations. Elastic accel-
erations are multiplied by the mode shape function evaluated
at the point of interest to yield the linear accelerations.

6-2

TABLE 6-2

A-END LOAD ACCELERATIONS ON A FULLY LOADED
FLATCAR AT A MID-SECTION EDGE (79 MPH)

Mode	Acceleration (g)
$\ddot{x}_o$	0.04 - 0.06
$\ddot{y}_o$	0.08 - 0.09
$\ddot{z}_o$	0.13 - 0.17
$\ddot{\theta}_*$	0.12 - 0.16
$\ddot{\phi}_*$	0.02
$\ddot{\psi}_*$	0.01 - 0.02
β_{zy1*}	0.03 - 0.05

TABLE 6-3

B-END LOAD ACCELEATIONS ON A FULLY LOADED
FLATCAR AT AN EXTREME CORNER (79 MPH)

Mode	Acceleration (g)
$\ddot{x}_o$	0.04 - 0.07
$\ddot{y}_o$	0.07 - 0.08
$\ddot{z}_o$	0.12 - 0.17
$\ddot{\theta}_*$	0.12 - 0.16
$\ddot{\phi}_*$	0.11 - 0.13
$\ddot{\psi}_*$	0.06 - 0.11
β_{zy1*}	0.03 - 0.10

little difference in mode accelerations. The small differ-
ences seen in trailer mode accelerations may be attributed
to differences in suspension characteristics and trailer
bogie positioning.

Accelerations for the A-end load on half-loaded flatcars can
be seen to be consistently greater than for the fully-loaded
configuration. Table 6-4 contains data for half-loaded
flatcars. The increase in acceleration levels is attributed
to the reduction in the total mass combined with the asymmetry
of the lading configuration.

Finally data are presented in Table 6-5 for the accelerations
of empty containers and trailers. These accelerations are
approximately double the values for loaded containers and
trailers. The difference is attributed to the mismatch
between load weight and suspension design.

TABLE 6-4

A-END LOAD ACCELERATIONS ON HALF-LOADED
FLATCARS AT AN EXTREME CORNER (79 MPH)

Mode	Acceleration (g)
$\ddot{x}_o$	0.04 - 0.08
$\ddot{y}_o$	0.08 - 0.11
$\ddot{z}_o$	0.12 - 0.21
$\ddot{\theta}_*$	0.14 - 0.18
$\ddot{\phi}_*$	0.13
$\ddot{\psi}_*$	0.08 - 0.14
β_{zy1*}	0.07 - 0.11

TABLE 6-5

EMPTY LOAD ACCELERATIONS (A-END)
ON HALF LOADED FLATCARS

Mode	Acceleration (g)
$\ddot{x}_o$	0.10 - 0.12
$\ddot{y}_o$	0.15 - 0.19
$\ddot{z}_o$	0.29
$\ddot{\theta}_*$	0.23 - 0.28
$\ddot{\phi}_*$	0.25 - 0.32
$\ddot{\psi}_*$	0.17 - 0.20
β_{zy1*}	0.13 - 0.17

6.1.2 CARBODY

Data, similar to that recorded for the loads, were tabulated
for the carbodies and listed in Tables 6-6 through 6-9. The
carbody locations of interest were the points of contact
with the load, where vibrational energies were directly
transferred to the loads. For trailer lading, the locations
of interest were the kingpins and the wheel well centers,
and for containers the bracket locations were evaluated.

Certain modes were observed to have consistent zero values
in many cases. This occurs when the location of interest is
at or very near the node for that particular mode. Thus,
there is no contribution to vibration from that mode.

In most cases the TTAX shows marginally lower accelerations;
this difference is attributed to the difference in weight
and the use of the same spring groups on all three cars. The
acceleration differences can be considered sufficiently small,
thus, the overall performance of the flatcars is comparable.

TABLE 6-6

KING PIN ACCELERATION CONTRIBUTIONS AT 79 MPH

	2 Loaded Trailers			1 Loaded Trailer			Empty		
	TLDX 61	TTAX-A	TTAX-B	TLDX 61	TTAX-A	TTAX-B	TLDX 61	TTAX-A	TTAX-B
$\ddot{x}_0$	0.034	0.047	0.047	0.040	0.037	0.037	0.042	0.037	0.037
$\ddot{y}_0$	0.064	0.050	0.050	0.085	0.066	0.066	0.110	0.083	0.083
$\ddot{z}_0$	0.075	0.061	0.061	0.075	0.070	0.070	0.140	0.132	0.132
$\ddot{\theta}_*$	0.052	0.075	0.073	0.065	0.090	0.091	0.124	0.155	0.155
$\ddot{\phi}_*$	0.022	0.022	0.140	0.025	0.028	0.166	0.029	0.034	0.222
$\ddot{\psi}_*$	0.012	0.009	0.064	0.013	0.011	0.083	0.018	0.019	0.154
a_{yz1*}	0.096	0.086	0.221	0.115	0.113	0.265	0.163	0.153	0.323
a_{yz2*}	0.018	0.023	0.134	0.021	0.025	0.139	0.026	0.032	0.183
τ_{xz1*}	0	0	0	0	0	0	0	0	0
τ_{xz2*}	0	0	0	0	0	0	0	0	0

TABLE 6-7

WHEEL WELL CENTER ACCELERATION
CONTRIBUTIONS AT 79 MPH

	2 Loaded Trailers			1 Loaded Trailer			Empty		
	TLDX 61	TTAX-A	TTAX-B	TLDX 61	TTAX-A	TTAX-B	TLDX 61	TTAX-A	TTAX-B
$\ddot{x}_0$	0.034	0.047	0.047	0.040	0.037	0.037	0.042	0.037	0.037
$\ddot{y}_0$	0.064	0.050	0.050	0.085	0.066	0.066	0.110	0.083	0.083
$\ddot{z}_0$	0.075	0.061	0.061	0.075	0.070	0.070	0.140	0.132	0.132
$\ddot{\theta}_*$	0.054	0.069	0.067	0.065	0.076	0.080	0.129	0.138	0.138
$\ddot{\phi}_*$	0.139	0.128	0.030	0.151	0.163	0.037	0.185	0.203	0.046
$\ddot{\psi}_*$	0.087	0.070	0.016	0.105	0.082	0.020	0.140	0.142	0.035
a_{yz1*}	0.109	0.170	0.085	0.126	0.203	0.103	0.189	0.339	0.136
a_{yz2*}	0.045	0.076	0.038	0.049	0.076	0.040	0.640	0.100	0.051
τ_{xz1*}	0.108	0.007	0.046	0.108	0.007	0.047	0.159	0.061	0.057
τ_{xz2*}	0.060	0.073	0.046	0.060	0.073	0.045	0.086	0.091	0.054

TABLE 6-8

INBOARD CONTAINER BRACKET ACCELERATION
CONTRIBUTIONS AT 79 MPH

	2 Loaded Containers		1 Loaded		Empty	
	TLDX 62	TTAX	TLDX 62	TTAX	TLDX 62	TTAX
$\ddot{x}_0$	0.034	0.027	0.046	0.031	0.052	0.037
$\ddot{y}_0$	0.042	0.045	0.067	0.064	0.117	0.083
$\ddot{z}_0$	0.082	0.069	0.092	0.075	0.169	0.132
$\ddot{\theta}_*$	0.037	0.042	0.048	0.061	0.156	0.138
$\ddot{\phi}_*$	0	0	0	0	0	0
$\ddot{\psi}_*$	0.006	0.006	0.009	0.008	0.013	0.013
a_{yz1*}	0.101	0.105	0.124	0.124	0.171	0.162
a_{yz2*}	0	0	0	0	0	0
τ_{xz1*}	0	0	0	0	0	0
τ_{xz2*}	0.013	0.020	0.020	0.036	0.042	0.062

TABLE 6-9

OUTBOARD CONTAINER BRACKET ACCELERATION
CONTRIBUTIONS AT 79 MPH

	2 Loaded Containers		1 Loaded		Empty	
	TLDX 62	TTAX	TLDX 62	TTAX	TLDX 62	TTAX
$\ddot{x}_0$	0.034	0.027	0.046	0.031	0.052	0.037
$\ddot{y}_0$	0.042	0.045	0.067	0.064	0.117	0.083
$\ddot{z}_0$	0.082	0.069	0.092	0.075	0.169	0.132
$\ddot{\theta}_*$	0.037	0.042	0.648	0.061	0.156	0.138
$\ddot{\phi}_*$	0.163	0.144	0.194	0.170	0.209	0.216
$\ddot{\psi}_*$	0.072	0.065	0.105	0.097	0.155	0.151
a_{yz1*}	0.258	0.211	0.180	0.237	0.399	0.304
a_{yz2*}	0.129	0.115	0.149	0.124	0.152	0.157
τ_{xz1*}	0.139	0.006	0.092	0.048	0.179	0.114
τ_{xz2*}	0.026	0.037	0.046	0.064	0.085	0.112

The effect of lading configuration on carbody accelerations is seen to follow the same pattern as loads. The lowest magnitudes are seen for the fully loaded configuration and the greatest magnitudes are seen for empty containers and trailers. Again, there is no difference between accelerations at the A-end and B-end for fully loaded cars.

6.2 OTR DATA

The most significant finding in the OTR data was the identification of hunting. This finding is explained in detail in Section 7.0. For purposes of evaluating load configuration effects, however, it is useful to discuss hunting briefly at this point.

Hunting did not occur to any significant extent during the first RVT, but it was observed in the OTR testing, at which point approximately 10,000 miles of revenue service had been accumulated. The TTAX displayed the largest amount of hunting, therefore, the data for the TTAX were examined for all load configurations to identify the full extent of hunting.

Hunting was observed as a strong low-frequency energy concentration in the sway and yaw modes, for all three mass elements. Hunting was largest for the half-laden configuration. The fully loaded configuration did not appear to hunt at any test speed.

The roll mode is also known to be indicative of hunting. For the fully laden configuration, roll PSD's were seen to consist of low- and high-frequency regions of energy, but for the half-laden configuration there was occassionally only one low-frequency concentration. This indicates that the low-frequency energy, associated in part with hunting, was great enough in the half-laden configuration to dominate the energy spectrum.

6-8

Finally, the effects on the carbody modes from container feedback were observed to continue in the same fashion as for the RVT's. This phenomenon, discussed in detail in Section 4.3, is the result of rigid physical contact between the container and carbody without the benefit of a suspension interface as with a trailer. The geometric motions of the carbody appear directly in the related container modes, whereas the trailers are not directly related to the carbody and behave in a relatively consistent manner dictated largely by their suspension characteristics.

7.0 LADING ACCELERATION ENVIRONMENT

The Over-the-Road tests (OTR) were conducted to quantify the vibrational environment of the flatcars under actual revenue service conditions. For these tests, the flatcars were attached to a revenue freight train. The data were processed and analyzed in the same manner as the RVT data. Unlike the RVT's, there was no control over train speed.

7.1 OTR AND RVT DATA

Comparison of the OTR and RVT data revealed numerous simularities. Because speed was not constant through the OTR test zones, it was necessary to estimate an average speed so that an appropriate RVT test could be used for comparison.

Upon comparing similar OTR and RVT data, the rms values were found to be in agreement. PSD's were observed to display similar signatures, with differences being attributed to speed variations in the OTR. For example, OTR PSD's seldom displayed the well-defined spike typical of RVT data which could be identified as response to rail joint input due in part to the use of welded rail in the OTR test zones. For the tests in which the speed variations were minimal, however, there were concentrations of energy at frequencies corresponding to a 39-foot wavelength.

PSD's for axles were more white in character because of speed variations. Carbody and load PSD's continued to indicate the effects of suspension characteristics with concentrated energy at the natural frequency of the system. Trailers continued to behave in response to the low-pass filtering effects of their suspension coupled with carbody suspension, and containers produced consistent feedback patterns into carbody PSD's.

7.2 LATERAL INSTABILITY (HUNTING)

Hunting was observed and recorded in many instances during the OTR tests. The vast majority of the hunting was observed on the TTAX flatcar. There is no one factor to clearly attribute this difference, since the differences between the flatcars are complex and involve weight, elastic properties and component wear.

Hunting was recorded on strip charts (Figure 7-1) during the test. The upper strip is a sample of lateral acceleration of the BB-axle for the TTAX; the lower strip is a sample of the BB-axle lateral motion for the TLDX-61. Both flatcars carried one trailer loaded on the A-end. The two strips are seen to be similar at the left end of the record. Near the middle of the strip, a change is observed in the record for the TTAX axle. Acceleration magnitudes become greatly increased and a low-frequency sinusoidal plot is visible. This pattern was observed on the strip chart during the test in conjunction with the observation of hunting in the flatcar behavior. The chart speed was approximately 20 mm per second, and thus the frequency associated with hunting, in this instance, is approximately 3 Hz.

This sample of strip chart was chosen from the record of Test Zone 8. The entire strip chart for this particular test was examined and a record was made of the time periods during which hunting was observed. This data was then plotted in Figure 7-2(b). The shaded areas represent time periods during which hunting was observed.

The periods of hunting are presented in this fashion to facilitate comparison with the rms acceleration histories. The rms acceleration histories, described in Section 3.3.3 are a time domain presentation of the relative contributions to overall acceleration levels from each of four octaves in the 30 Hz frequency domain. The line labeled "5" represents the total acceleration level at any given time.
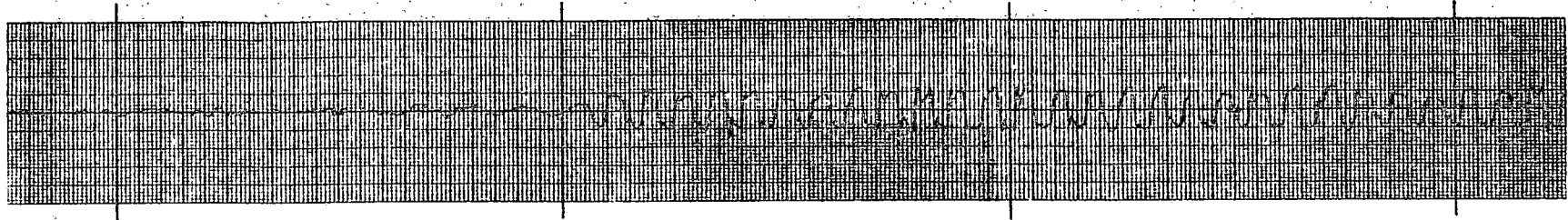
TTAX
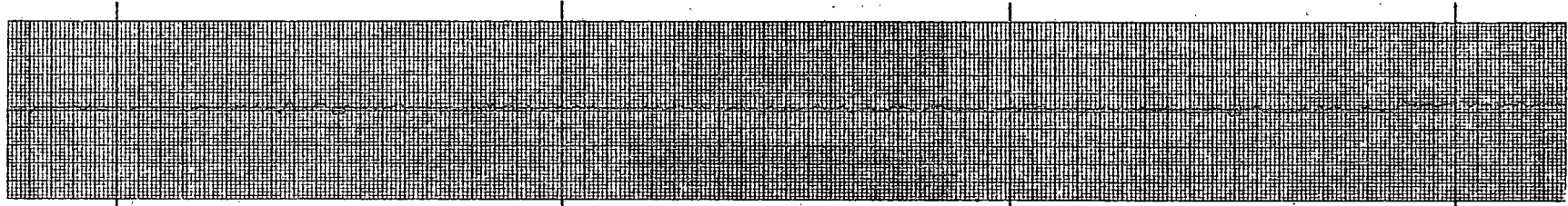
TLDX-61

Figure 7-1. BB-Axle Lateral Acceleration History

SEC

SWAY −BB −AXLE

(TTAX   TEST ZONE 8   LWFC 6   1LT   AXLES)
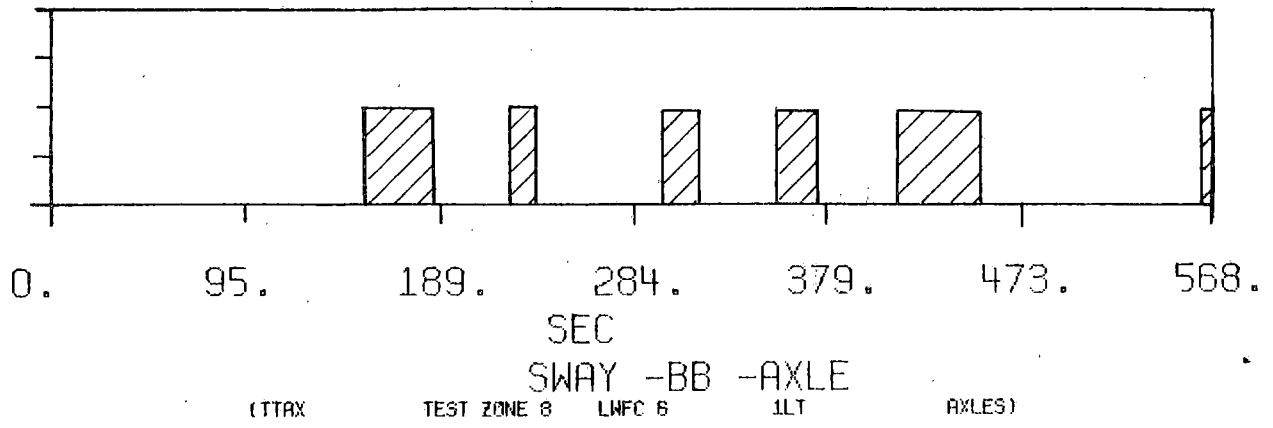
(b) Periods of Hunting for TTAX
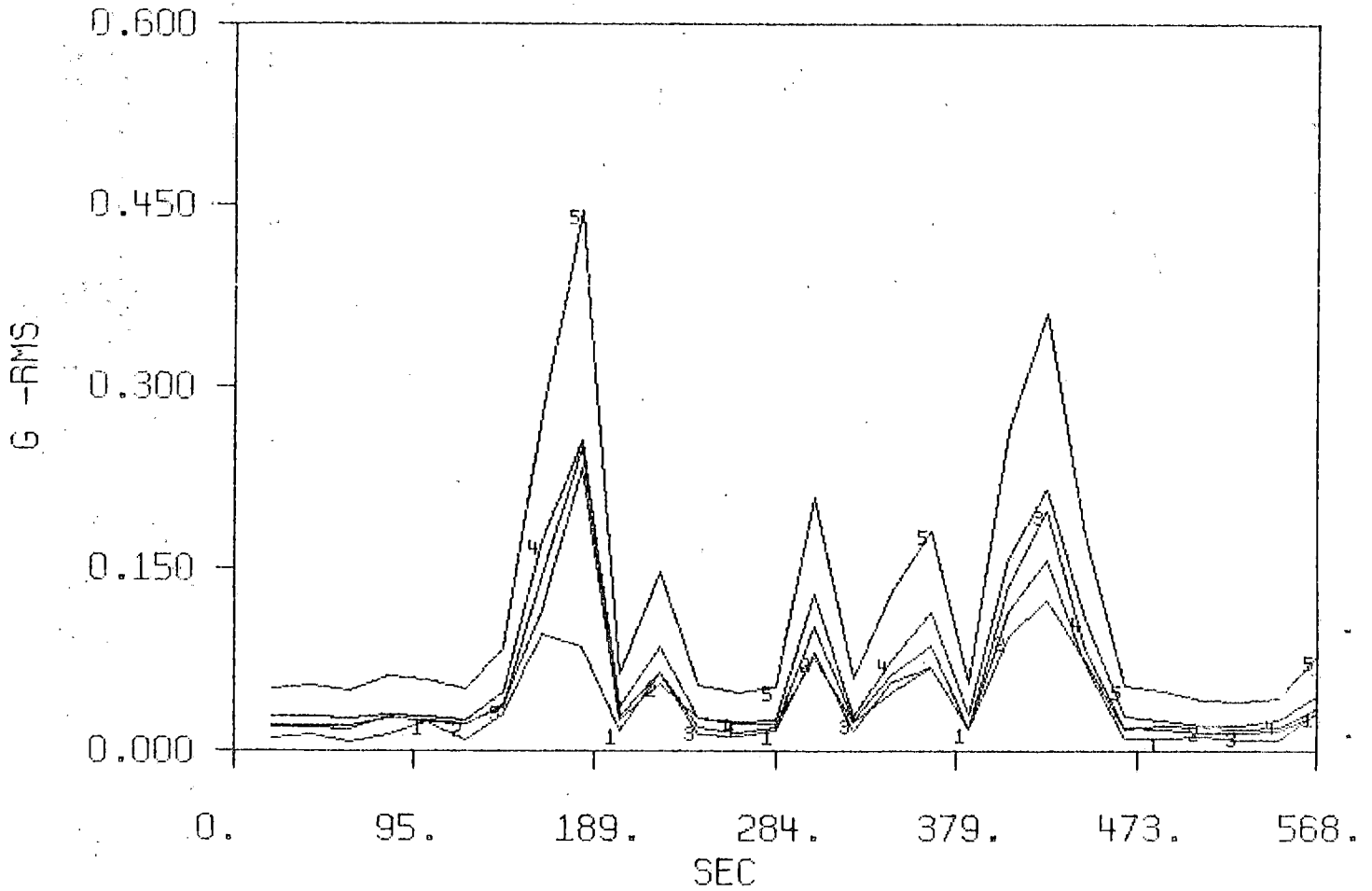
(a) RMS Acceleration History

Figure 7-2.   Comparison of Hunting with the rms
Acceleration History for the TTAX

7-4

The rms acceleration history shown in Figure 7-2(a) contains
several distinct peaks, or periods of high dynamic energy.
These peaks are directly associated with the periods of
hunting presented in Figure 7-2(b). The differences in the
magnitudes of the peaks are attributed not to the severity
of the hunting but to the time span involved; the time
history is actually not a continuous history but a sequence
of averages calculated over time spans of 20 seconds. Thus,
a period of hunting which was less than 20 seconds would be
indicated by a peak which included quiet data (periods of
no hunting). Even periods greater than 20 seconds will be
affected by the placement of the 20-second window which
could possibly overlap into quiet data. Complete accelera-
tion histories for both the TTAX and the TLDX-61 are included
in Appendix F.

Several observations can be made from this data. First,
where hunting is indicated for the BB-axle, there is very
little indication of hunting by the AA-axle. In this case,
hunting was primarily associated with the rear truck. Second,
hunting also appeared in both sway and yaw axle accelerations.
Finally, the rms acceleration peaks associated with hunting
appear in the rms acceleration histories for load yaw and
carbody yaw and sway. To a lesser degree, hunting was also
indicated by load sway and carbody roll.

The high energy levels associated with the peaks in the rms
acceleration histories are also apparent in the PSD's at the
3 Hz hunting frequency determined from strip chart measurements.
Shown in Figure 7-3 are the sway mode PSD's for the BB-axle
for the TTAX and TLDX-61. The PSD for the TLDX-61 shows a
sufficiently smaller concentration of energy which keeps the
scale factor (YMAX) low enough to allow higher frequency
energy to become visible. A significant decrease in rms
acceleration was also observed. A small peak is present at
3 Hz; this energy is associated with the minor occurrences
of hunting by TLDX-61.

YMIN = .00000E 00 · YMAX = .75730E-03   X-AXIS SCALE .19866E 02 REAL DATA POINTS PER INCH
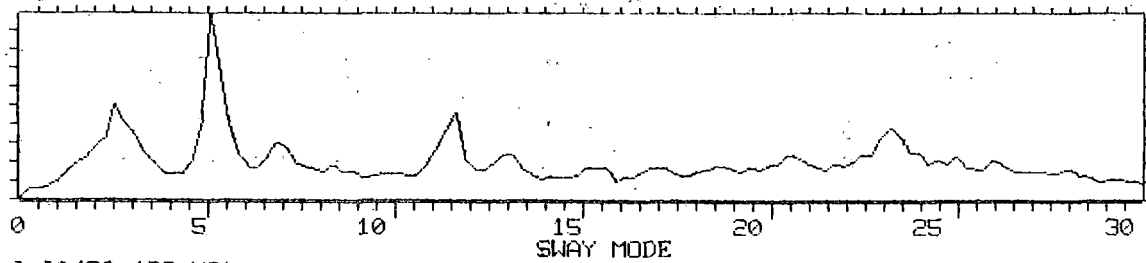
POWER IN BAND (0 - 30) = 0.00420 (GS-MS)
                    RMS = 0.06483

(a) TLDX-61

YMIN = .00000E 00   YMAX = .11150E-01   X-AXIS SCALE .19866E 02 REAL DATA POINTS PER INCH
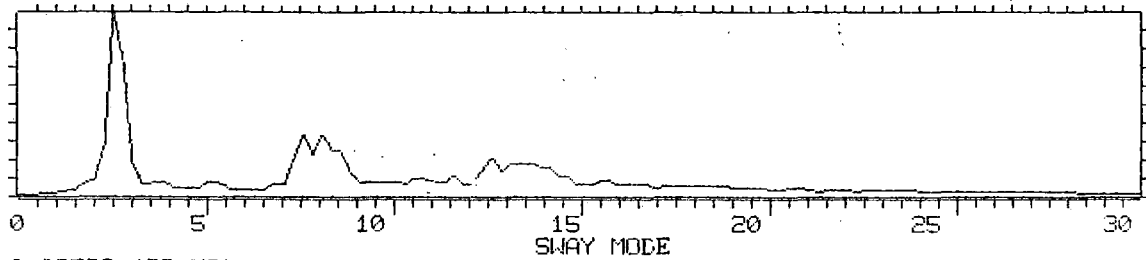
POWER IN BAND (0 - 30) = 0.02522 (GS-MS)
                    RMS = 0.15881

(b) TTAX

Figure 7-3. A Comparison of BB-Axle Sway (Zone 8)

The evidence of hunting is seen in the PSD's for several modes of the loads and carbodies. Shown in Figure 7-4 is a set of PSD's of carbody sway and yaw modes for the TTAX flatcar. The similarities between the sway and yaw PSD's in each set are attributed in part to the neutral response to hunting. The PSD's in Figure 7-4(a) are dominated by a peak at 3 Hz. The signature for the second set (Figure 7-4(b)) includes, besides the peak at 3 Hz, additional energy representative of more normal behavior. The rms acceleration values for Figure 7-4(b) are significantly lower than the values for Figure 7-4(a), due to the reduced occurrence of hunting.

Beyond the identification and characterization of hunting, the preceding analysis has additional significance in terms of the overall evaluation of the statistical data from the test series. Concentrations of energy at 3 Hz have previously been attributed to either of two sources - rail joint input at 40 or 79 mph, and vibration at the natural frequency for a spring mass system. The inclusion of hunting as a third source of 3 Hz energy increases the possibilities for a thorough data interpretation and additionally provides new insight into the troublesome phenomenon of hunting.

CAR BODY
TTAX   ZONE 8   1LT   LWFC 6

YMAX = .50547E-02   X-AXIS SCALE   .19866E 02 REAL DATA POINTS PER INCH

SWAY MODE

TOTAL POWER IN 30 HERTZ BAND   .373316E-02   G'S MEAN SQUARE
                                 .610996E-01   RMS

YMAX = .27078E-02   X-AXIS SCALE   .19866E 02 REAL DATA POINTS PER INCH

YAW MODE

TOTAL POWER IN 30 HERTZ BAND   .223261E-02   (RAD/SEC/SEC) MEAN SQUARE
                                 .472505E-01   RMS

(a)

CAR BODY
TTAX   ZONE 9   1LT   LWFC 6

YMAX = .35424E-03   X-AXIS SCALE   .19866E 02 REAL DATA POINTS PER INCH

SWAY MODE

TOTAL POWER IN 30 HERTZ BAND   .131487E-02   G'S MEAN SQUARE
                                 .362611E-01   RMS

YMAX = .20717E-03   X-AXIS SCALE   .19866E 02 REAL DATA POINTS PER INCH

YAW MODE

TOTAL POWER IN 30 HERTZ BAND   .108918E-02   (RAD/SEC/SEC) MEAN SQUARE
                                 .330027E-01   RMS

(b)

Figure 7-4.   A Comparision of Carbody Sway and Yaw

7-8

8.0 WEAR MEASUREMENTS

Another objective of the LWFC Program was to determine the
relationship between component wear and accumulated mileage
in revenue service. Appendix B contains the vehicle component
measurements made by American Steel Foundaries using their
standard service wear measurement form. Measurements were
also made of wheel tread wear and draft gear wear. A complete
set of measurements was made at accumulated mileage levels
of 0, 50,000, and 125,000 miles with the exception of draft
gear wear which was measured at 0 and 125,000 miles.

8.1 COMPONENT DAMAGE AND MAINTENANCE

Before discussing the trends in component wear resulting from
mileage a brief summary of events and damage incurred during
the 125,000 miles of service is required. The intent of the
LWFC Program was to subject all the flatcars to the rigors
of normal usage. As a consequence, a certain amount of damage
and repair work was incurred.

American Steel Foundries presented an excellent summary of
wear effects on flatcars in a letter* to FRA dated 4 December
1978. Excerpts from the letter follow:

> "Wear as indicated by the latest inspection (RVT_3)
> generally appeared to follow the moderate trends
> established by Inspection No. 2 (RVT_2) from October
> 1977. Qualitatively and from brief quantitative
> review, we found the trucks to be performing satis-
> factorily and in a reasonably normal manner. A few
> scattered wear data points indicated negative wear
> (wrong direction) relative to the previous inspections,
> but such were inconsequential to the extent of data
> gathered. They are probably attributable to some
> variations in measurement position or misapplication
> of a gauge. In retrospect, data acquired should
> provide a statistically useful study."

* Letter American Steel Foundries/H.G. Tennikait/4 December
   1978

"Various isolated occurrences were observed which should be brought to your attention as an aid to your evaluation. These include:

Those bolsters using a horizontal center plate liner were subject to liner retention weld failure around the king pin hole. The plates were then free to move somewhat, therein causing some localized plate damage (small broken pieces), through contact with the weld metal. These liner pieces then apparently gouged the car body center plates around their king pin holes. All-in-all, this condition did not represent a functional degradation, but the plate movement essentially restricts study of bolster center plate wear to a more averaging approach, and subjects analysis to some error relative to initial measurements when the welds were intact.

The L-2 inner pocket slope liner plug welds of TLDX 62 failed. The plate was in position at disassembly, however, and appeared to have caused no functionally significant damage. It was rewelded into position for re-assembly.

The side frame column friction plate in the R-1 position of the TTX car displayed some weld cracking in all six retention positions and both attachment bolts were missing. The plate was not loose, however, and due to the normal retention lugs, could not be expected to cause trouble. As a precaution, undersize carriage bolts were installed upon re-assembly. Should plans be made for the trucks to be used for additional test purposes of extended duration, this plate should be reworked.

The side bearing clearance of the TLDX 61 AL corner was zero at the time of measurement. Adjustment or another check would be desirable before deploying for additional testing.

Wheels on the B-end truck of TLDX 61 had been substituted some time prior to the inspection with wheels in rather poor condition, as noted by the trend contours, attached. There was also considerable shelling in the treads. We have no idea why the substitutions were made or where the original wheels are. These particular wheels should be modified before any additional testing. While on the wheel subject, all others were in generally good shape, with some sporatic but minor shelling.

> Bearing adapters were found rotated 180°
> out of original position in two cases, and for
> the B-end of TLDX-62, had been swapped L-1
> to L-2 and R-1 to R-2. These discrepancies were
> probably the result of truck work relating to
> tests or wheel changes. Data are provided for
> and adapters reinstalled in the original
> orientations."

In addition to the replacement of the two axles on the B-truck of the TLDX-61 mentioned in the ASF letter the B-axle (axle 2) of the TLDX-62 was replaced. After RVT_2 the BB-axle (axle 1) of both the TTAX and TLDX-61 were turned into a narrower flange contour due to spalling.

During the first wear measurement, it was found that on all three cars only the B-truck had a king pin liner. During the second measurement, it was found that the liner horizontal weld had cracked on both the TTAX and TLDX-61. These were repaired before the flatcars were returned to service. Some evidence of various maintenance and component changes was found throughout the program. The most notable evidence concerned the roller bearing wedge adapters on the left side of the TLDX-62 B-truck which had been turned around and all four keepers which were missing.

During preparation for the second RVT, the cut bar support assembly on the TLDX-61 was found to have been damaged. Also, one of the containers (XTRU-871264) had had a latch broken off. In summary, the three test flatcars had seen 125,000 miles of service typical to that experienced by any flatcar in inter-modal service.

8.2 COMPONENT WEAR

The draft gear of all three flatcars showed little wear after the 125,000 miles of service; however, the TTAX shank butt height at the B-end did reach the condemning limit at the end of the program. This may be attributed to a variation in the

butt design between the draft gear of the two lightweight flatcars which were manufactured in January 1967 and the draft gear of the TTAX which was manufactured in December 1974. The measurements of the wheel contours (Appendix B) indicate normal wear and the turning of the wheels due to spalling. Wheel wear took place primarily in the throat area. There is no direct correlation between wheel wear and axle position which agrees with the observations made in previous sections concerning lateral instabilities or hunting. It should, however, be noted that all the wheels turned and the axles replaced were on the B-trucks.

Wear measurements made on other truck components show a steady wear rate trend on the order of 0.05 to 0.1 inches per 100,000 miles of service. The ASF letter points out exceptions to the general wear rate trend.

One interesting wear surface to examine is the truck bolster center plate. Sufficient measurements were made on this surface to provide a statistical data base. Measurements were made every 45° around three concentric rings. Tables 8-1, 8-2, and 8-3 summarize these measurements in terms of the mean value, μ, and the standard deviation, σ, about the mean for each of the three cars. Each table shows four sets of these parameters, one each for the outer, middle and inner rings as well as an overall set which is the mean of all measurements.

These statistics show that the overall wear rate ranges from 0.04 to 0.1 inches after 125,000 miles of service. The rate of wear seems to be more or less constant for a given car. The TLDX-62 exhibits the smallest amount of wear (0.04 inches) followed by the TTAX (0.06 inches). The TLDX-61 shows by far the most wear -- almost twice that of the other cars.

Although there is no clear cut trend in the standard deviation
of the measurements, which may be thought of as an irregularity
or roughness in the surface, it appears as though there may
be a tendency to smooth the center plate surface with use.
This observation is obscured by the weld failures around the
king pin liners. The standard deviation does, however,
establish the limit of resolution in the mean which permits
the comparison of the three flatcars.

TABLE 8-1

TTAX TRUCK BOLSTER CENTER PLATE WEAR MEASUREMENTS

Truck	Mileage	Outer		Middle		Inner		Overall	
		μ	σ	μ	σ	μ	σ	μ	σ
B	0	.3863	.0176	.3813	.0156	.3729	.0143	.3801	.0162
	50,000	.3584	.0176	.3633	.0122	.3628	.0099	.3615	.0132
	125,000	.3206	.0090	.3163	.0083	.3000	.0055	.3134	.0115
A	0	.3705	.0476	.3595	.0349	.3545	.0208	.3615	.0352
	50,000	.3555	.0435	.3458	.0282	.3393	.0175	.3468	.0309
	125,000	.3181	.0488	.3094	.0332	.2969	.0141	.30825	.0347

TABLE 8-2

TLDX-61 TRUCK BOLSTER CENTER PLATE WEAR MEASUREMENTS

Truck	Mileage	Outer		Middle		Inner		Overall	
		μ	σ	μ	σ	μ	σ	μ	σ
B	0	.3795	.0229	.3710	.0139	.3605	.0073	.3703	.0172
	50,000	.3566	.0264	.3698*	.0156	*	*	.3601	.0221
	125,000	.2900	.0314	.2669	.0196	.2613	.0133	.2727	.0252
A	0	.3203	.0281	.3083	.0210	.3049	.0111	.3111	.0214
	50,000	.2906	.0164	.2925	.0135	.2905	.0088	.2912	.0127
	125,000	.2043	.0205	.2128	.0149	.2169	.0149	.2113	.0171

* TLDX-61 (RVT$_2$) the horizontal weld around the king pin liner was broken allowing the liner to rise and show negative wear.

TABLE 8-3

TLDX-62 TRUCK BOLSTER CENTER PLATE WEAR MEASUREMENT

Truck	Mileage	Outer		Middle		Inner		Overall	
		μ	σ	μ	σ	μ	σ	μ	σ
B	0	.3634	.0168	.3593	.0157	.3526	.0118	.3584	.0150
	50,000	.3420	.0214	.3618*	*	*	*	*	*
	125,000	.3216	.0161	.3179	.0083	.3141	.0085	.3179	.0115
A	0	.3355	.0194	.3389	.0113	.3253	.0127	.3332	.0154
	50,000	.3080	.0110	.3153	.0081	.3100	.0121	.3111	.0105
	125,000	.2896	.0102	.2948	.0071	.2943	.0100	.2929	.0091

* Weld broke around king pin/liner rise allowed negative growth.

9.0 CONCLUSIONS AND RECOMMENDATIONS

The Lightweight Flatcar (LWFC) Evaluation Program has provided a complete representation of the dynamic performance of the conventional TTAX flatcar and the two prototype lightweight flatcars. An analysis of this information has provided valuable insight into the relative merits of these two types of flatcar. In addition, several fundamental findings were made regarding the dynamic performance of flatcars in general. The LWFC Program has provided useful data for future flatcar design and has demonstrated the means for future railcar test and evaluation.

9.1 SUMMARY OF IMPORTANT FINDINGS

The first objective of the LWFC Program as stated in Section 1.2 was to obtain a quantitative comparison between conventional and lightweight flatcars. To this end, a great deal of data was analyzed to determine if the overall performance of the flatcars studied was comparable. By comparable, we mean that with the exception of certain isolated cases, the mode accelerations were typically 20 to 30 percent different between cars. In some instances, the lightweight flatcars exhibited lower levels of acceleration and in other situations the conventional flatcar provided lower levels of acceleration. Thus, lightweight flatcars are comparable to conventional flatcars in terms of their dynamic performance. One exception to this was the bounce mode in which the TTAX consistently experienced lower acceleration levels. This is due to the type of spring groups used during this study which were designed for the heavier car (TTAX). As a result, the lightweight flatcars were relatively stiff and experienced somewhat higher levels of vertical acceleration. Modification of the spring groups for the lightweight flatcars, therefore, offers a potential improvement in their performance.

Before further discussing the relative performance of the flatcars, we must consider the sources of vibrational input

to each system. Examination of axle accelerations has shown
that for the most part each flatcar did indeed receive similar
inputs. Exceptions to this were seen during the first Ride
Vibration Test (RVT_1) where TLDX-61 (trailer) apparently had
a defective truck and during RVT_2 where TLDX-62 (container)
apparently had a flatspot on the wheel. Also the flatcar
coupled directly to the locomotive (TLDX-62) experienced
somewhat larger longitudinal inputs than did the two trailing
flatcars.

An analysis of axle accelerations revealed certain fundamental
features of the rail environment useful in establishing the
physical validity of the data. First, the regular spacing
of joints at 39 feet produced a pronounced input to the vehicle
system; the frequency of this input was a linear function of
speed. This was useful in identifying the paths of input trans-
mission and the causes of certain vehicle response character-
istics. Also, the staggering of rail joints every nineteen
and one half feet provided similar information for those modes
which depend on the differences in track inputs from both rails.

The level of axle acceleration was observed to increase with
the square of the speed. This was anticipated because the
wheel remained in contact with the rail at all times. In
contrast, the acceleration experienced by the carbody and load
increased linearly with speed. This was again anticipated since
these masses are mounted above the truck suspension which acts
as a filter to any input. Thus, as the speed and the track
input frequency increase, the input is filtered more and more.
These facts helped establish confidence in the data and thereby
the credibility of the conclusions drawn from them.

The second objective of the LWFC Program was to quantify the
load acceleration environment under typical operating conditions.

The Over-the-Road (OTR) test series was conducted to accomplish
this objective. Basically these results were in agreement with
those of the RVT series with some differences related to
differences in train handling (controlled versus uncontrolled)
and track inputs (tangent versus curved). These differences
basically appeared as wider energy peaks in the power spectral
densities of the OTR results caused primarily by variations
in speed. Also hunting was more prevalent during the OTR test
series. The levels of acceleration were found to lie in the
range of .01 to .2 g rms during the OTR test series. There
were, however, instances where the level of instantaneous
accelerations on the axle exceeded one g; e.g., during hunting.

The third objective was to determine the relation between wear
and dynamic performance. A trend towards increasing accelera-
tion levels for all three flatcars was found to occur with
accumulated mileage and increased wear. The actual rate of
increase was small, and as a result unplanned events, such as
axle replacement and other repairs, obscured the trend and,
in some cases, caused a reduction in acceleration levels. A
pattern was, however, observed in which occurrences of resonant
behavior became increasingly frequent with wear. In some
cases, this resulted in a relative maximum in the accelera-
tion versus speed curves. Overall the results were found to
be in line with the expected values for this study. That is
simply, wear causes increases in acceleration levels.

The fourth objective of the LWFC Program was to determine
the relation between accumulated mileage and wear. Those
surfaces designed to wear were found to wear normally with
accumulated mileage. These surfaces typically wore at a rate
of one-tenth of an inch per one hundred thousand miles. In no
case was wear found to be more than a quarter of an inch and,
in most cases, less than one-tenth of an inch during the entire

program. There were, however, occasional failures and cracks which developed resulting in larger changes than caused by simple wear.

The fifth program objective was the determination of load configuration influence on dynamic performance. The lading configuration was seen to have a significant effect on flatcar performance. The fully-loaded flatcars experienced the lowest acceleration levels while the empty flatcars experienced the highest levels. The most extreme lading acceleration environment was observed on the outside corners of the load in the half-loaded configuration.

Trailers were observed to experience a vibrational environment composed almost exclusively of low frequency energy due to the filtering effect of their suspension systems. Containers experienced vibration similar to that of the carbodies themselves, and complicated due to feedback. Energy was transferred from one mode to another through the geometry of the mass system comprised of the carbody and the loads.

One additional finding was made concerning hunting. Hunting was identified on three levels or domains of data representation. In the time domain hunting appeared as large sinusoidal oscillations on the strip chart records of lateral acceleration. In the octave rms histories, which are a graphical combination of the time and frequency domains, hunting was indicated by peaks several factors larger than the normal acceleration levels. In the frequency domain, the indication for hunting was a peak in the PSD at approximately 3 Hz.

Hunting was virtually nonexistent when the trucks were new (RVT_1) but considerable hunting was observed when approximately 10,000 miles of service had been accumulated. Hunting was observed primarily for the conventional flatcar and almost exclusively for the half-laden configuration.

9.2 CONCLUSIONS AND RECOMMENDATIONS

The results of the Lightweight Flatcar Program indicate that the performance of the lightweight flatcars is comparable to conventional flatcars. Indications are that normal service will be feasible and in the long run the benefits associated with weight reduction will be gained without incurring penalties in other areas.

The LWFC Program has provided an extensive data base which will lend itself to further analysis and can be used in guiding future test planning. Several observations have already been made which warrant further investigation, such as hunting, and axle frequency. Another observation was that hunting occurred primarily for the half-laden configuration after some wear had been accumulated on the trucks. Further investigations to determine whether extensive wear will result in significant hunting for fully laden flatcars as well may be warranted. The answers to such questions are important to the successful operation and future development of rail transport systems. The results of the Lightweight Flatcar Program have contributed answers to specific questions and have provided a stepping stone for future analytical programs.

Finally the LWFC Program has developed a highly useful methodology and tool which can be used in the evaluation of other vehicles and/or components. Volume I of this report describes in detail the technique and general procedures of modal analysis. Use of the modal analysis technique and the data base established by this program should serve as a guideline for future studies of dissimilar vehicles.

APPENDIX A

TRANSDUCER LOCATIONS
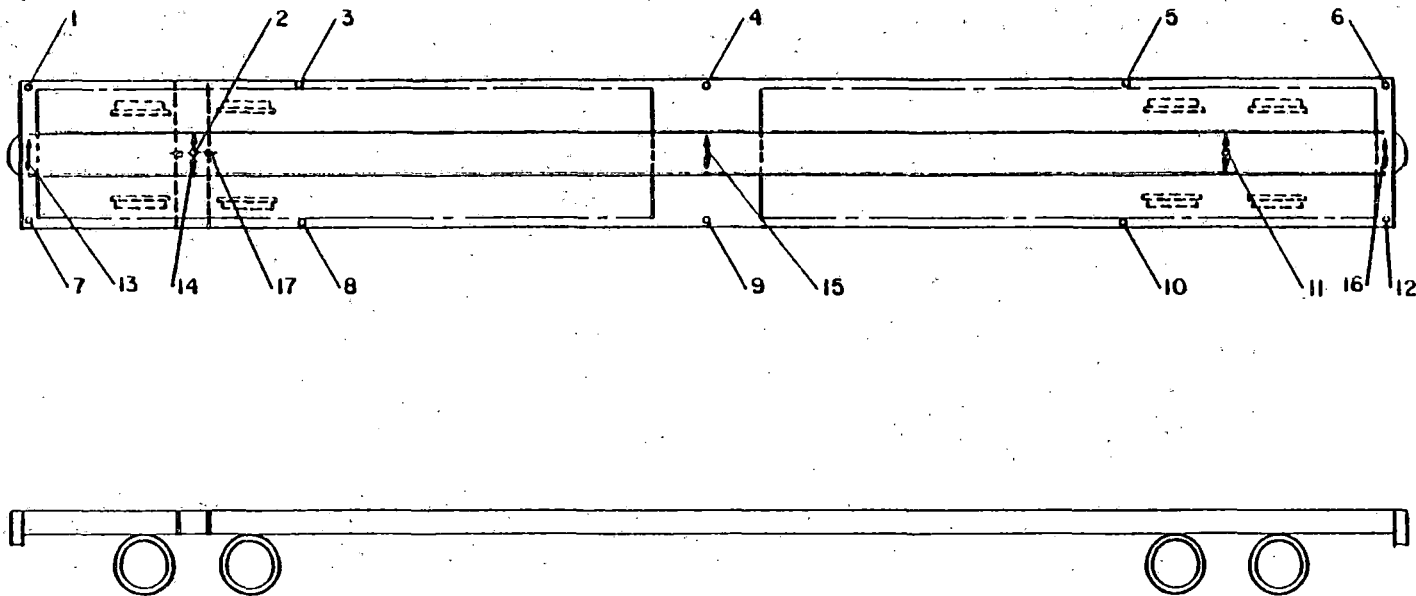
Figure A-1.. Transducer Locations on TTAX Car

TTAX TRANSDUCER LOCATIONS
(L/2 = 45 Feet)

VERTICAL

Number	ID	x	y
1	34.0 V	43'9-1/2"	-4'3/4"
2	32.0 V	31'10-7/8"	7-5/8"
3	31.1 V	16'6"	-4'3/4"
4	30.0 V	-8-1/2"	-4'3/4"
5	29.1 V	-16'6-1/4"	-4'3/4"
6	28.0 V	-43'9"	-4'3/4"
7	49.0 V	43'9-1/2"	+4'3/4"
8	49.1 V	16'5-1/4"	4'3/4"
9	50.0 V	7-1/2"	4'3/4"
10	50.1 V	-16'6-1/2"	4'3/4"
11	29.0 V	-32'1/4"	7-5/8"
12	51.0 V	-43'6-3/4"	4'3/4"

LATERAL

13	33 L	44'5-5/8"	1'8-1/2"
14	32 L	33'9-1/2"	9-1/4"
15	31 L	3-1/4"	-1'2-3/8"
16	29 L	-32'2-1/2"	-1'4"

LONGITUDINAL

17	32 H	31'1-3/4"	7-5/8"

Figure A-1 (Cont.). Transducer Locations on TTAX Car
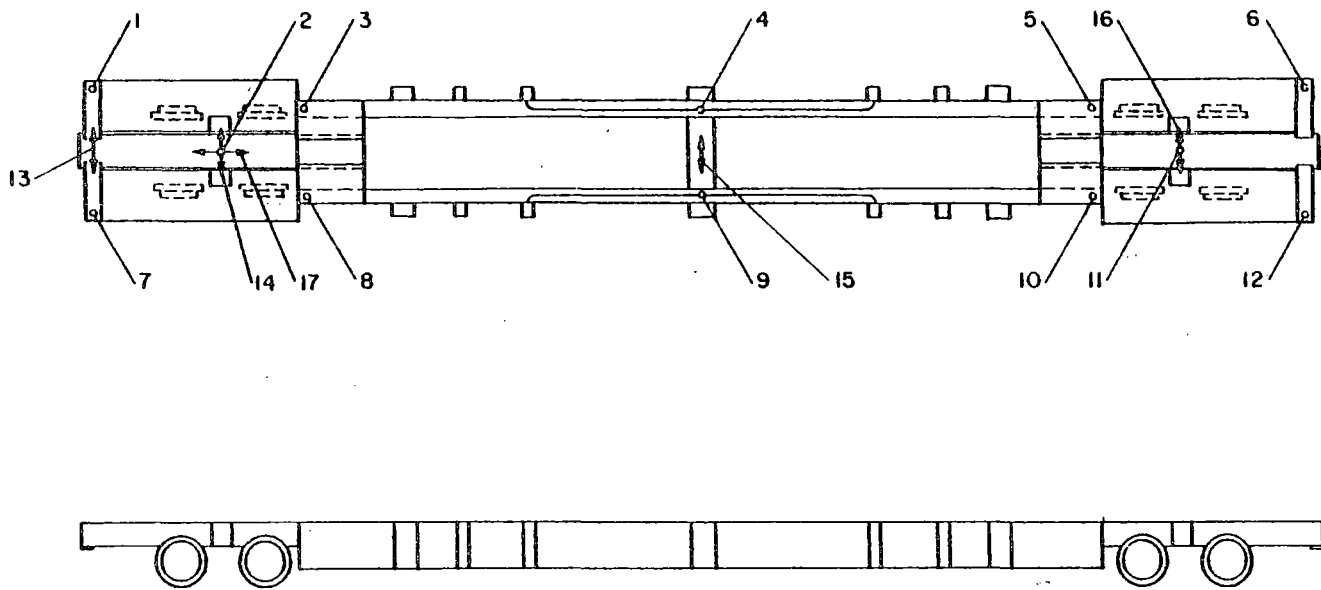
Figure A-2. Transducer Locations on TLDX-61 Car

TLDX-61 TRANSDUCER LOCATIONS
(L/2 = 41'5")

VERTICAL

Number	ID	x	y
1	27 V	40'6-1/2"	-4'2-7/8"
2	25 V	31'3"	-10-1/2"
3	24 V	23'3-1/2"	-2'11-7/8"
4	22 V	3-3/8"	-2'10-3/4"
5	21 V	-23'2-3/8"	-2'11-7/8"
6	19 V	-40'7-1/2"	-4'3-1/2"
7	52 V	40'6-1/8"	4'3-1/4"
8	53 V	23'3-7/8"	3'1/8"
9	54 V	3-1/2"	2'10-5/8"
10	55 V	-23'3-5/8"	2'11-3/4"
11	20 V	-37'7-3/4"	-10-1/2"
12	56 V	-40'6-1/4"	3'-1/8"

LATERAL

Number	ID	x	y
13	26 L	41'1-3/4"	1'5"
14	25 L	30'10-5/8"	1'4-3/8"
15	23 L	-1-3/4"	2'7-1/2"
16	20 L	-33'9-5/8"	1'4-1/4"

LONGITUDINAL

Number	ID	x	y
17	25 H	30'1-5/8"	10-1/2"

Figure A-2 (Cont.). Transducer Locations on TLDX-61 Car
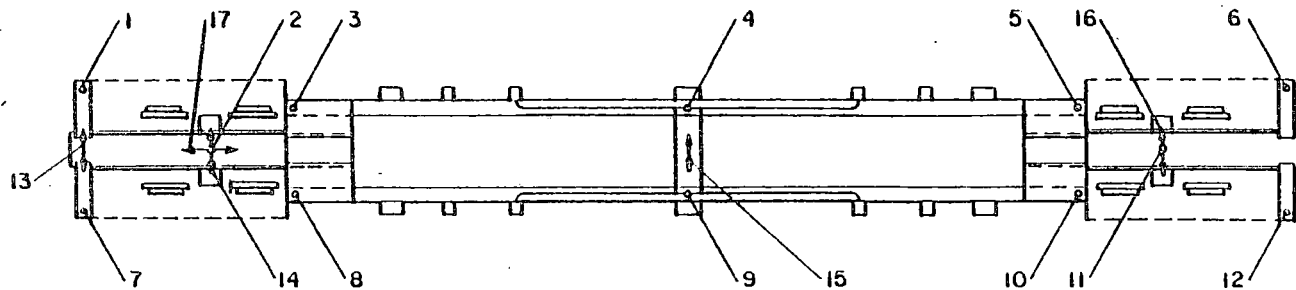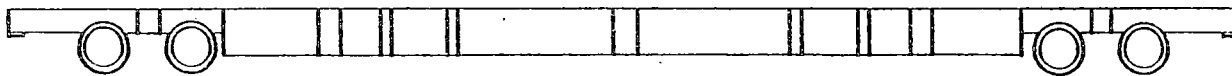
Figure A-3. Transducer Locations on TLDX-62 Car

TLDX-62 TRANSDUCER LOCATIONS
(L/2 = 41'5")

VERTICAL

Number	ID	x	y
1	43 V	39'4-3/4"	-3'5-1/4"
2	41 V	31'1-3/8"	10"
3	40 V	22'8-5/8"	-2'11-7/8"
4	38 V	10-3/4"	-2'10-3/8"
5	37 V	-22'9-7/8"	-2'11-7/8"
6	35 V	-39'4-1/8"	-3'5-1/2"
7	44 V	39'4-3/4"	3'5"
8	45 V	22'9"	2'11-5/8"
9	46 V	9-5/8"	2'10-7/8"
10	47 V	-22'9-3/4"	2'11-5/8"
11	36 V	-33'10-1/4"	10-1/2"
12	48 V	-39'3-3/4"	3'5-1/4"

LATERAL

13	42 L	39'4"	1'9"
14	41 L	31'9"	1'4"
15	39 L	1'6-1/8"	2'7"
16	36 L	-33'3-5/8"	1'4-1/2"

LONGITUDINAL

17	41 H	31'1-3/8"	10"

Figure A-3 (Cont.). Transducer Locations on TLDX-62 Car
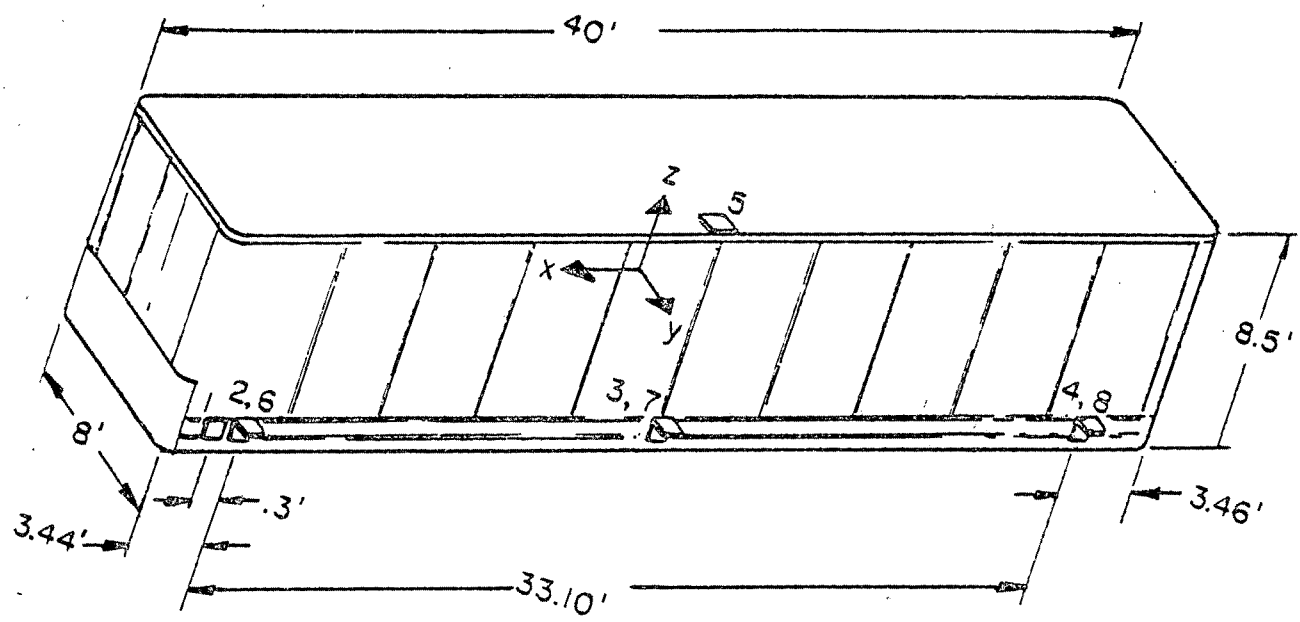
Figure A-4. Trailer Transducer Locations

Number	x (Feet)	y (Feet)	z (Feet)
1	-		
2	16.5		
3	0.0	4	
4	-16.7		-4.12
5	0.0		-3.83
6	16.5		-3.83
7	0.0	4	-3.83
8	-16.7	4	4.75
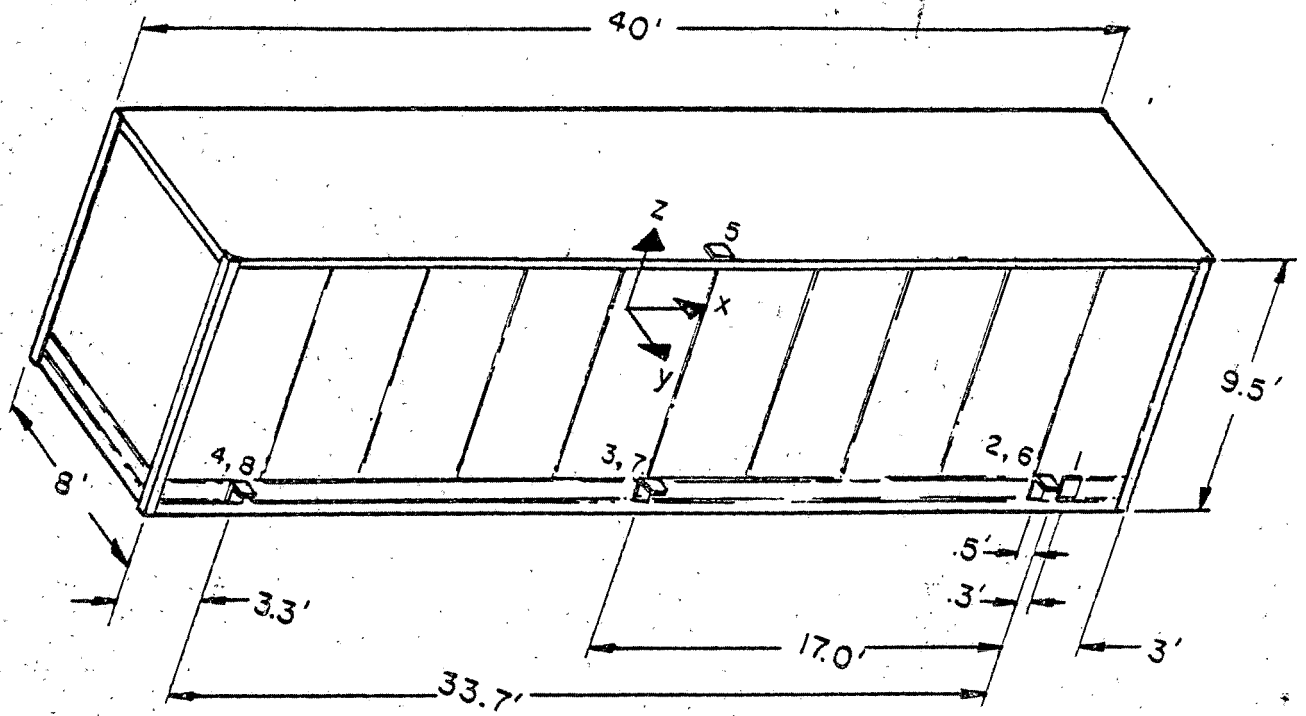
Number	x (Feet)	y (Feet)	z (Feet)
1	16.86	4.17	-3.33
2	16.56	4.33	-2.90
3	0.00	4.33	-2.90
4	-16.54	4.33	-2.90
5	0.00	-3.48	4.54
6	16.56	4.17	-3.33
7	0.00	4.17	-3.33
8	-16.54	4.17	-3.33

Figure A-5. Container Transducer Locations

A-8

LATERAL ACCELEROMETER
ON RIGHT SIDE OF
TRUCK ONLY

$7\frac{1}{2}"$

$1\frac{7}{8}"$

$1\frac{5}{8}"$

L   H

V

$6\frac{1}{2}"$

$4\frac{3}{8}"$

$5\frac{5}{8}"$

DISTANCE BETWEEN VERTICAL
ACCELEROMETER ON ADJACENT
AXLES

$7'\,4\frac{1}{2}"$

DISTANCE BETWEEN VERTICAL
ACCELEROMETERS ON OPPOSITE
SIDES OF SAME AXLE

Figure A-6.   Axle Transducer Locations

A-9